DEPARTMENT OF EARTH SCIENCES
ADDIS ABABA UNIVERSITY
SCHOOL OF GRADUATE STUDIES

LITHOLOGICAL AND STRUCTURAL MAPPING OF THE CENTRAL AND NORTH WESTERN PART OF ETHIOPIA IN VIEW OF PETROLEUM EXPLORATION.

BY

ZELALEM SHIFERAW

ADDIS ABABA
JUNE 2005

Lithological and structural Mapping of the central and North Western part of Ethiopia in View of Petroleum Exploration.

A THESIS PRESENTED TO
THE SCHOOL OF GRADUATE STUDIES OF
ADDIS ABABA UNIVERSITY

In partial Fulfillment of the requirements for the Degree
Master of Science in Earth Sciences.

BY
ZELALEM SHIFERAW
JUNE 2005.

ADDIS ABABA UNIVERSITY
SCHOOL OF GRADUATE STUDIES

Lithological and structural Mapping of the central and North Western part of Ethiopia in View of Petroleum Exploration.

By
Zelalem Shiferaw
Faculty of Natural Science
Department of Earth Sciences.

Approval By Board of Examiners

Dr. Dereje Ayalew _____
Chairman, Department
Graduate Committee

Dr. Tesfaye Korme _____
Advisor

Dr. Bekele Abebe _____
Advisor

Dr. Asfawossen Asrat _____
Advisor

Dr. Solomon Tadesse _____
Examiner

Dr. Danagchew Legesse _____
Examiner

Dr. Wollela Ahemed _____
Examiner (external)

Declaration

I, the under signed, declare that this thesis is my original work and has not been presented for a degree in any other university, and that all sources of material used for the thesis have been dully acknowledged.

Dr. Tesfaye Korme (Advisor)

Signature_____

Name : Zelalem Shiferaw
Signature:_____

Date and Place of submission, July 2005, Addis Ababa.

Acknowledgements

In connection with paper that is through now, I would like to take this opportunity to extend my thanks the people and institutions that have a lot to the complete of my work.

First of all would like to thank Dr. Tesfaye Korme, my academic advisor and initiator of the work presented here. Dr Tesfaye has established a research group with a very pleasant working atmosphere that made everybody works with appreciable high interest for the expected results.

Dr. Bekele Abebe and Dr. Asfawosson Asrat (both from department of earth science of Addis Ababa University),have gone through pains taking exercise of checking earlier version of the manuscript and have given important suggestions and valuable comments, which greatly helped in improving the quality of this thesis. However, any errors and imperfections that remain in the thesis are entirely my responsibility.

Ato Shiferaw Demissie, Manager gold and base metal project, National Mining Corporation (NMIC), reviewed this work. I wish to particularly express my gratitude to Ato Shiferaw (my Father) for willingly shared his Ethiopian and African Geology with me . His enthusiasm for my work has been a special motivation for me. He also has spent much effort in creating a large network of scientific and social contacts that I am glad I was able to use. My research benefited much from it.

I am grateful to the staff member of AAU, the Earth Sciences staff member, the department head and the department secretary for their continued assistance in areas where I needed their corporation and help. I am also grateful to the K & S Pvt. Company for their kindness providing me with field accommodation, vehicles and having covered some of my field expenses. I also like to thank the Ministry of Mines Petroleum Operation Department and the Ministry of Water Resource Development for allowing using company reports.

I am especially greatly indebted to my brother Abraham and his wife Mrs. Sara Pleasant for their kindness of letting me their computer. I am also grateful to my mother W/O Ayelech Amare for her wonderful advice, encouragement, endless support and love. A Special thank for all of my family members for being on my side when things seemed to work out wrong, I appreciate that a lot.

Wondesson has been my friend for two years, which I enjoyed both for social and scientific reasons. During my research I enjoyed the company of collogues of the earth science department and various other department and science faculty of Addis Ababa University. Addisu, Yodit and Sewit never hesitated to take endless coffee or tea breaks with long conversations about far-from scientific topics. I thank my friends for their interest during all these years and for all the fun that we have had (and are going to have of course).

At last but not least especial thank is for W/O Minasse for typing the entire thesis and for her rewarding friendship.

DIGITAL IMAGE PROCESSING, INTERPRETATION AND GIS DATA INTEGRATION.....19

3.1 Digital image processing..... 19

3.1.1 Image rectification……19

3.1.2 Contrast stretching…….22

3.1.3 Spatial filtering and edge enhancement…….23

3.1.4 Principal Component Analysis……..29

3.1.5 Band Combination…….31

3.2 GIS Technologies as an aid for Hydrocarbon Exploration……..31

LITHOLOGICAL MAPPING AND DESCRIPTION……...36

4.1 Digital Image Processing……...…..36

4.2. Field Mapping and Description……...42

4.2.1 Stratigraphy Section……...42

4.2.2 Lithologic Description……...45

STRUCTURAL MAPPING AND ANALYSIS…….54

5.1. Image Interpretation…… 54

5.1.1. NW-SE to WNW-ESE lineaments…….54

5.1.2. NE-SW lineaments…….57

5.1.3. E-W lineaments…….....59

5. 2. Field Structural Mapping…….60

CONCEPTUAL MODEL AND DISCUSSION…….....65

6.1 Structural and Stratigraphic interpretation…..... 65

6.2 Conceptual Model…….. 68

6.3 Implication To Petroleum Potential of the Blue Nile basin…… 71

CONCLUSION AND RECOMMENDATION……. 73

7.1 Conclusion……... 73

7.2 Recommendation…… 76

Reference..... 77

List of Table Page

Table 3.1 Image to Map Ground Control Points Table.....21

Table 3.2 Standard deviation.....29

Table 3.3 Eigenvalue.....29

Table 3.4 Correlation Matrix 29

Table 4.5 Covariance Matrix.....30

Table 3.6 Eigenvectors.....30

Table 5.1 Table presenting the measurement and characteristics
of dyke swarm studied during the field survey..... 62

3.9 A) And B) High-pass Kernel and E-W Lineaments respectively 28

Fig. 3.10 Principal Component Analysis of band 75432 A) PC1, PC2
and PC3 In RGB;B) Band 7543 PC1,PC2 and PC3 in RGB order
respectively..... 30

Fig. 3.11 Base map generated with the aid of GIS data Integration techniques..... 32

Fig. 3.12. SRTM of: A) Were Ilu and A DTM after draping
A geological map on the Grid B) Dera respectively..... 33

Fig. 3.13 Draped image..... 34

Fig 3.14 Drape image of the Principal component on the DEM..... 35

Fig. 4.1. A drape image of principal component of band 75432
of PC1, PC2, and PC3 in RGB order respectively over the DEM..... 37

Fig 4.2 The HIS drape over the DEM enhance the boundary of
the volcanics and Mesozoic sediment..... 39

Fig. 4.3. False color satellite imagery of band 754 in RGB order revealing
rills on the Antalo limestone at the flanks of the Weleka river valley..... 40

Fig.4.4 Digital Terrain Model Of the Dera Sub basin Area
depicting the geological unit After drape the DEM..... 41

Fig.4.5. Geological map of Dera Sub basin as interpreted from
satellite imagery. 42

Fig. 4.6 Major composite stratigraphic sections of the area..... 44

Fig. 4.7 Photograph showing the fossiliferous Antalo
Limestone bedding at the Jara stream..... 47

Fig. 4.8 The Left panel showing the Coarsing upward upper sandstone around
Wenchit stream and the right panel showing the Upper and
lower traps at Were Ilu.....49

Fig. 4.9 DEM of the central and west part of the study area.....50

Fig 4.10 profile section..... 51

Fig. 4.11 Geological Map of Were Ilu..... 52

Fig. 4.12 Lithological map of the study area..... 53

Fig. 5.1. Lineaments identified in the western escarpment of the
MER and Afar.....55

Fig. 5.2 NW-SE and NE-SW Lineament..... 56

Fig 5.3. NE-SW lineaments..... 58

Fig. 5.4. E-W running lineament in the study area..... 59

Fig. 5.5. Dikes close to Kabe village..... 62

Fig. 5.6 Digital Terrain Model of the study area, presenting
the general morphology, structure, lithology , and geology..... 64

Fig. 5.7 Structural map of the study area..... 65

Fig. 6.1. Conceptual model of the study area. 70

Fig. 6.2. Oil seepage along fractures at the Mechela river bed.....71

The general nature of the transport network is highly influenced by the distribution of the existing settlements and development areas. Asphalted roads largely radiate from Addis Ababa in all directions linking major towns and important economic areas. These include the Addis Ababa - Debre Birhan - Dessie road segment; Addis Ababa - Djibouti port, passing through major towns and from Addis Ababa - Gojam road segments. In addition, all weathered gravel and dirt roads branch from the main asphalted roads and, in terms of length, constitute the most important part of the whole transport network in the area. The third type of roads are rural roads. These are constructed by local people. Accessibility by rural roads is strongly affected by the seasonal distribution of rain. There are some interconnected foot paths that crosses the area . Off-the road access within the area is very difficult due to steep slopes that reaches up to 100% in some localities, bushes and scrub covers.

1.1.2 Drainage and physiography

The area is characterized by very undulating morphology. The Blue Nile, Beshilo, Weleka, Jema and Mugher Rivers and their affluences have deeply dissected the area forming very rugged terrain. The altitude in the area changes from about 1,100m west of WereIlu, 3,500m near Mehal Meda and falls to about 600m in the Afar floor. The average elevations ranges from 2,000 to 2,500m above sea level. Extensive faulting and major displacements along the Tertiary faults together with wide spread of volcanism; out pouring of basic lava & pyroclasts have at best determined the forms of landscape. The streams are characterized by sub-parallel and parallel drainage patterns indicating strong structural control.

1.1.3 Climate

The climate falls under warm sub tropical climatic conditions. It receives rainfall twice in a year, heavy precipitation (June to September) and light to moderate precipitation (February to march). In general, there is low infiltration rate and high rainfall. Mean annual rainfall gradually decreases towards the northeast and east. In central and north central part, the annual amount is moderate, about 1100 mm. There are some pockets where it amounts to over 2000 mm towards east. The mean annual rainfall is about 700 mm and less than 700 mm over most of the Afar region. The mean annual temperature varies from over 30^0C in the tropical lowlands to less than 10^0C at very high altitudes (EMA, 1988).

1.1.4 Land use and Land cover

Intensively cultivated land, bush land, shrub land, salt flats and rock exposures are the observed land use and land cover types in the study area. The intensively cultivated land includes areas of intensively cultivated peasant mixed agriculture as well as state farms. This land use and land cover type accounts for about 58% of the total area (EMA,1988). This includes land used for rain fed peasant and livestock grazing. The major areas of these types of land use are found on the highlands of Welo, Semien Shewa, Gojam and Gonder. In these regions it is estimated that about 70% of the land during the rainy season is under annual crops such as "Teff", Maize, Barely, Wheat, etc. The remaining 20% of mostly uncultivated land is used for grazing(UNFAO, 1984). The state farms are found mostly in the low land and account for about 10% of the total area (EMA, 1988) producing mainly Sugar cane, cotton, horticulture, etc.

Bush land and shrub lands accounts for about 20% of the study area and consist of intermediate zone humid and semiarid parts (EMA, 1988). They are usually intermixed with the wood land and moderately cultivated land regions. Pastoral livestock grazing and browsing and, in some parts, charcoal and incense harvesting are the main activities. The denser bush land occurs on the humid side of the region and consists of multi-storied bushes. In the west, low land bamboo bush land of pure stands are common. The shrub land occurs on the semi-arid side and often consists of patches of shrubs interspersed grass land with some scattered low trees.

The salt flats account for about 0.5% of the study area and are most common in the Danakil depression of Afar at Dubti and Hertale. In the study area bare rock exposure and sand surface account for about 21.5%. In the northeast, the region consists mostly of recent lava flows with scattered small patches of shrubs and scrub. Extensive fracturing occurred in the late Oligocene although caused an outpouring of volcanic products in the central and north western plateau. Mesozoic rocks are frequently observed in deep river cuts, particularly in the Abbay canyon, Beshilo, Mugger, Jemma and Weleka rivers.

1.2 Background to the problem

The energy crises affects all countries in the world. Considering the price scenarios, many countries in Africa initiated to explore various energy resources. Ethiopia is one of the countries that depend up on imported crude oil. To overcome this problem extensive and intensive studies will be carried out for the possible estimation of oil reserve.

Petroleum exploration in Ethiopia dates back to the 1930's. Since then, various oil companies have been actively engaged in exploration activities in different basins of Ethiopia. The demand for petroleum resources is constantly expanding from time to time to support the industrial economy. In order to attract investment in the field of petroleum and to achieve success in oil exploration, selection of effective exploration targets is an important step. Oil seep at Wereilu that appears along a fracture zone, is proved to have a source of a marine rock of the Jurassic age (MME, 1992). Presence of such an oil seep makes the Blue Nile Basin worthy of more attention to look for petroleum objectives.

Several studies were conducted on the study area, and reviewing of the available data reveals that many are dealing elaborately with the Stratigraphy and sedimentation history based on a regional and reconnaissance context. Few give account on surface lithological mapping based on ground surveys, drawn from observations along random traverses and extrapolations of insufficient work. Moreover, the region of difficult access remains unexplored. Most of the studies failed to account and to focused on major structural elements in the study area, the age relationships of the structural elements and their possible effect including the temporal and spatial relationships with the Blue Nile basin development. To overcome the problem and unravel the resource potential of the basin Remote sensing methods with conventional ground survey and GIS data integration techniques is unquestionable.

1.3 Previous Studies

The study area has been investigated by several researchers. Kernkel (1926), Stefanini (1933), Merla, G., and Minucci, E. (1938), Jepsen and Athearn (1961 a,b), Meral (1973) and Mohr (1962 and 1974) has been carried out a concise account of Geological work prior to 1975. Kovaiac, J. (1975), Getaneh Assefa (1987 and 1991), Zanettin et, al (1973, 1974, 1976 and 1978), Peccerillo and Bekele Megerssa (1992), Russo et al. (1994), Serawit and Tamrat

(1999, 1996 and 1995), Tamrat and Tibebe (1997), Wolela Ahmed (1997 and 2004), were amongst those who made a valuable contributions to understanding of the region.

The name Adigrat formation was originally named as Adigrat sandstone after Adigrat town in Tigray region (Blanford, 1870). The terminology "strata of Abbay" was first introduced by Kernel (1926) for Liassic to early Callovian Mesozoic formation; "Abbay Series" by Stefanini (1933); "shale–Gypsum unit" by Jepsen and Athearn (1961 and 1964) and Dainelli (1970); and "Abbay Beds" by Mohr (1962). Kazmin (1972 a,b), in the legend of the new geologic map of Ethiopia used the term Abay beds in the same manner as Mohr (1962). Getaneh Assefa (1987) has defined this unit as Gohatsion formation. The Antalo formation was first named by Blanford (1870) at the type locality as Antalo Limestone in Tigray region, and later described in detail by Mohr (1963), Kazmin (1972 and 1975) and Merla (1979).

The name Ambaradom formation was introduced by Blandford (1870); Merla and Muncil (1938); Mohr (1962), Merla et, al. (1973) to describe the upper sandstone unit of late Kimmeridgan to Cenomamian age. Getaneh Assefa (1991) classified the Upper sandstone as Mugger Mudstone and Debre Libanose sandstone in the Abay River basin. Raben et al. (1980) and Beicp (1985) elaborately discussed the Stratigraphy and history of sedimentation in the Abbay basin.

Zanettin et al. (1978) explained that the earliest volcanism is that of Ashangi formation erupted in a pre-Oligocene rift; then unconformably overlain by Aiba and Alaje Silicic volcanism of the Oligocene-Miocene stage. In the upper Oligocene to lower Miocene stage the volcanism changed to central type volcanism of strato and shield volcanoes of the Tarmaber formation. However, (Ukstins et al., 2002) investigated that, the oldest dated pre-rifted flood basalt unit in the northern sector of the western escarpment produce a plateau age of 30.90 $\pm$ 0.11 Ma. According to Wolfenden et al.,(2004) volcanism may have initiated between 32 and 33 Ma with the greatest eruption rates and volumes occurring ~31 to 28 Ma, and the total duration of the flood volcanism was at least 4 Ma. Previous age estimates (16-13 Ma) and a reported age of 13 Ma (Mohr, 1967 b) for the shield volcanoes are significantly older than the study provides by (Tadiwos Cherenet et al., 1998) which is 10 Ma for the northern western shield volcanoes.

The Integrated Master plan of the Abay basin by the Ministry of Water Resources is a complete compilation which gives a highlight about the basin (MWR, 1999). Others, like The Review of Hydrocarbon potential of the Blue Nile basin, By Wolela Ahemed (2004); Sedimentology, Diagenesis and hydrocarbon potential sandstone in hydrocarbon perspective Mesozoic rift basin, By Wolela Ahemed (1997); Sedimentary evolution of the Blue Nile basin by Russo et al., (1994); Petrological and geochemical variations associated with the transition from plateau Basalt to central volcanoes along the Mugher-termaber transect by Peccerillo and Bekele Megersa (1992); Report on oil seepage occurrence south of Dessie in the province of Wello. By Kovacik, J. (1975); Stratigraphy and sedimentation of the Gohatsion formation (Lias-Malm), Abay river basin by Getaneh Assefa (1987) and Lithostratigraphy and environment of deposition of late Triassic to early Cretaceous sequence of the central part of northwestern plateau, Ethiopia by Getaneh Assefa (1991) are the prominent works.

1.4 Objective

The principal aims of the study are classified into two groups, namely general objectives and specific objectives. Both are presented below:

General objectives:

1) To gain a better understanding of surface geology of the Blue Nile basin and to examine the occurrence of suitable stratigraphy and structural traps for petroleum accumulation as interpreted from satellite imagery data.

2) To produce georeferenced digital map and data base required for delineating preferable potential areas for subsequent detailed petroleum exploration.

3) To test if, and by how much, integration of remote sensing and digital terrain modeling (DTM), facilitate and give hint to further geophysical survey in the understanding of subsurface geology.

Specific objective:

1. Lithologic mapping at 1:500,000 scale from Landsat-ETM+ images

- Identification of major lithologic units;
- Delineation of sedimentary basins including those beneath the trap cover;
- Mapping Tertiary volcanic centers and edifices within the basin and along basin boundary;
- To study dyking in the basin and its relationship with basin tectonics;
- To establishing regional Stratigraphy for each basin; and
- To construct the profile geological section.

2. Structural mapping from Landsat-TM images and Digital Elevation Model
   - To outline structural elements of the basin from satellite data;
   - To identify faults defining the basin boundary;
   - To study faults crossing the basin belonging to the Ethiopian Rift System; and
   - To propose basin's structural model.

1.5 Materials and Methods

The results of this work were derived from the following sources:

- 12 Landsat ETM+ scene which are Scene number 170-52, 170-53, 170-54, 169-52, 169-53, 169-52, 168-52, 168-53, 168-53, 167-52, 167-53, 167-52 of ACQUISITION_DATE at September 23,1999.
- Topographic map of the study area with 1:250,000 scale.
- The Shuttle Radar Terrain Model (SRTM) of Ethiopia.
- Existing digital information supplied from the Ministry of water Resources and Ethio GIS.
- Previous reports and publications relevant to the study area.
- Field structural and lithological mapping.
- Computer and digitizing table.
- Different types of remote sensing and GIS software such as ENVI 3.5, Idrsi for Window 2.0, Microdem, 3 DEM, Map Info, Arc view GIS 3.2, Carta Linx, and Microsoft office application software are among those software used during data encoding, manipulation, modification, processing, interpretation, analysis and report writing.

First, the topographical maps were encoded to the computer by digitizing using Cartalinx software on a digitizing table. The Landsat ETM+ satellite imageries were georeferenced to Ellipsoid Clark 1880 projection System. Then a Mosaic of the images was generated followed by resizing to get the desired size of the study area. Georeferencing and image rectification process was done with the aid of selected ground control points (GCPs) from topographic maps and GPS survey in the field. The time consuming exercises were applying Mathematical transformation, various image processing and enhancement techniques on the raw Landsat ETM+ Scenes. These include contrast stretching, band rationing, spatial filtering, edge enhancement, Principal Component Analysis (PCA) and various band combinations to obtain false color composite image. This was made to increase the visual interpretation of image data, to highlight and extract very subtle information that would have been invisible by using conventional photo geologic interpretation techniques, by enhancing the spatial and multi spectral resolution of the image.

The enhanced image had been exported to Arc View GIS 3.2 software and information from the image such as lithological boundaries as polygon features, Drainage, faults and linear elements as polyline features, location of city, and oil seep as a point features generated as directly interpreted from the computer screen. The road network, drainage pattern, major cities and other necessarily data was also updated using the merged satellite image and from digital data obtained from Ministry of Water resource and Ethio GIS.

The topographic contours digitized and elevation points collected with the help of GPS were interpolated using the Triangulated Irregular Network (TIN) method to generate the Digital Elevation Model (DEM). In order to generate the Digital Terrain Model (DTM), the Landsat ETM+ images were draped over on the SRTM and DEM. These analyses were carried out both in MICRODEM and Arc view 3.2 GIS software using the 3D analyst module. Similarly the lithological and the structural map were draped over the TIN to produce digital models for better 3D visualization.

Field check had been accomplished with supervisors and utilizing available maps and GPS. In the field, important lithological and structural features were studied. The age relationships between the structural elements and their spatial and temporal relation with the lithological units, the orientation of the structures, attitudes of beds, (dip and strike measurement) were carefully studied and measured.

Finally, data merging followed by various multi-disciplinary thematic layer data analysis and interpretation procedures were done to achieve the necessary target. The general approach is listed in the following flowchart below (Fig 1.2).

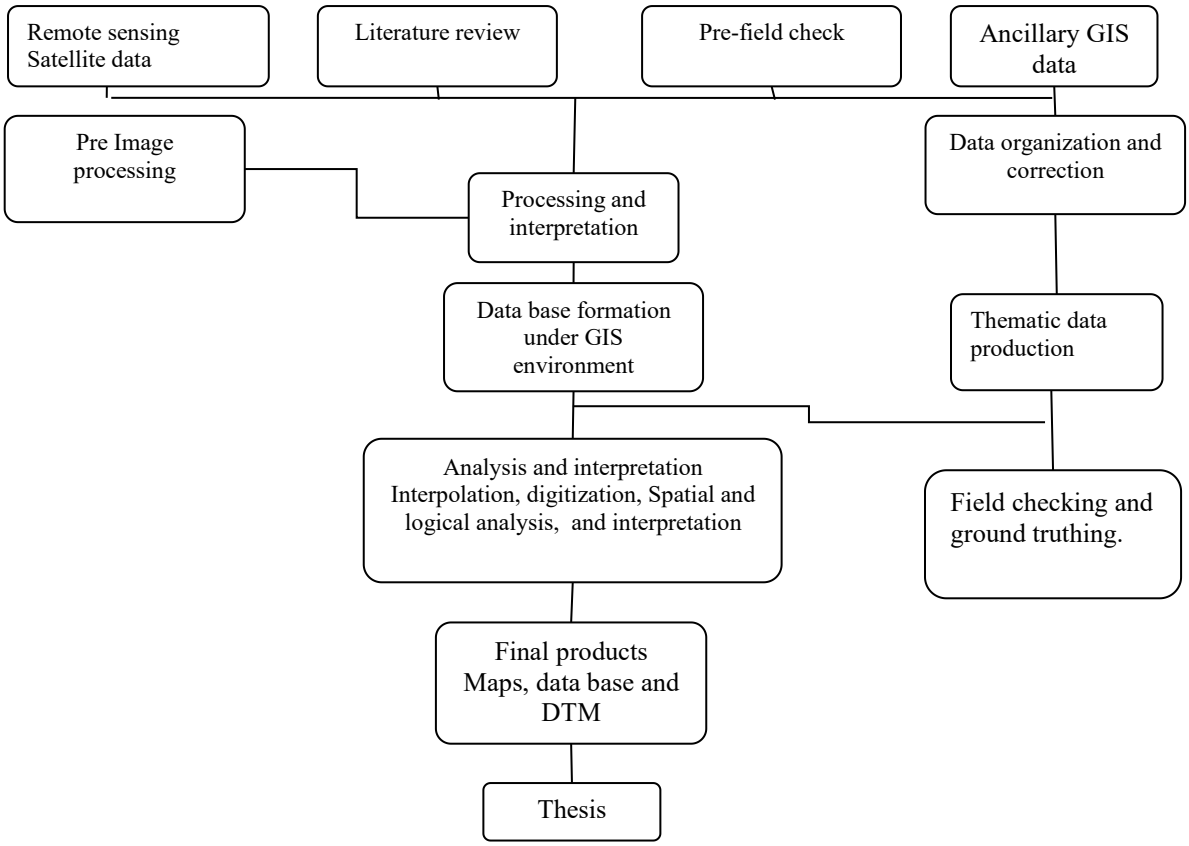

Fig.1.2. Methodology flow chart.

1.6 Structure of the Thesis

The thesis presented here has eight Seven. The first chapter gives the background to the problem; the objective and scope of the works and relevant literature reviewed on the subject matter. In this chapter the general over view of the study area including , physiographic and drainage pattern, the climatic variations of the area, landuse and land cover and its accessibility has discussed briefly. The thesis would summarized the general geological setting, Major formations and basin evolution in chapter two. The regional geology and discussion has limited to the early Triassic to Liassic Adigrat sandstone formation to younger

rocks of the blue Nile basin. Chapter three focused on the processing stages that outlines in the proposed methodology The crucial steps in this chapter were digital image processing methods to enhance the surface geology interpretation. In chapter four, distinction has been made on the co-registered image data and DEM data among the basement complex the Mesozoic sedimentary sequence and the tertiary volcanic cover. Chapter five addresses the spatial and temporal relationships between lineaments and faults identified in the study area as interpreted visually from the enhanced Landsat ETM+, the DTM and conventional field survey. Chapter six presented, a conceptual model which shows evolution of the Blue Nile basin, the sedimentation process and the possible effect of the structures in basin development with six developmental stages. The discussion, in addition explained important implications to petroleum potential of the Blue Nile basin, besides the assent of the oil seepage at the floor of the Mechela river. The thesis ends with conclusion and more general discussion of the obtained results and their implications, as well as some possible direction of further research.

CHAPTER 2

REGIONAL GEOLOGICAL SETTING AND BASIN EVOLUTION

2.1 Regional Geological Setting

Rabben et al., (1979) and Beicip (1985) elaborately discuss the stratigraphy and history of sedimentation in the Abay basin. Based only on surface geology and previous studies, the stratigraphy of the Blue Nile basin is assumed to comprise a crystalline basement, Paleozoic sediments, Adigrat sandstone, Gohatsion formation, Antalo limestone, Ambaradom sandstone and Tertiary volcanism (Fig. 2.1). The Precambrian and Paleozoic sediments are not significantly important to the subject of this paper. The stratigraphic sequence to be reviewed will be limited to Adigrat sandstone (Triassic-Liassic) and younger. As the Triassic and Jurassic sediments contain important source & reservoir rocks in the Blue Nile (Wolela Ahmed, 2004).

2.1.1 Triassic to Liassic Adigrat sandstone formation

The Adigrat sandstone previously known as lower sandstone unit generally overlies the basement, but in some place it overlies unconformably the Paleozoic continental sediments (Russo et al., 1994). The Adigrat sandstone formation, in the Blue Nile basin attains a thickness of 100m in the Jemma river section (Mohr, 1962); 120m in Arjo area (Gethaneh Assefa, 1987); 450m in the Dejen - Gohatsion section (Wolela Ahmed,1994); 800m in Amuru - Jarty; 450m in Gindeberet - Jeldu (Tamrat and Tibebe, 1997); and 150m in Ejere area (Serawit and Tamrat, 1994).

According to (Bosselini et al., 1989), large-scale down warping occurred in Triassic to Jurassic time, resulting in the deposition of the alluvial fan, fluviatile, lacustrine or swampy facies of this unit in the Blue Nile Basin (Wolela Ahmed, 1997, 2004).

2.1.5 The Shale Gypsum Unit

It is equivalent to the Gohatsion formation (Getaneh, 1981) the Abbai beds (Mohr, 1962), Abbai strata (Kernel, 1926) in the Blue Nile basin; and to the Middle Hamanlei formation (Wolela Ahmed, 2004) in the Ogaden basin. This unit attains a thickness of 290m in the Jema river section (Serawit and Tamrat, 1996), 300m in the Mugher area, 150m in Gendeberet Jeldu area (Tamrat and Tibebe, 1997).

The unit is represented in the lower part by alternating dolostones and shales. The dolostones are greenish, gray or brown, with flute casts at the base of beds, ripples and flaser bedding on the lower part, and parallel lamination at the top (Russo et al., 1994).

The middle part of the unit is characterized by several cycles of non - fossiliferous shale, marlstone or dolostone with few scattered small bivalves, fine-grained, cross laminated sandstone and thick beds of gypsum (Russo et al., 1994). The upper part consists of gypsum and terrigenous materials composed of fine grained sandstone and siltstone. Generally the siltstone is observed almost at the top of this last part especially at the Mugher valley (Tamrat and Tibebe, 1997).

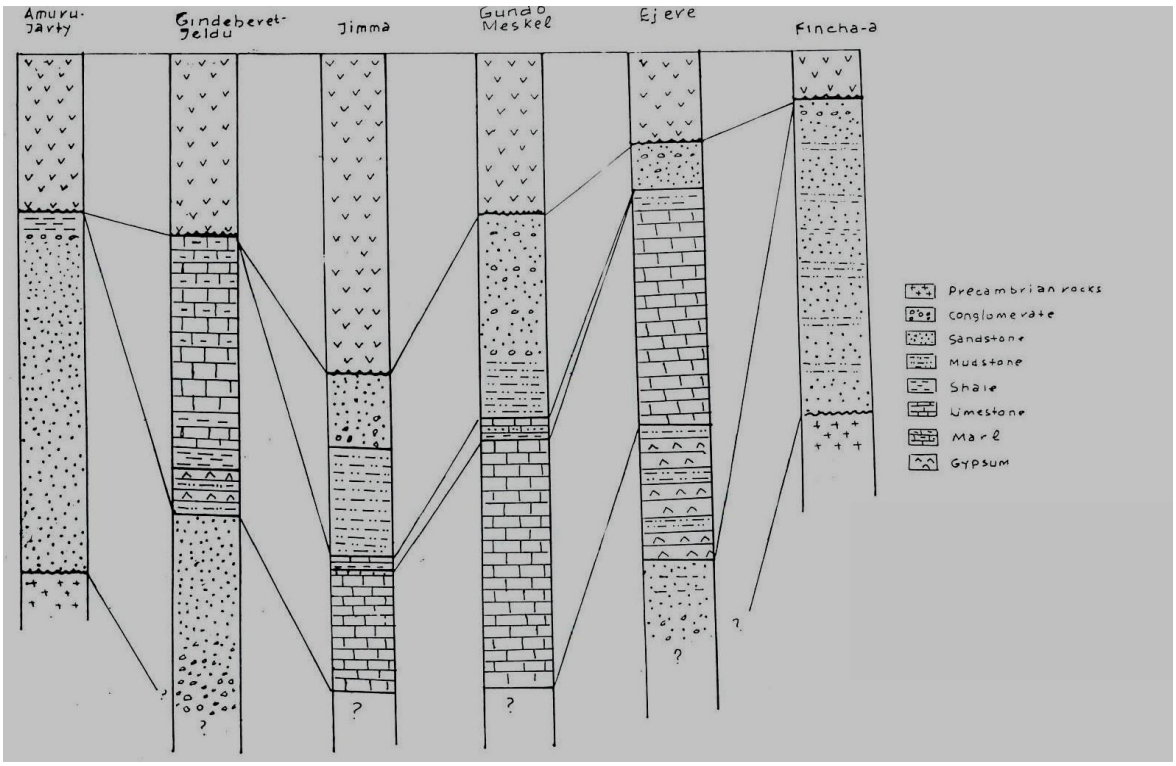

Fig.2.1. Stratigraphic correlation of different unit in the Blue Nile Basin (after, Wolela Ahmed, 2004)

2.1.5 The Antalo limestone

The Gohatsion formation described previously, grades upward in to scarcely fossiliferous and burrowed mudstone, and then in to an oolitic limestone rich in corals, stromatoporoids,

bivalves gastropods, echinoids, foraminifers and ostracods, (Russo et al., 1994). The Antalo limestone is exposed in the Jema River, Dejen-Gohatshion, Gendeberet Jeldu, Debre Libanoes and Mugher. It is composed of gray to yellowish gray, white dull-white to light yellow marly limestone, skeletal packstone - wackstone, oolitic - skeletal packstone and shales (Wolela Ahmed, 2004). The lower part of this formation is represented by fossiliferous marlstones, which vertically pass up in to oolitic limestone. 190 meter thick marly limestones silty limestone and oolitic limestone, which contain corals, bivalves gastropods, echinodis and foraminifera represent the middle and the upper part of the Antalo limestone. A transitional facies is developed between the Antalo limestone and the Mugher mudstone formation. The transitional interval is 10-30 meter thick in the Debre Libanoes - Lemi area, and it consist of shale sandstone, silty and sandy limestone, dolostone and evaporite (Wolela Ahmed, 2004). According to Wolela, the transitional zone in the Jema river valley is marked by alternating sequences of 15m thick red clay and 8m thick calcareous sandstone and limestone.

2.1.4 The Upper sandstone

Blanford (1869); (Merla and Muncil, 1938); (Mohr, 1962) and (Merla et al., 1973) described the Mugher mudstone and Debre Libanoes formation as Ambaradom in northern Ethiopia. (Getaneh Assefa, 1991) classified the upper sandstone formation as Mugher mudstone and the Debre Libanoes sandstone.

2.1.4.1 The Mugher mudstone

The name of the formation is derived from the Mugher river. It comprises mainly mudstone and sandstone with gypsum and dolomite. It is exposed in the Mugher valley, Zega Wedom, Wencit, Wesena Adabai and Jemma river section (Russo et al., 1994; Getaneh Assefa 1991). The lower part is consists of dolomite and shale, where as the upper part is constituted of a 240m thick mudstone. The gypsum, bluish gray to white in color, occurring in layers ranging from 4mm to 1.5m in thickness lenses of dolomitize in micrite and shale are closely associated with it. The gypsum occurs as vugs and vein fillings in the dolomicrite and shale (Getaneh Assefa, 1991). Dolomitic algal stromatolites are common. Small-scale mud cracks and birds eyes filled with spray calcite. The shale is laminated and contains a few thin laminae and vein-lets of gypsum (Getaneh Assefa, 1991). The upper part consists of interbeded mudstone, siltstone and fine to medium - grained sandstone. The mudstone shows massive bedding, thin laminae and ripple lamination.

A discontinuous thin bed of lignite and carbonaceous siltstone is thinly bedded and commonly contains cross - lamination and convolute bedding. The sandstone consists of fining upward sequences and thick massive beds (Getaneh Assefa, 1991).

2.1.4.2 The Debre Libanose formation

This unit is widely exposed in the valley of the Zega Wodem River and it is tributaries. It consists of sandstone, pebbly sandstone and local lenses of conglomerate and clay stone. It conformably overlies the Mugher mudstone formation and is, in turn overlain by trap volcanoes. The sandstone attains a thickness of 280m near Lemi; 200m in the Jema River; 230m in Debre Libanoes; 312m in the Mugher River section and pinch out towards the Abbay River Gorge (Wolela Ahmed, 2004). The main sedimentary structures of the sandstone are large and small-scale planar tabular and asymmetrical through cross-beds, convolute beds, flat beds, scoured and channel surface and massive beds. Some fining upward trends occur from medium- to fine grained sandstone up to laminated clay stones (Getaneh Assefa, 1991). This unit is interpreted as a deposit of sandy-braided rivers on a broad alluvial plan (Getaneh Assefa, 1991).

2.1.5 Tertiary and Quaternary Volcanoes

Mohr (1962) divided the Cenozoic volcanic rock of Ethiopia into Trap Series and Aden Series and explained the trap series for the flood basalts of the Ethiopian plateau and Aden series for the volcanics of the rift valley. Blanford (1869) described that the evolution of the Ethiopia - Yemen swells and it transacting rift valley during the Cenozoic has accompanied by profuse volcanism and subordinate intrusive activity. Tadiows Cherenet et al., (1998) described that the plateau portion of the transition zone exposed the upper stages of extensive and voluminous flood basalts collectively called Trap series.

The lavas are dominantly alkali olivine basalts with intercalation of felsic lava and pyroclastics (Gregnanin 1969; Le Bas and Mohr, 1970). They were supplied chiefly from fissures now preserved as dikes along the warped rift margins (Mohr, 1971). A major unconformity exists within the flood basalts of the east central Ethiopian plateau (Mohr & Rogers, 1966; Zanettin and Justin-Visentin, 1973). Zanettin and others (1978) explained that the earliest volcanism is that of Ashangi formation erupted in Pre-Oligocene rift; then uplifting and erosion had formed Ashangi peneplain which was later uniformly fractured and flooded by Aiba flood basalt and Alaje fissural silicic volcanism of the Oligocene - Miocene stage. In upper Oligocene to lower Miocene stage the volcanism changed to central type volcanism of strato and shield volcanoes of the Tarmaber formation, which cover older volcanics by edifices of different size. However, (Ukstins et al., 2002) investigated that, the oldest dated pre-rifted flood basalt unit in the northern sector of the western escarpment produce a plateau age of 30.90 $\pm$ 0.11 Ma. According to Wolfenden et al.,(2004) volcanism may have initiated between 32 and 33 Ma with the greatest eruption rates and volumes occurring ~31 to 28 Ma, and the total duration of the flood volcanism was at least 4 MYr. Previous age estimates (16-13 Ma) and a reported age of 13 Ma (Mohr, 1967 b; Kazmin et al., 1980) for the shield volcanoes are significantly older than the study provides by (Tadiows Cherenet et al., 1998) which is 10 Ma for the northern western shield volcanoes.

2.1.5.1 The Lower Trap

The Lower Trap represents the oldest fissural flood basalt volcanism of the Blue Nile basin. They are strongly weathered, highly fractured, tilted basalts interbeded with minor tuff, and are mainly exposed along deep valleys of major streams and rivers. It is equivalent to Ashangi formation and consists of predominantly mildy alkaline basalts with interbeded pyroclastics and rare rhyolites (Ethio Geo-Technical Services, 2000). It is commonly injected by dolorite sills and dikes. The upper part of the Ashangi formation consists of tuft and interbeded lacustrine deposit with lignite seams. It is forming 200-1000m thick sequence over the Mesozoic sedimentary sequence.

It forms the "Kola" plains and the steep walls of Chilga and Gunda Rivers and attains about 500m of thickness in the Ajbar-Saynt that consists of degraded olivine basalts with tuff interbeds. In the Yeshum valley at Mekane Selam, the Ashangi formation attains about 550m thick sequence that is highly weathered with minor tuff beds, representing about 250m thick sequence of strongly weathered basalt in Were Ilu (Ethio Geo-Technical Services, 2000).

2.1.5.2 The Upper Trap

The Aiba basalts represent the second major pulses of fissural basalt volcanism in the Blue Nile basin. The Amba Aiba formation rests uncomfortably over Ashangi formation. At places where Ashangi formation is missing, it overlies Debre Libanoes sandstone formation. It is represented by the Upper Trap in this thesis.

It represents aphyric columnar basalts with rare intercalation of tuff. The basalt flows are mainly of a distinctive tholeiitic nature with transitions to mildy alkaline varieties. The thickness of the formation in the study area ranges from 200m to 500m, however, the common thickness is 200m. The formation consists up to 6 lava flows that are characterized by open to tight columnar jointing indicating variable stress release during emplacement (Ethio Geo-Technical Services, 2000). It outcrops in the northern and southern parts of Ajbar-Syant attaining 240-420m thick sequence over Ashangi formation about 300m thick and forms cliff with stream beds in the Mekane Selam has cliff forming morphology about 250m thick sequence with columnar joint spacing varies from close to wide observed at Wegeltena. Amba Aiba formation is wide spread in the Werilu area. It occurs either under thin cover of Tarmaber of Alaje formations or as streamed rocks. It under lies the drainage basin of at Atari and Tumele streams. The basalt flows are aphyric columnar joint spacey varies from close to wide observed at Wegeltena. Amba Aiba formation is wide spread in the Were Ilu area. The unit attains about 200m thickness over Ashangi formation in Were Ilu area. However, in Rema it has a total thickness of about 200m over Debre Libanoes sandstone (Ethio Geo-Technical Services, 2000).

The Alajae formation mainly consists of aphyric flood basalts associated with alkaline to peralkaline rhyolites ignimbrites alkaline and alkaline trachy rholylites; also considered as the lower Trap in this work. The basalts are tholeiitic of transitional type. It occur conformably overlying Amba Aiba formation in the Blue Nile basin but in some places for example in Kassem Gorge and Mugher canyon it directly overlies on the Mesozoic sediments. It's thickness varies from 300 to 450m in the northern part to less than 100m in the southern part of the Blue Nile basin. The Alajae formation contains basalts transitional to tholeiitic in nature and an increase in alkalinity is observed in the younger members of the formation (Ethio Geo-Technical Services, 2000).

2.1.5.3 The Shield Volcanoes

The chief extensive out crops exposed in the Blue Nile Basin is the Tarmaber Formation now and then called the shield volcanoes in this work. It overlies unconformably the older volcanic centers and elevated plains. It thins out to less than 100m in the northern, southern and western parts of the area. Tarmaber formation is made of often-lenticular basalts with large amount of flows and often interbeded with typical red paleosoils (Ethio Geo-Technical Services, 2000).

Zanettin et al.(1974a) recognize very felsic basalts, fine grain, basalts with large plagiocalse phenocerysts, zeoltised basalts, phenolities, alkaline-trachytes trachy phenolites and subordinate alkaline and peraelkaline rhyolites.Occerence in the Blue Nile Basin reported at Ambo Sirro Hill, In Kutaber, adjacent to north eastern, at Gugftu spring in Gimba plain, Sayint-Ajibar, Werilu especially at Jegola and Kuntab rivers and Tenta market place (Ethio Geo-Technical Services, 2000).

2.2 Basin Evolution.

The break-up of Gondwanaland, which began in the late Paleozoic and persisted up to Jurassic time, produced aulacogen-like basins around the borders of the mega continent. The Blue Nile basin of Ethiopia is one of the northern most failed arms of these trough systems (Russo et al, 1994). The sedimentary evolution of the Blue Nile River succession appears to have been controlled by the following geodynamics stages.

1) Peneplain stages: It corresponds to the Pan-African metamorphic peneplain, probably covered with a veneer of pediment sediments (Russo et al., 1994).

2) Intracontinental rift stage: It is equivalent to the early stage of Karoo rifting. The break-up of eastern Gondwanaland through transtensional stress in a NW-SE direction along the African continent produced graben and half-grabens and a number of rift basins stretching from South Africa to eastern Ethiopia (Bosselini et al., 1989). The early sedimentation of the karoo rift in eastern Ethiopia commenced with the deposition of the alluvial fan deposits of the calub sandstone formation, the lacustrine Bokh shale formation, and the fluvitile Gumburo sandstone formation (Wolela Ahmed, 2004).

3) Post rifting stage: This stage corresponds to the deposition of the Adigrat sandstone formation (Russo et, al., 2004).

    a) Early Flooding: Corresponds to the early transgression by the sea and flooding of the craton, due to the rifting and thermal subsidence of the East African continental margin. The thermal subsidence and eustatic sea level changes caused the southern arm of Tethys to spread westward over the Arabo-Ethiopian shield (Bosselini et al., 1989). The beginning of the marine transgression is documented by the deposition of the Gohatsion formation in the Blue Nile basin (Getaneh Assefa, 1987).

    b) Drowing of craton: A major transgression, dated as Callovian-Early Oxfordian over the entire East Africa, is documented by the Antalo Limestone (Russo et al., 1994). This is probably related to the drifting phase and major sea level high stands.

    c) At the end of the Jurassic time, the sea began to withdraw from the Horn of Africa probably as result of the intraplate effect of the separation of South America and Africa (Bosellini et al., 1989). The subsequent deposition was characterized by restricted marine evaporite sediments in Somalia and southern Ethiopia, and by lagoonal, sabkha sediments and continental sandstones in the Abay River and northern Ethiopia.

4) There were successive events of uplifting and subsidence from late Creataceous to Lower Miocene. This Tectonic activity created graben and half-graben, in which Tertiary sedimentation took place. These sediments are mostly covered by late- stage volcanic activity. According to Wolfenden et al.(2004)) the earliest volcanism may have initiated between 32 and 33 Ma with the greatest eruption rates and volumes occurring ~31 to 28 Ma, and the total duration of the flood volcanism was at least 4 Ma. Wolfenden et al., (2004) as well as indicates the first silicic ignimbrite in the study area was erupted at 30.2 Ma and bimodal flood volcanism continued until 25.3 Ma. In upper Oligocene to lower

Miocene stage the volcanism changed to central type volcanism of strato and shield volcanoes of the Tarmaber formation, which cover older volcanics by edifices of different size (Zanettin et al., 1978). However, (Cherenet Tadiwos et al., 1998) indicates it is 10 Ma for the northern western shield volcanoes.

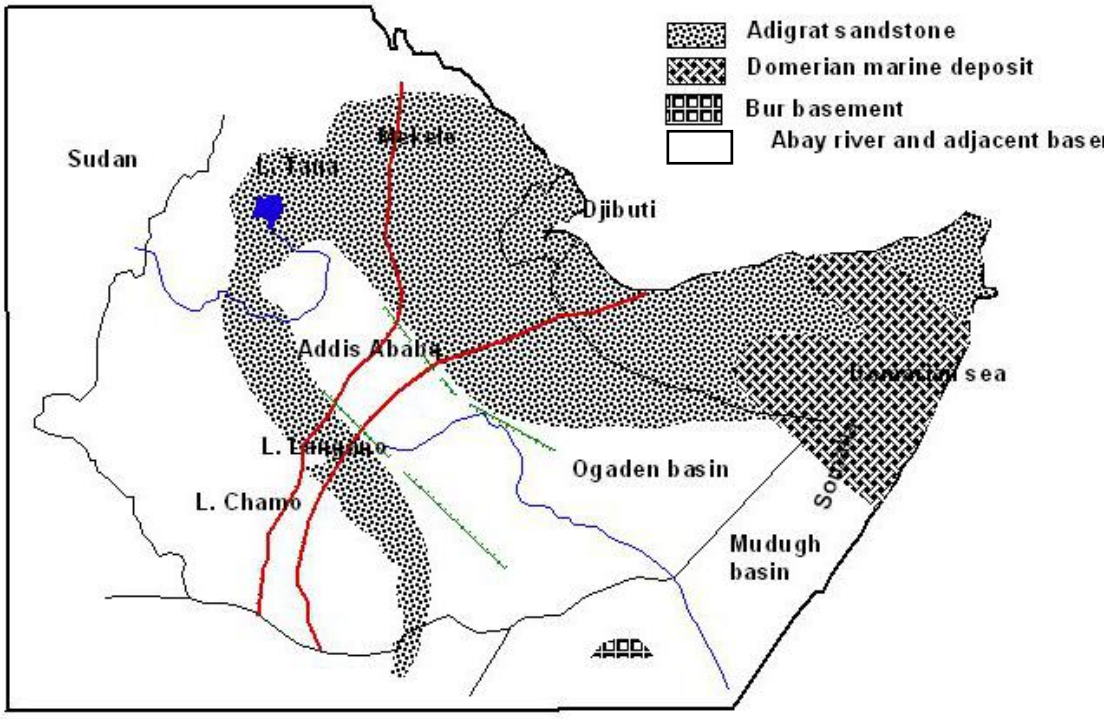

Fig. 2.2. Paleogeography map of Ethiopia and Somalia in the early Middle Jurassic (After Bosselini, 1989).

CHAPTER 3

Digital image Processing, Interpretation and GIS data Integration

To extract various types of lithology and complex tectonic setting of the study area, digital image processing and mathematical transformation have been performed on LANDSAT ETM+. The technique has produced valuable products in comparison to the raw data. Most of the digital technique depends on the radiance properties of images and uses special algorithms designed to perform various types of spectral analysis. A number of geological features has been identified and separated into map products such as rock type, lineaments, faults, and others with the aid of GIS data integration techniques. In this chapter, suitable procedure of using remote sensing and GIS techniques for geological studies has been conducted.

3.1 Digital image processing

3.1.1 Image rectification

Image rectification is one of the major processing tasks which handle the corrections of errors frequently observed in the geometry and radiometry of digital images. The types of errors and their major causes which are frequently observed on the raw satellite imagery have already been discussed elsewhere (Drury, 1993). Image rectifications have been applied to satellite images which are used in mapping the lithology and structure of the study area. The absolute geometric correction process involves identification of image coordinates of several clearly discernible points, called Ground Control Points (GCP) (Fig. 3.1, the red points in the image), in the distorted image and matching them to their true positions in geographic coordinates. 22 true GCPs were collected from 1: 250,000 topographic maps and Global Positioning System (GPS) during the field survey (Table 3.1). The coordinates help to georeference the digital image to Ellipsoid Clark 1880 projection system that is Universal Transversal Mecator (UTM) coordinate system, Datum Adindan and Zone 37 N (Fig, 3.2). The geometric correction applied to the digital images or bands involved linear affine coordinate transformation which has used bilinear spatial interpretation for the recalculation of pixel values at their new geographic position. The accuracy of the geometric corrections has been assessed with the Root Mean Square (RMS) error assessment technique which has shown error value of 0.94.

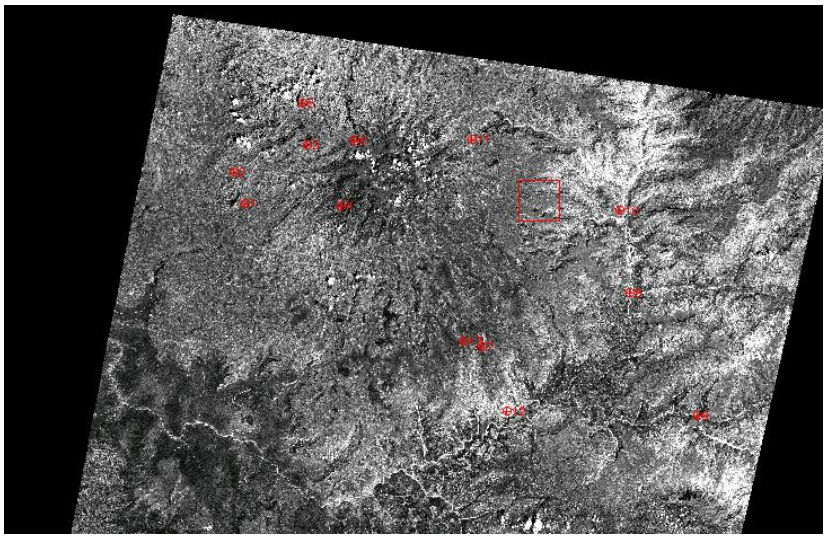

Fig. 3.1. Selected ground control points.

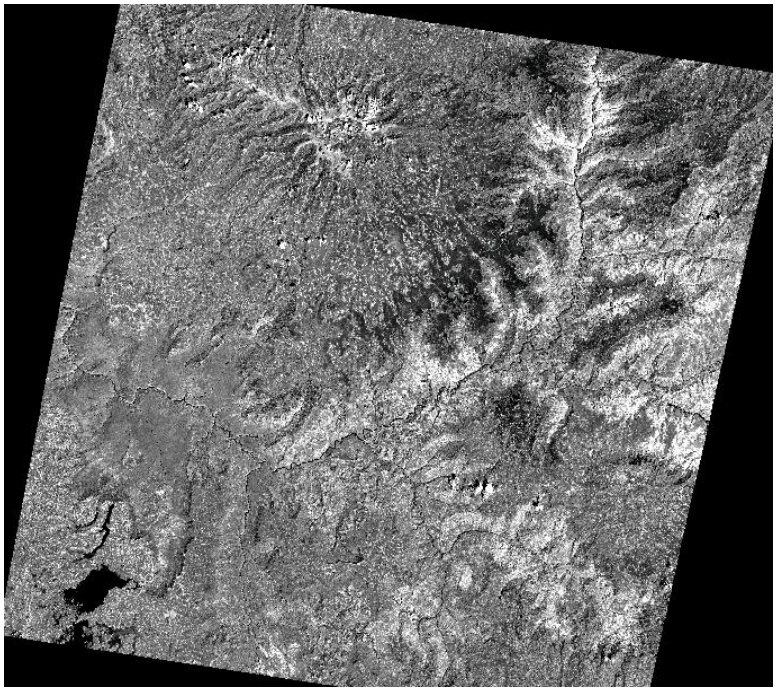

Fig. 3.2. Geographical corrected image

Groungd Control Points (GCPs)								
Map X	**Map Y**	**Predict X**	**Predict Y**	**Error X**	**Error Y**	**RMS Error X**	**RMS Error Y**	**RMS Error (X,Y)**
170107.43	996113.7	1655.1	2704	1655.9	2704.68	0.79	0.68	1.04
280125.11	995362.22	1654.5	2370	1654.5	2369.76	-0.02	-0.24	0.24
390078.59	994911.79	1653	2034.3	1652.2	2035.04	-0.84	0.74	1.12
500000	994761.72	1649.2	1699.4	1648.9	1700.43	-0.28	1.03	1.07
609921.41	994911.79	1644.6	1365.1	1644.8	1365.83	0.17	0.73	0.74
719874.89	995362.22	1638.6	1029.3	1639.7	1031.13	1.09	1.83	2.13
940006.64	997167.34	1628.5	362.5	1626.8	361.09	-1.71	-1.41	2.22
937315.65	1218785.9	953.9	378.1	950.95	376.33	-2.95	-1.77	3.43
827877.82	1217508.7	957.5	708.8	958.54	709.26	1.04	0.46	1.14
609251.16	1216051.6	969.5	1373.6	970.37	1374.38	0.87	0.78	1.17
390748.84	1216051.6	977.4	2039.4	977.74	2039.17	0.34	-0.23	0.41
172122.18	1217508.7	982.4	2705.4	980.68	2704.38	-1.72	-1.02	2
171064.93	1106808.7	1318.7	2704.8	1318.3	2704.68	-0.41	-0.12	0.43
280762.64	1105977	1317.6	2370.6	1317.1	2370.82	-0.47	0.22	0.52
500000	1105312.3	1312	1702.7	1311.8	1703.6	-0.23	0.9	0.93
719237.36	1105977	1301.9	1034.2	1302.4	1036.42	0.46	2.22	2.27
938727.76	1107974.9	1292.5	370.3	1288.9	368.51	-3.63	-1.79	4.04
935770.73	1329600.8	612.7	384.8	613.03	384.56	0.33	-0.24	0.41
826721.12	1328214	619	715	620.95	716.21	1.95	1.21	2.29
717763.2	1327224.8	626.5	1047	627.65	1047.6	1.15	0.6	1.29
608866.34	1326631.9	633	1379	633.14	1378.81	0.14	-0.19	0.23
500000	1326434.4	636.8	1711.5	637.42	1709.94	0.62	-1.56	1.68

Total RMS Error: 0.949212

Table 3.1. Image to map Ground Control Points.

3.1.2 Contrast stretching

The starting point is to point out that radiances measured by the sensors variation in intensity. The computer screen of a digital image processor, expresses radiances measured by the sensor in a range of intensity values. The values are restated as digital numbers (DNs) that consist of equal increments over a range from 0 (black) to 255 (maximum intensity), (Drury, 1993). The simplest manipulation of these DNs is to increase or decrease the range of DNs present and assign this new range, the gray levels available within the display screen for better visual interpretation. This is called contrast stretching.

It is one of the most widely used image enhancement techniques in lithological mapping. The original input brightness is expanded to make use of the total sensitivity of the output device. When the original input bands are displayed in CRT before contrast stretching is performed, less than one half of the full range of brightness values could be only displayed (Fig. 3.4). In these bands, brightness value between 9 to 149 and 122 to 255 are not to be used (Figs.3.3 and 3.5). It is difficult to visually interpret such an image. The upper panel is a raw (untstretched) histogram of LANDSAT ETM+. A Gaussian stretch and its raw image deploy next to and a Gausian stretch of histogram showing increasing DN values in the lower of the imagery.

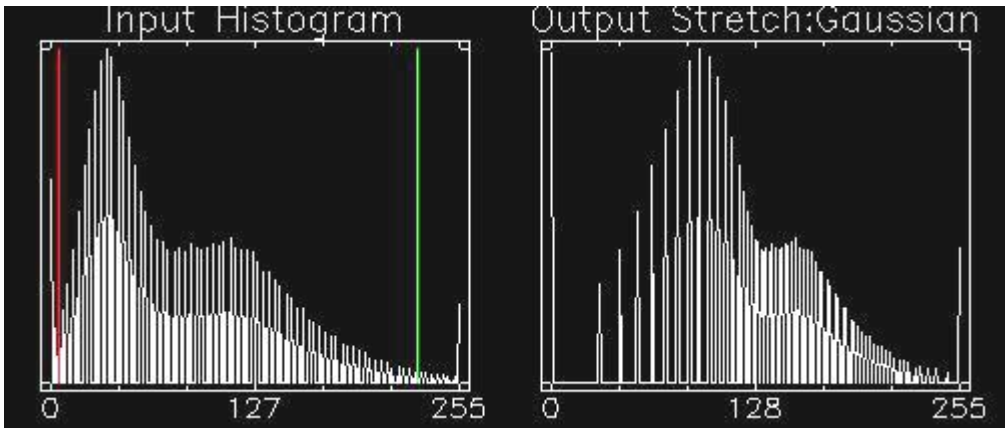

Fig. 3.3. Histogram of unstretched raw band 5 left from red to green and right the gausian stretched.

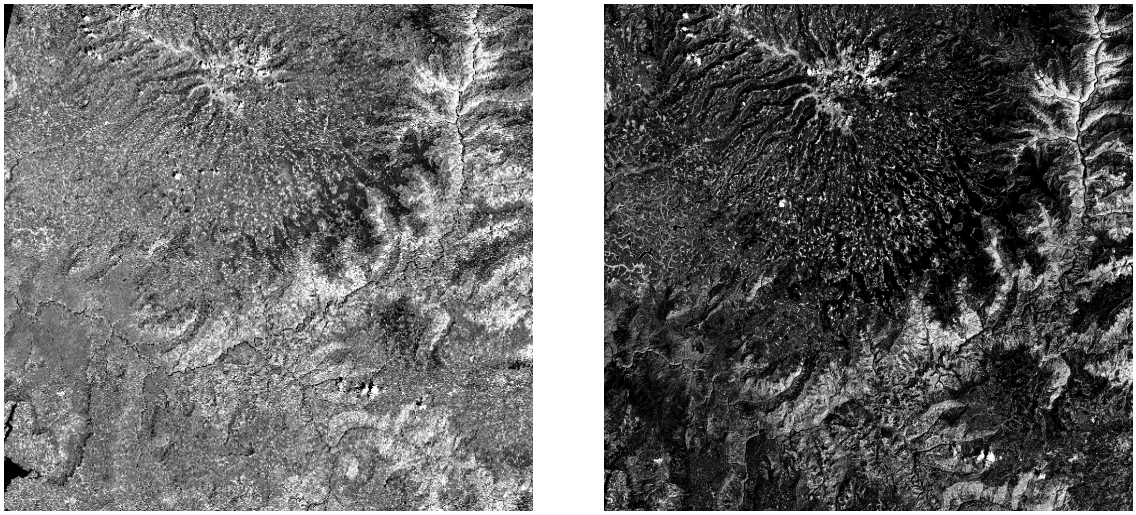

Fig. 3.4. LANDSAT ETM+ band 5 left Unstretched and right stretched.

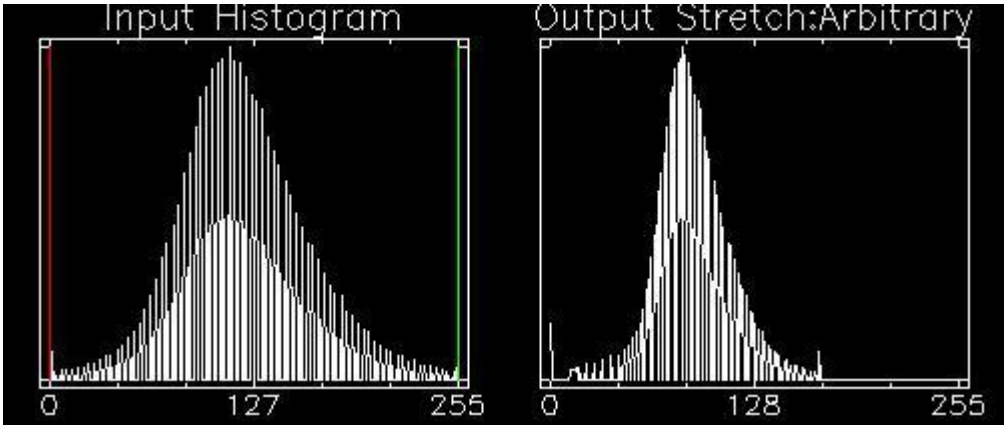

Fig. 3.5. Histogram of stretched LANDSAT ETM+ band 5 right input Image.

3.1.3 Spatial filtering and edge enhancements

Spatial filtering and edge enhancement are mathematical convolution methods that act on neighboring pixels of digital image. They highlight linear features such as faults, joints, dykes and regional lineaments and major lithologic boundaries and facies limits. Directional filters are high-pass spatial filter applied on digital images to increase the visibility of linear features such as faults in specific directions.

When Landsat image first became available, the most pleased and surprised persons were geologists, who had initially felt that the imagery would be too small-scale to be of assistance to them. In actuality, the smallness of the scale helped, displaying major geologic structure that had been previously unknown. The standard techniques include an initial stage of image processing using high-pass and directional filters that detect edge in the preferred orientation. It consists of selectively enhancing the high-, Medium- and low-frequency variations of digital number (DN) in an image.

Emphasizing the spatial frequency component of an image can further enhance obscure features or pick out features of interest hidden within a cluttered, highly textured, original image (Drury, 1993). This may be done by masking out part of the Fourier transform of the image, or more simply by passing rectangular kernels filter over the image. A mathematical technique for separating an image into its various spatial frequency component is Fourier analysis (Lillisand and Kifer, 2000). According to Lillisand and Kifer (2000), a high-pass and directional filter is a type of Fourier transform that enable high frequencies, amplitude and direction of an image to be emphasized by algorithm known as filters. A common filtering procedure involves moving a window of a few pixels in dimension (e.g. 3X3, 5X5, etc.) over each pixel in the image, applying a mathematical calculation using the pixel values under those windows, and replacing the central pixel with the new value. The window is over along both the row and column dimensions one pixel at a time and the calculations is repeated until the entire image has been filtered and new enhanced image has been generated (Figs. 3.6b, 3.7b, 3.8b and 3.9 b).

The following high pass kernels are used to enhance the structures in the study area(Figs. 3.6a, 3.7a, 3.8a and 3.9a). The low pass filtering including smoothing techniques can remove a noise and enhance the lithological units, but for non linear-high filter are not so useful for lithological distinguish but can enhance some geomorphological unit such as valley fill, erosional features, etc.

-1.414214	-0.707107	0.000000
-0.707107	0.000000	0.707107
0.000000	0.707107	1.414214

A)

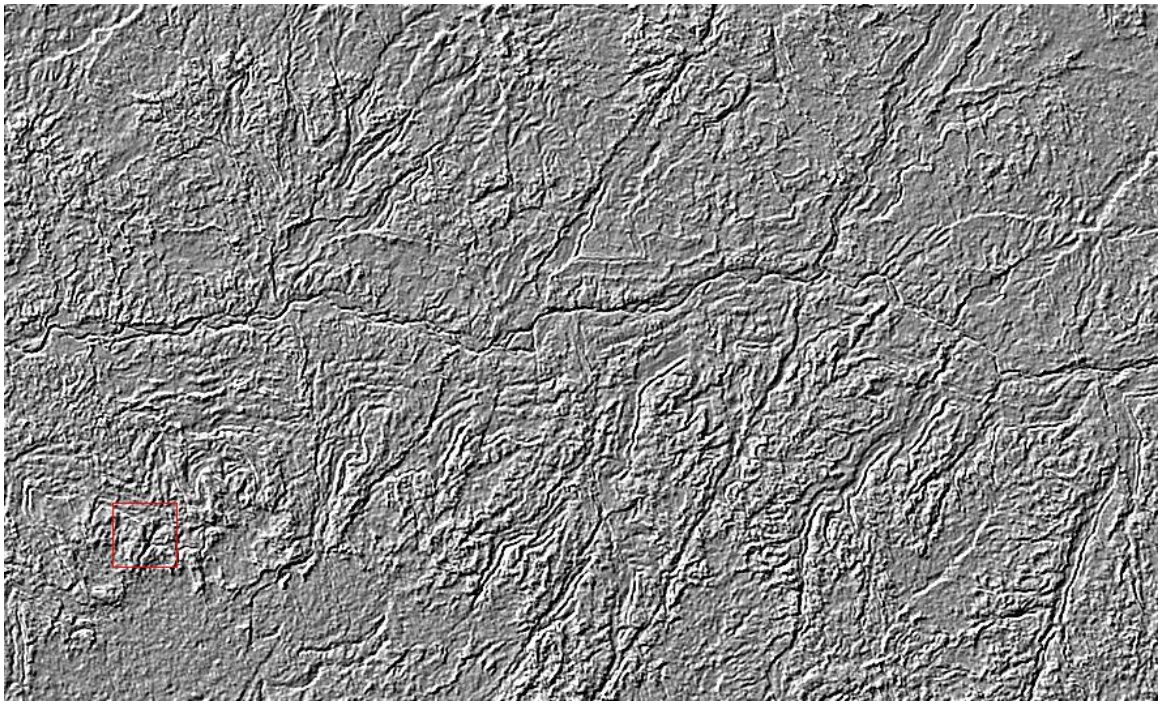

B)

Fig 3.6. (A) High-pass kernel used to enhance Image in the preferred orientation, (B) NE-SW lineaments observed after the high-pass filtering.

1.392729	0.573577	0.245575
0.819152	0.000000	0.819152
0.245575	0.573577	1.392729

A)

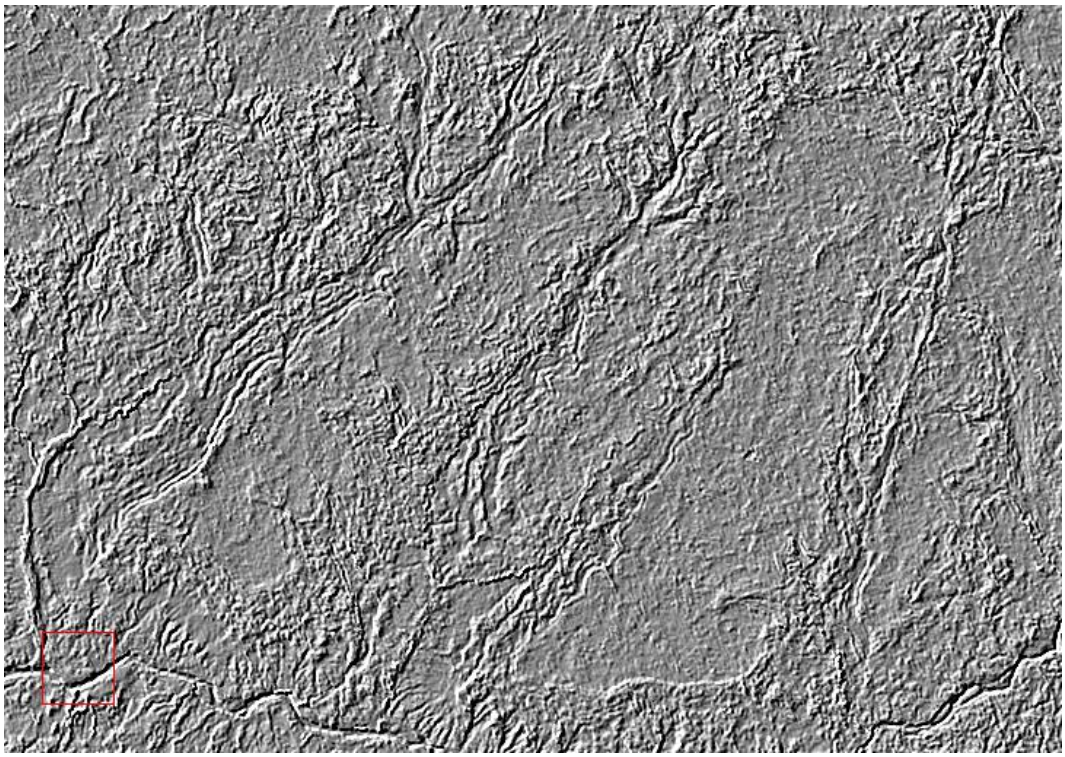

B)

Fig 3.7. (A) and (B) high-pass kernel which is used to enhance structural control stream and stream that trend in NE-SW direction over a kilometer.

-0.221231	-0.809017	-1.396802
0.587785	0.000000	-0.587785
1.396802	0.809017	0.221231

A)

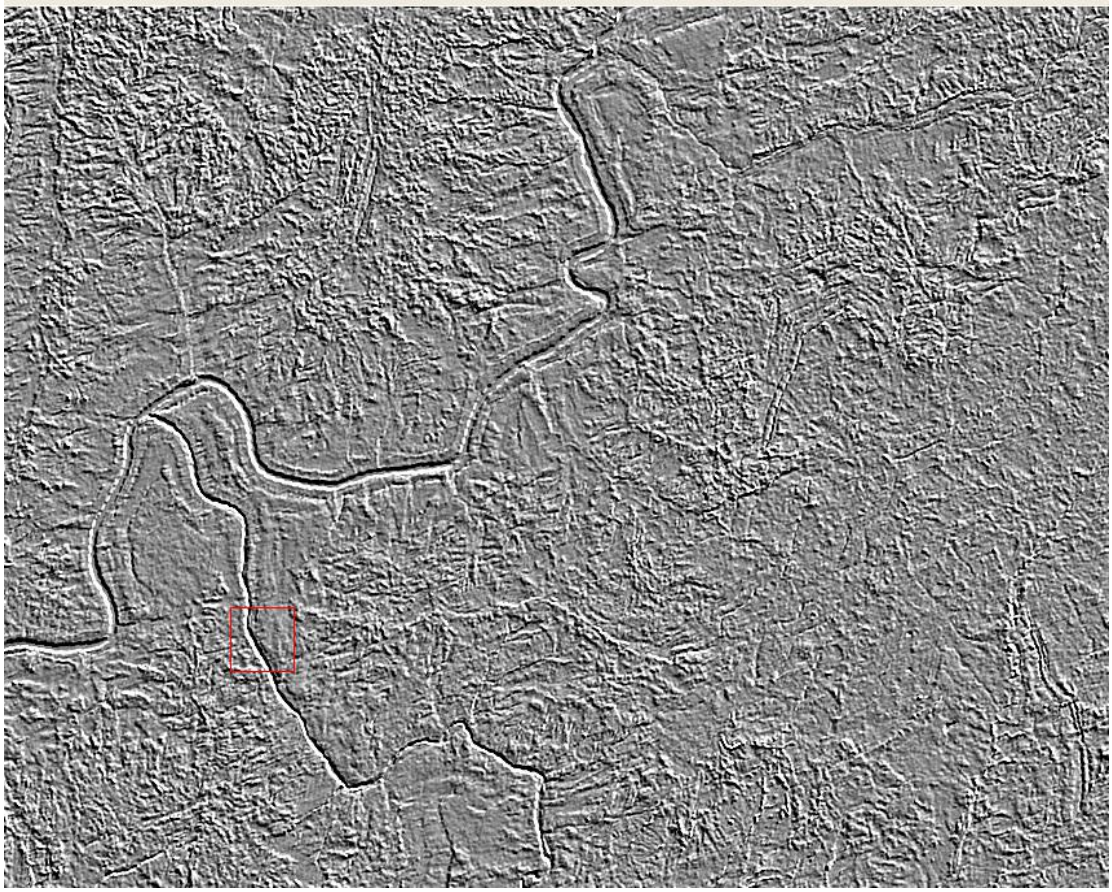

B)

Fig. 3.8. (A) High-pass kernel and (B) WNW-ESE lineaments at the Abbay and Jemma Confluence.

-1.000000	-1.000000	-1.000000
0.000000	0.000000	-0.000000
1.000000	1.000000	1.000000

A)

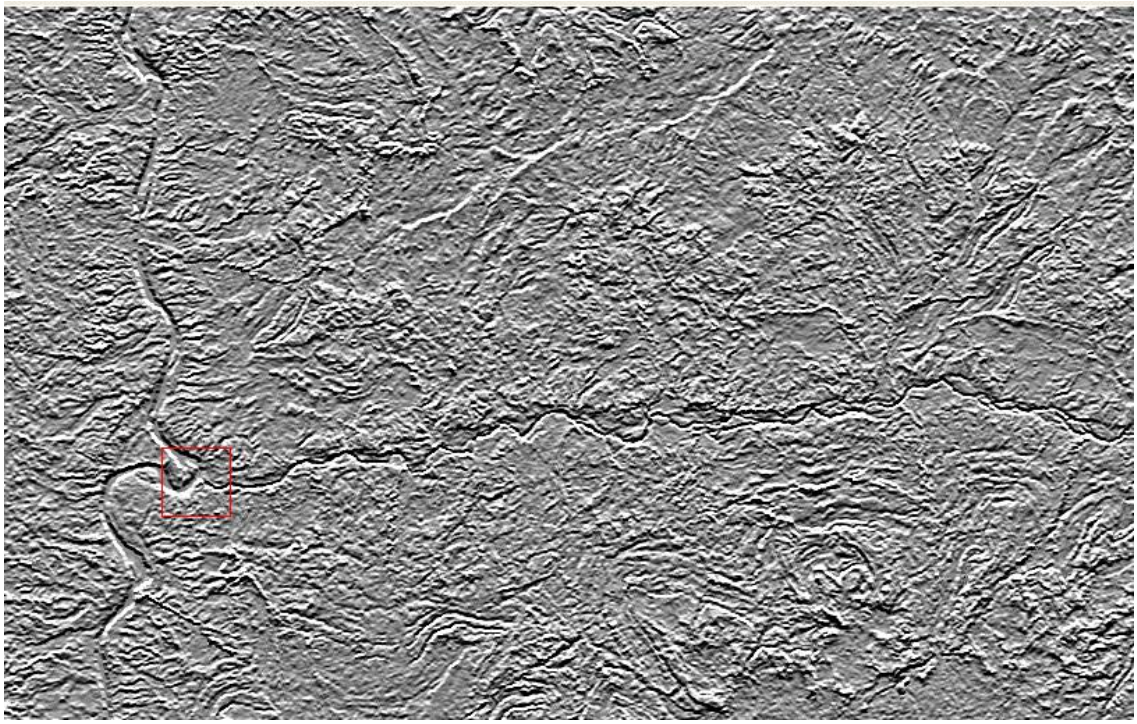

B)

3.9.(A) And (B) High-pass Kernel and E-W Lineaments respectively

3.1.4 Principal Component Analysis

Data from several bands that are set up from spectral data in the visible and near IR tend to be varyingly correlated for some wavelength or classes. This correlation can be minimized by reprocessing technique known as principal component analysis (PCA). In the process of decorrelation new PCA bands are produced, each containing some information not found in the others. The concentration of information in the upper PCA is governed by statistical variables called eigen value (λ) and eigen vectors (ν) (Tables 3.3 and 3.4) derived from matrix of inertia Table.

Band	**Min**	**Max**	**Mean**	**Stdev**
1	0	255	120.975074	61.367988
2	0	255	132.452298	60.624305
3	0	255	137.731351	59.226267

Table 3.2. Standard deviation

Num	**Eigenvalue**
1	4072.726034
2	3715.544957
3	3160.815979

Table 3.3. Eigenvalue

Band	**Band 1**	**Band 2**	**Band 3**
1	3766.029962	177.703565	-8.438342
2	177.703565	3675.306317	-402.899923
3	-8.438342	-402.899923	3507.750692

Table 3.4. Correlation Matrix

Band	**Band1**	**Band2**	**Band 3**

1	1.000000	0.047765	-0.00232
2	0.047765	1.000000	-0.11221
3	-0.00232	-0.11221	1.000000

Table 3.5. Covariance Matrix

Eigenvec	**Band 1**	**Band 2**	**Band 3**
1	0.437008	0.729221	-0.526555
2	0.881514	-0.230878	0.411860
3	0.178767	-0.644152	-0.743714

Table 3.6. Eigenvectors

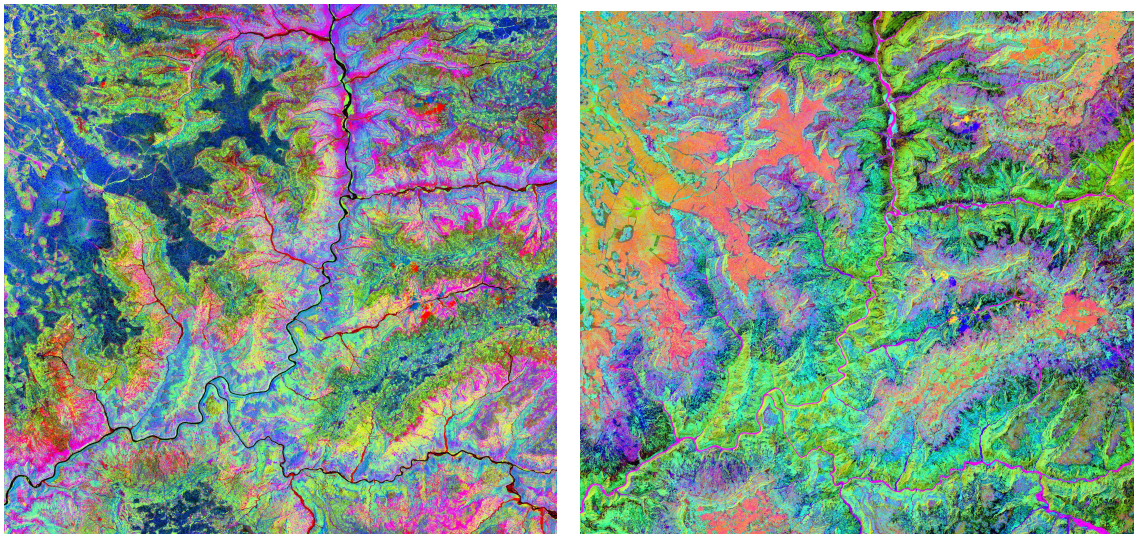

A) B)

Fig. 3.10. Principal Component Analysis of band 75432 (A) PC1, PC2 and PC3 In RGB; (B) Band 7543 PC1,PC2 and PC3 In RGB order respectively.

3.1.5 Band Combination

Any three bands each covering a spectral range from a multispectral image set, either stretched or unstretched, can be combined to produce a color composite of true colors or false color. The color combination techniques could be either in additive colors Red, Green and Blue order or in subtractive color mode Cyan, Yellow and Magenta or even in advanced hybrid color mode Intensity (I) Saturation (S) and Hue (H). In using the LANDSAT image for lithology mapping 35 different possibilities of combinations have been used. However, most of the bands are highly correlated and hence the color contrast and information content were low in several combinations. Therefore, least correlated bands using their coefficient of correlation have been selected (Tables 3.3, 3.4 and 3.6) and combined them to obtain the images indicated in Appendix i. In these images, the color variations are directly related to lithologic differences and to some extent to the degree of alteration as well.

3.2 GIS Technologies as an Aid for Hydrocarbon Exploration

Hydrocarbon Exploration in geologically complex and highly rugged terrain's, like the Blue Nile basin, is always faced with difficulties. In such cases, it is imperative that such exploration technology be used, which are cost effective and relatively accurate. An integrated approach of remote sensing and geographic information system (GIS) can suffice not only for geological mapping, but also for geological interpretation. In between Ethio GIS and an integrated master plan of the Abay basin, an extensive GIS data base has been build up for the study area through standard procedures, so as to utilize the data not only to generate map outputs, but for lithological descriptions and structural interpretation. Thematic layers generated by digitization include, lithological contact and geological information, lineaments (linear features), roads, lakes, drainage, cities and topographic contours (Fig. 3.11).

The processing stage is to combine the enhanced image with Digital Elevation Model (DEM) to produce a digital terrain model (DEM) to further improve the interpretation of the surface geology. Elevations individual points, are commonly collected from systematic grids of geographic significance as surveyed during the field survey with the aid of GPS and digitizing from topographic map of the study area. The topographic contours and elevation points were interpolated using triangular regular network (TIN) method to generate DEM with the aid of Arc view GIS software using surface module. The enhanced image were draped with the DEM using three dimensional GIS overlay techniques. Digital elevation data for this study

were also obtained from shuttle radar terrain model of Ethiopia (SRTM) (Fig 3.12 a and b). These data have a pixel resolution of 90mX90m.

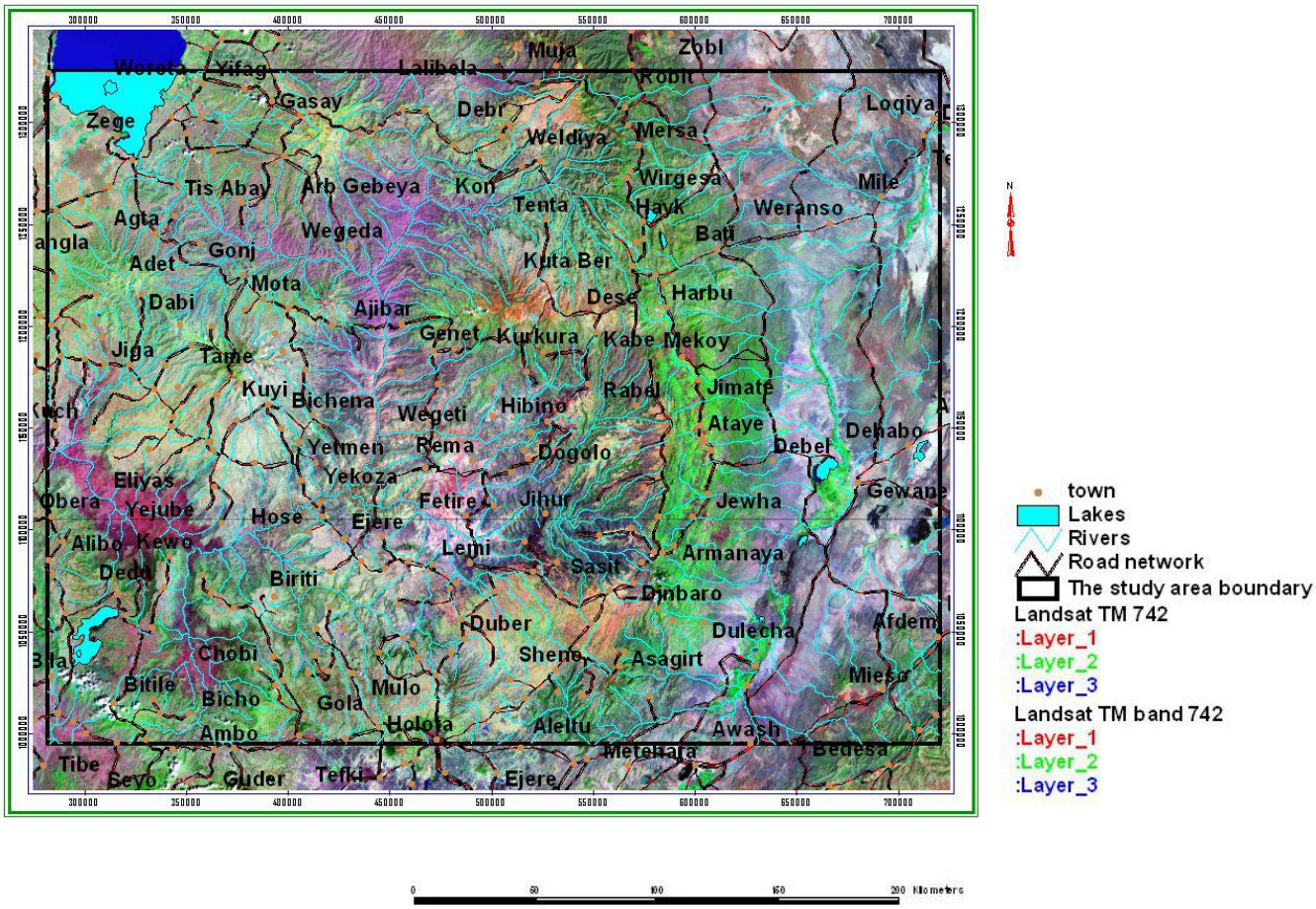

Fig. 3.11 Base map generated with the aid of GIS data Integration techniques

The processing stage was accompanying with the help of three commercially available software packages in combination with micro DEM, 3 DEM and Arc view GIS 3.2 all the software system used into this study are personal computer version mounted Pentium 4 under windows.

In this study, the integration of co-registered image data and DEM data displayed in three dimensions was found to significantly increase the ease of interpretation of rock types.

The land sat ETM+ used has a 28.5m pixel resolution, so that the SRTM data resembled from 90m pixel resolution to 28.5m pixel resolution. The study area is the north western and central plateau where lithological contacts are associated with subtle slope brakes on the cliff faces. The integration of co-registered DEM data and enhanced image data displayed in three dimensions is a more effective method for interpreting surface lithology the traditional 2D image interpretation approach. The results of these techniques will demonstrate, in chapter 4, in which the distribution of lithology is easily interpreted and better understood, through a 3D combination of DEM and image data.

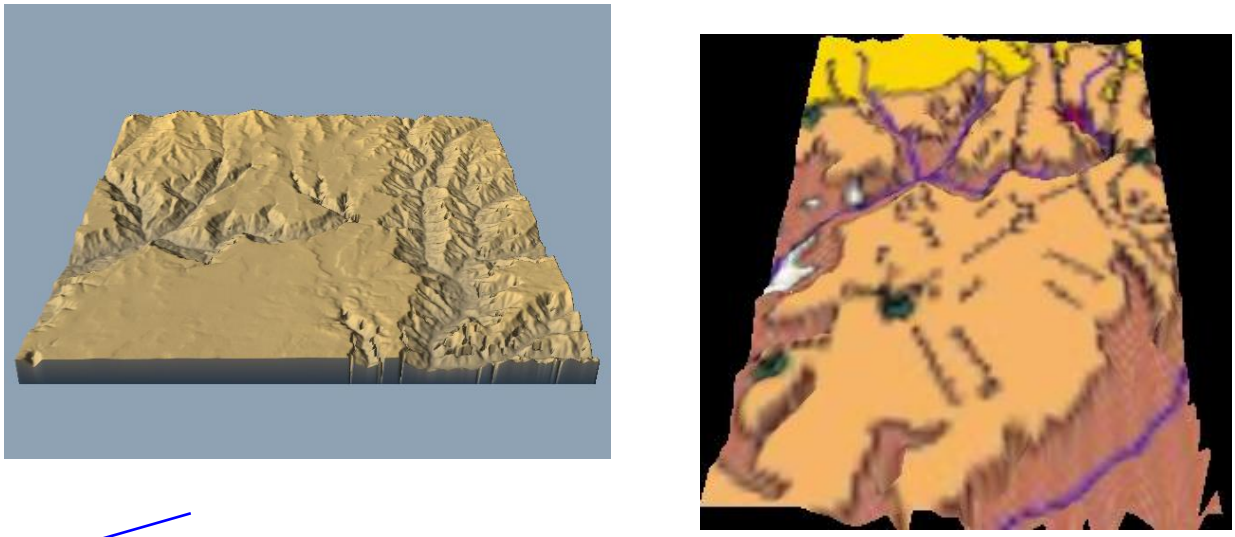

A)

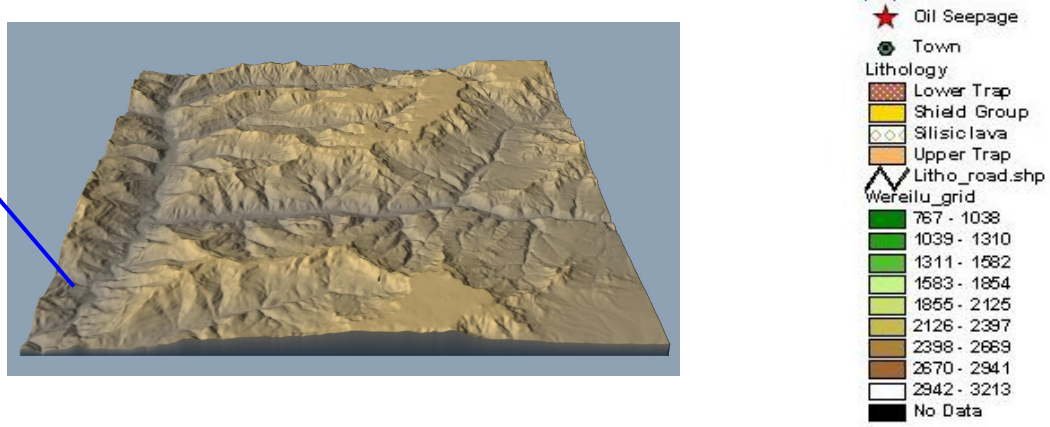

B)

Fig. 3.12. SRTM of: A) Wereilu and a DTM after draping a geological map on the Grid B) Dera respectively.

In addition to the lithological interpretation, integration of co-registered DEM data and enhanced image is provides an automated determination of strike and dip measurements. This can be improve and has been demonstrated in this study. The image data were from a decorrelated principal components image from land sat ETM+ bands 1,2,3,4,5,6 and 7, in which the first three PCs where displayed in RGB (Fig. 3.14). The image and DEM data were rectified to the Ellipsoid Clark 1880 (Adindan UTM zone 37N) coordinate system and the image data were resembled to 90m by 90m pixel resolution to much the SRTM resolution. Validation was with the topographic map contour and field GPS survey data. The result of this approach will be discussed in chapter 5.

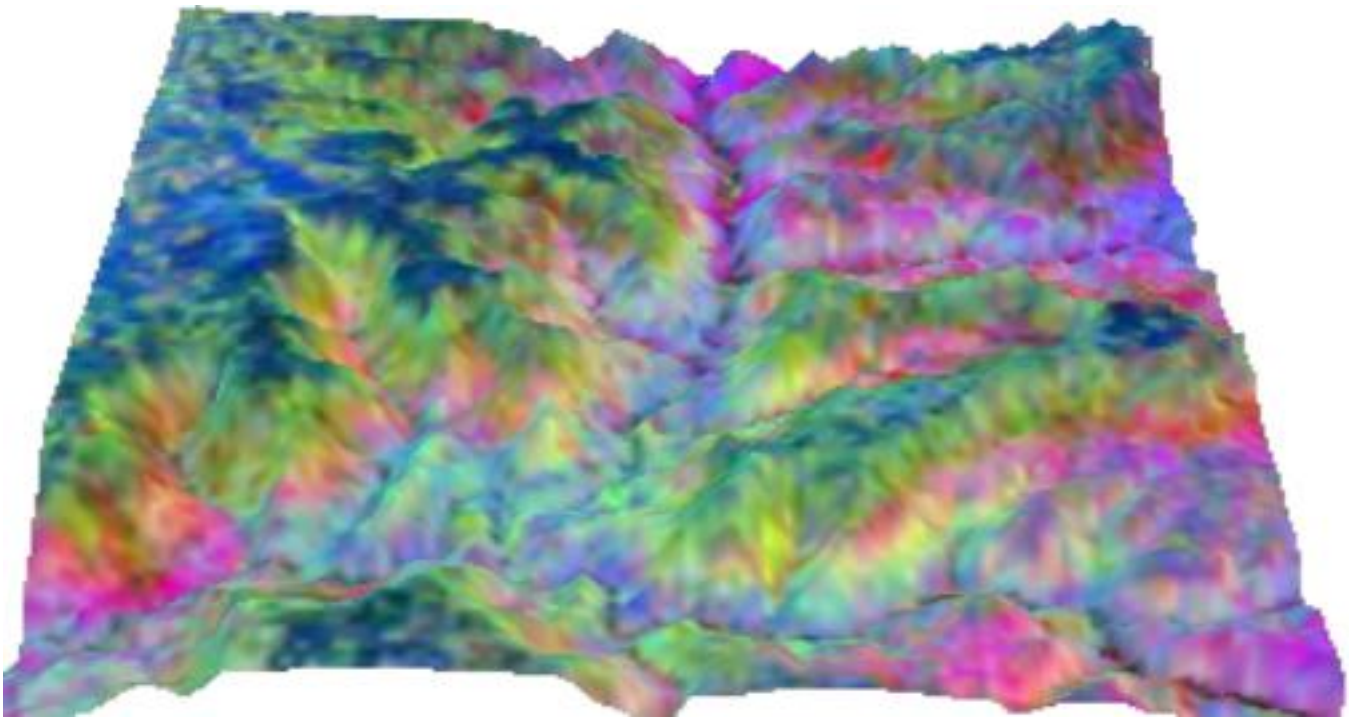

Fig. 3.13. Draped image of band 75432 PC1,PC2 and PC3 In RGB order respectively on the DEM

The other full potential of co-registered imaged data and DEM is for the construction of the profile section of the study area (appendix ii). The topographic contours and elevation points were interpolated using the triangular irregular network (TIN) method to generate the digital elevation model (DEM) of the study area. In order to generate digital terrain models (DTMs), the enhanced land data ETM+ were draped over the DEM (Fig.13). These analyses were carried out in Arc view GIS 3.2 and micro DEM using the 3D analyst module.

The profile section is cut on the Microdem Los module and exported to Arc view with vertical exaggeration 5X. The interpretation result of this approach will discuss in chapter 6. The present study is an example of how remote sensing and GIS can be used in geology in morphological complex terrain like the north western and central plateau of Ethiopia.

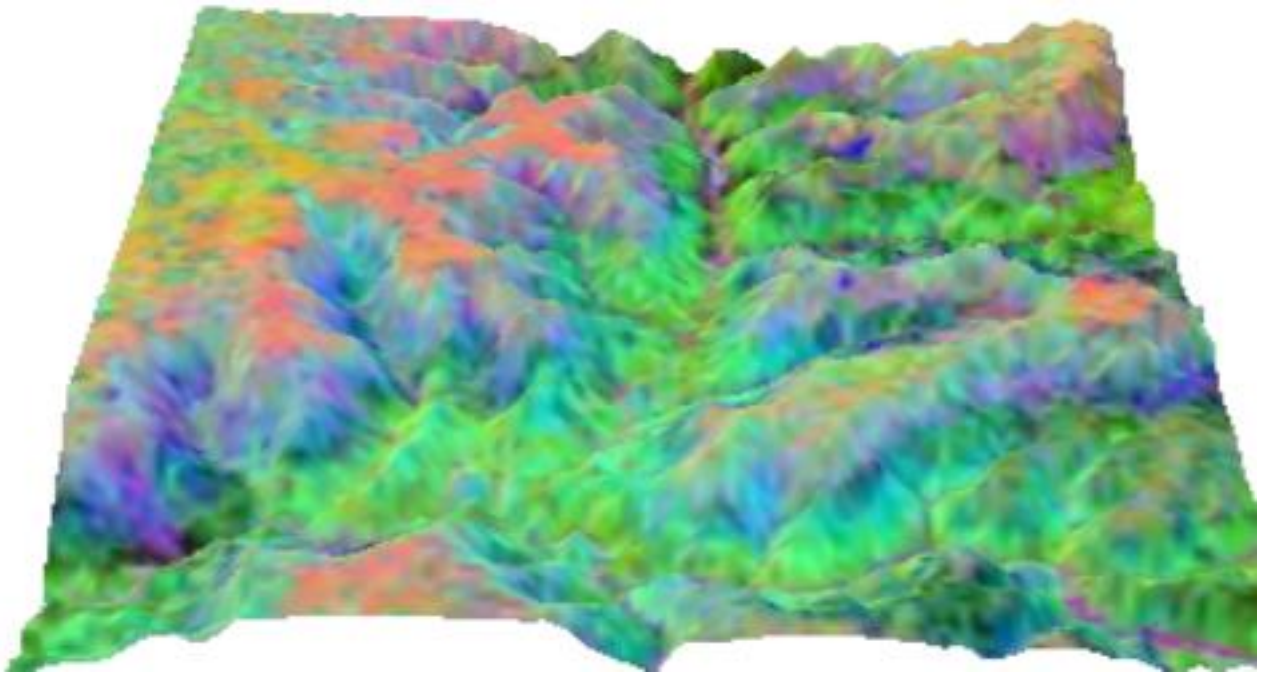

Fig 3.14. Drape images of the band 7543 of the Principal component PC1,PC2 and PC3 in RGB order respectively on the DEM.

are dominantly observed on the upper trap, while dendritic drainage patterns are observed on the weathered and fractured lower Trap.

Furthermore, the shield volcanoes are observed in topographically elevated area, underlain by the upper Trap. The lower Trap basalts are identified in lower relief as compared to the above two unit, probably due differential weathering and erosion. Intrusive (dikes) can also be recognized from linearly stretched false color composite LANDSAT ETM^{+} images, by their distinct landforms (linear or curvilinear topographic expressions) and their structural relations to the surrounding rocks.

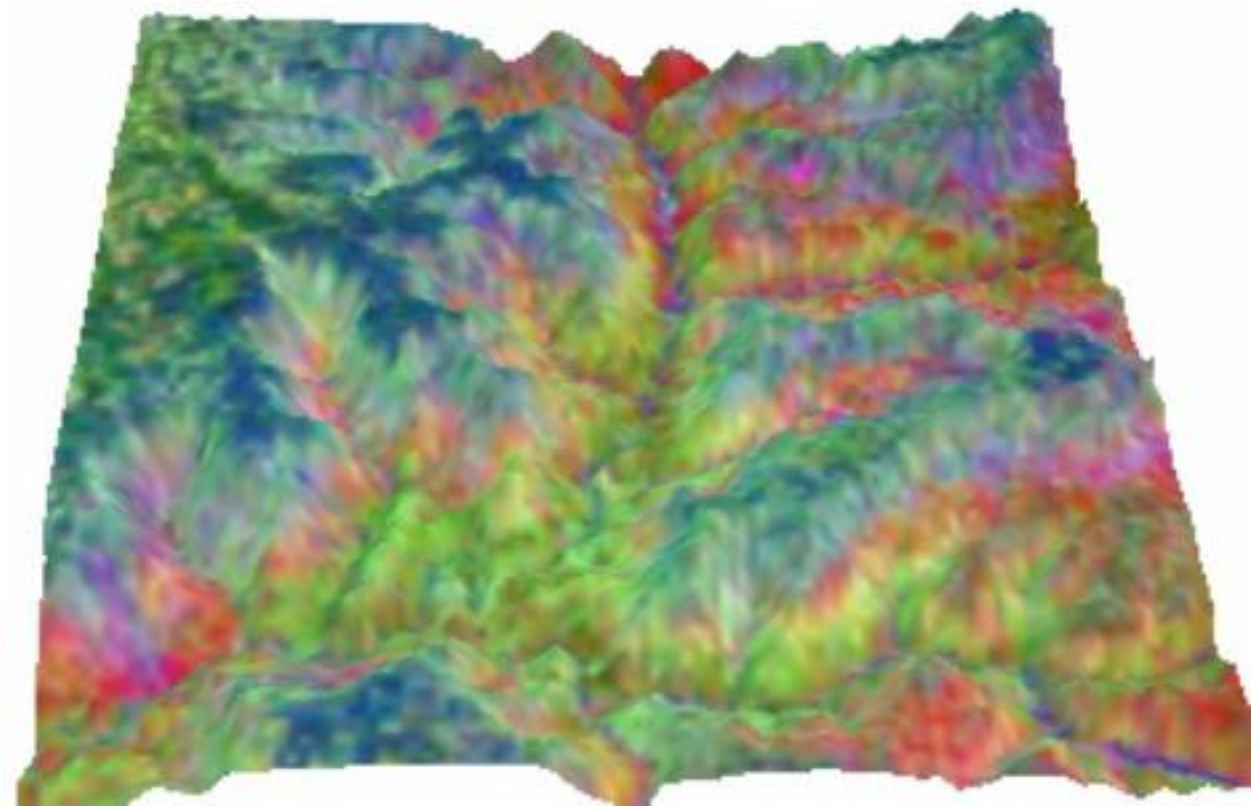

Fig. 4.1. A drape image of principal component of band 75432 of PC1, PC2, and PC3 in RGB order respectively over the DEM.

East of the Tana Lake, the satellite imagery marks the shield volcanoes at Mekit woreda along 10 and ½ latitude. Further south, at legambo woreda the shield volcano is clearly identified from the imagery. Exactly south of lake Tana is represented a shield volcano with a general NW-SE orientation northwest of Debre Work, Felege Berhane and Bichena town. Another shield is clearly identified south of Dessie comprising Guguftu, Akesta, Buso, and Mekane Selam. Shield volcanoes are also marked by enhanced satellite imagery at the northern part of Wer Ilu underlying the Jegola stream catchment.

The upper Trap basalt marked by the satellite imagery by forming steep walls of Chilage and Gunda rivers in Ajabar, in the Yeshum valley at Meakane Selam, Tenta and in Werilu. The landsat imagery reveals the wide spread exposures of the lower trap basalt in the northern and southern parts of Ajbar forming cliff with streambeds in Mekane Selam. The co-registered landsat ETM+ and DEM reveals that this unit is widely exposed in Werilu, underlying the drainage basins of Atari and Tumele streams. This unit is also identified at Kassem gorge, Mugher canyon and in most outcrops in the western margin of the rift escarpment.

In the Mesozoic sedimentary sequence of the study area, lithological boundaries are easily recognized yielding more information on the imagery, especially in the Abbay river canyon, Jemma and Mugger river valleys (Appendix i). The standard false color composites especially bands 742, 754, 753, 523 in RGB and a three-band decolerated principal components (PC) image (bands 1,2,3,4,5 and 7 with PC 1, 2, 3 displayed in Red, Green, Blue (RGB), respectively reveal better detail of the distribution of rock types. These images give better details than the original raw data in both topographically low and elevated terrains, but each band combination contains different information.

The principal component images, which combine the first, second and third order principal components from the area in RGB order easily distinguish the Goha Tshion formation from the Antalo limestone. The co-registered image and DEM integration shows the Antalo limestone as cliff forming, while the Goha Tshion formation has a gentle slope and lower relief. In addition, this formation develops a very fine close-spaced, ramified dendritic drainage pattern with deep incision valleys. This helps to identify the presence of fine clays. The above-mentioned

characteristics indicate this unit to consist of two or more members, each having a pronounced differential resistance to erosion. The enhanced false color components of different combination mark the presence of this formation at the Abbay canyon, the Jemma river valley and other deep river valley cuts.

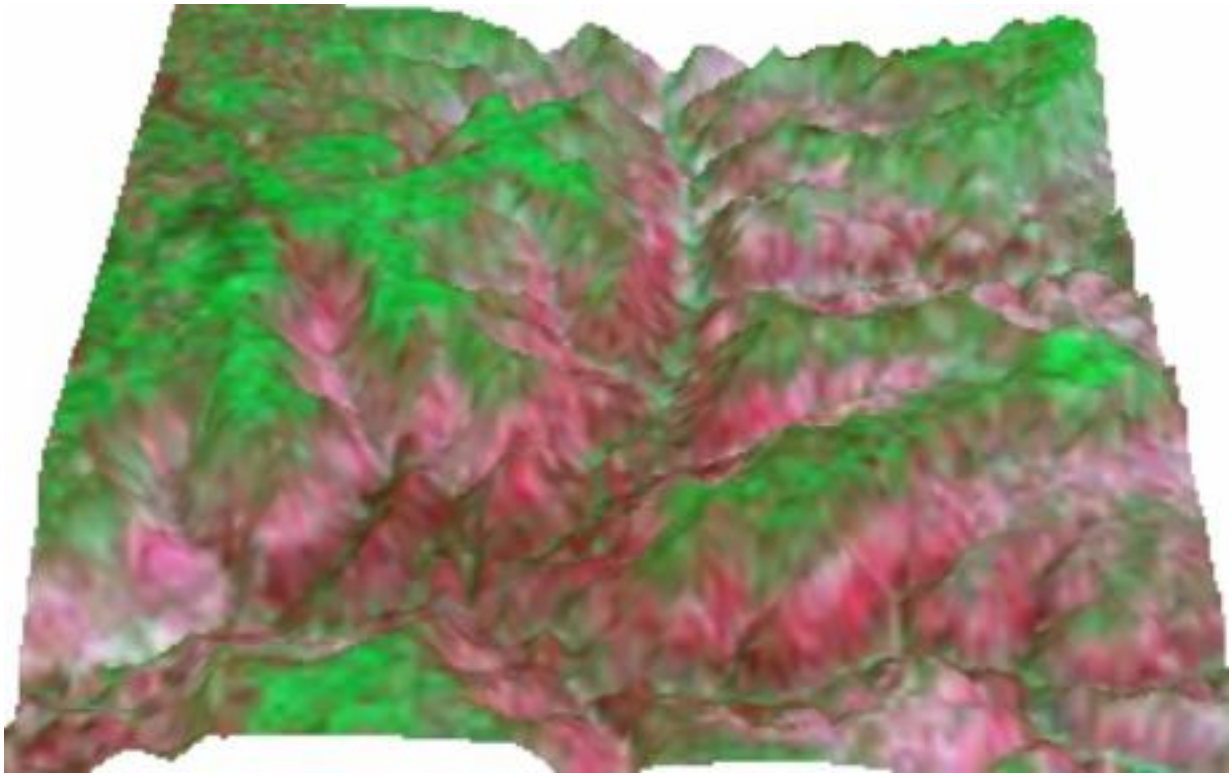

Fig 4.2. The HIS drape over the DEM enhance the boundary of the volcanics and Mesozoic sediment.

The limestone unit, especially in the Weleka river valley shows rills and bowls (Fig. 4.3). The rills form channels and seem to be tilted on the satellite imagery, and can be identified as the beds of the Antalo limestone. The rilled surface looks wrinkled as marked on the satellite imagery. This probably indicates that the rills are connected with fractured or solution surface. The landsat

ETM$^+$ reveals the presence of these units in the Abbay river valley, in the Jemma river valley, North of Cheka Genet in a dip river cut and in the Weleka river valley.

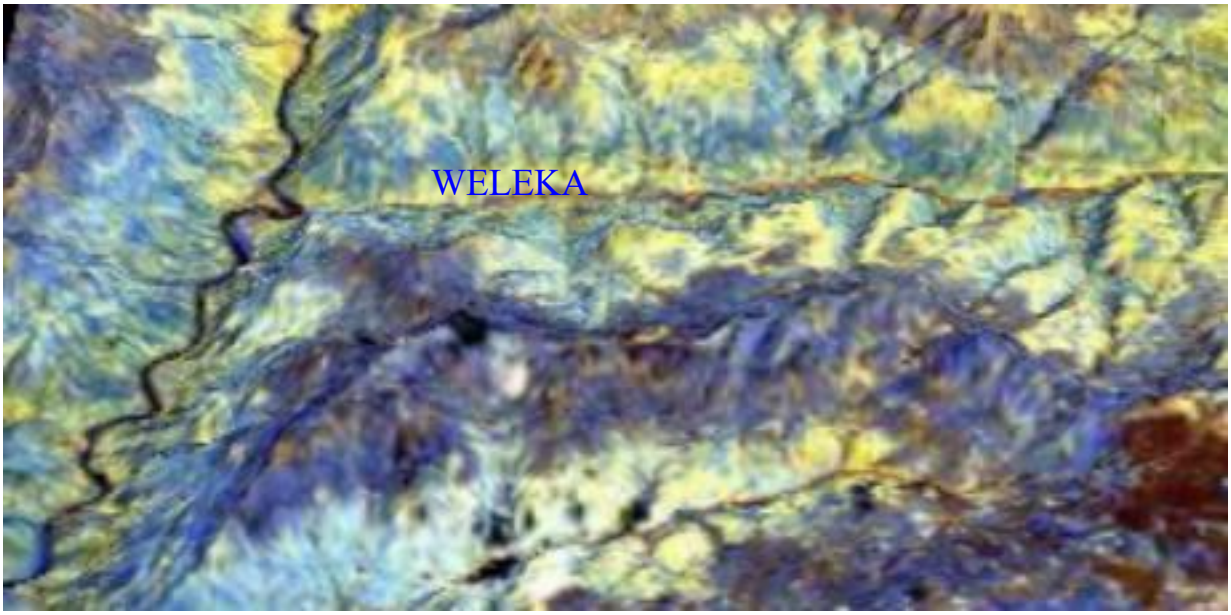

Fig. 4.3. False color satellite imagery of band 754 in RGB order drape over the DEM revealing rills on the Antalo limestone at the flanks of the Weleka river valley.

The landsat ETM$^+$ image reveals the surface that comprises the upper sandstone unit to be texturally smooth and the tone consequently lighter. This unit does not show a predominant surface drainage pattern on the landsat TM imagery. The co-registered landsat ETM$^+$ and the DEM depict the sandstone as having a rolling topography. This can be due to the weak cementing and less susceptibility to chemical weathering. In some places, the satellite imagery marks this unit to have a wrinkled surface, probably indicating the lenticular & cross-bedded structures. This unit is clearly identified on the enhanced composite false color imagery at Lemi, at the foot of Gundo Meskel ridge underlying the lower Trap, in the Jara and Wenchit streams, north of Rema, in the Jema river valley and in all the areas east of the Gundo Meskel ridge. The landsat imagery does not indicate the existence of this unit in the Weleka river section and in the areas west of the Gundo Meskel ridge and the Abbay canyon (Fig.4.4). The Adigrat sandstone is represented only in the lower reaches of the Abbay canyon forming steep cliffs (fig 4.4).

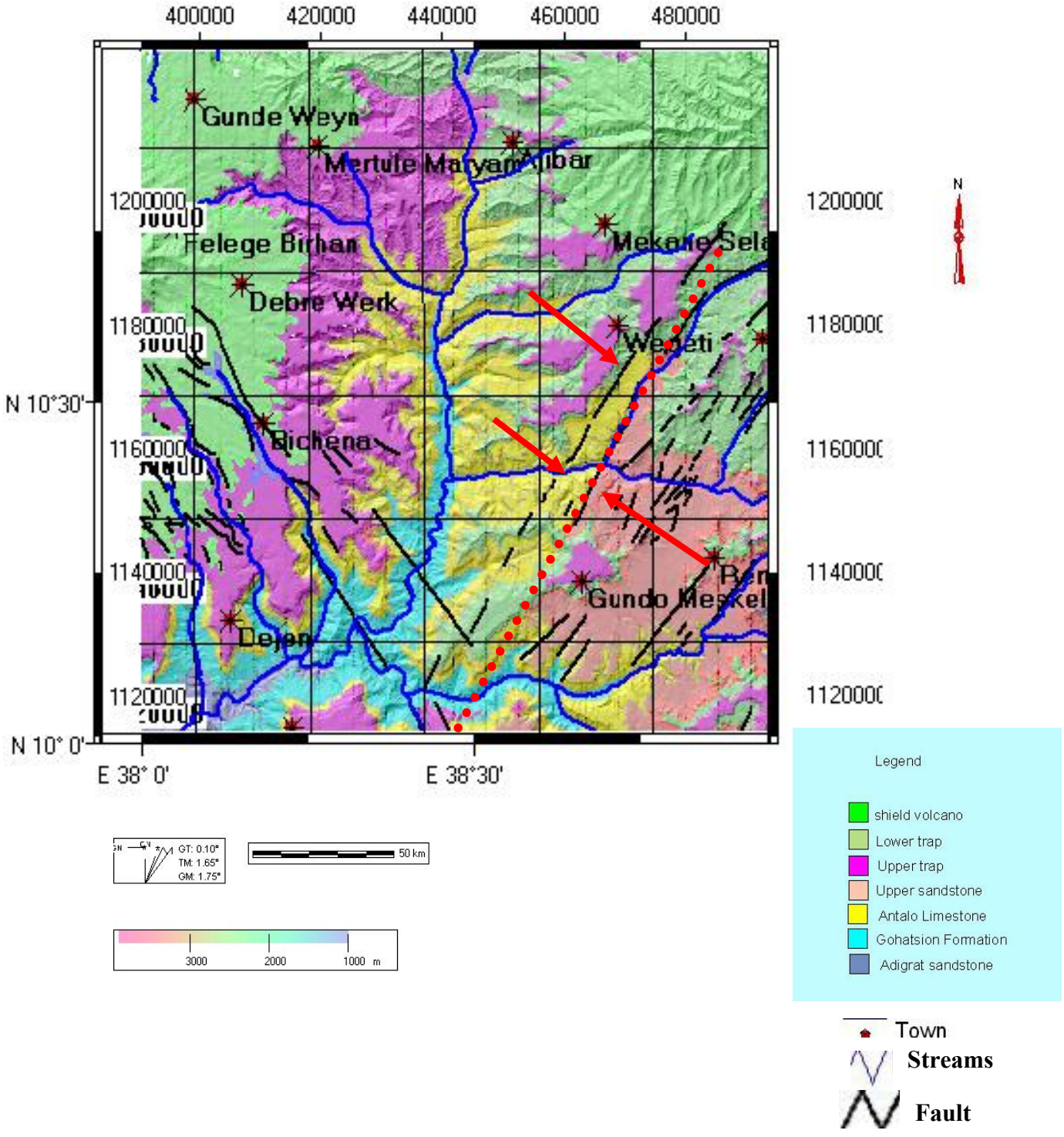

Fig.4.4. Digital Terrain Model Of the Dera Sub basin (east of the red dot line) depicting the geological unit after drape on DEM, N.B The Upper sandstone restricted east of the red dot line.

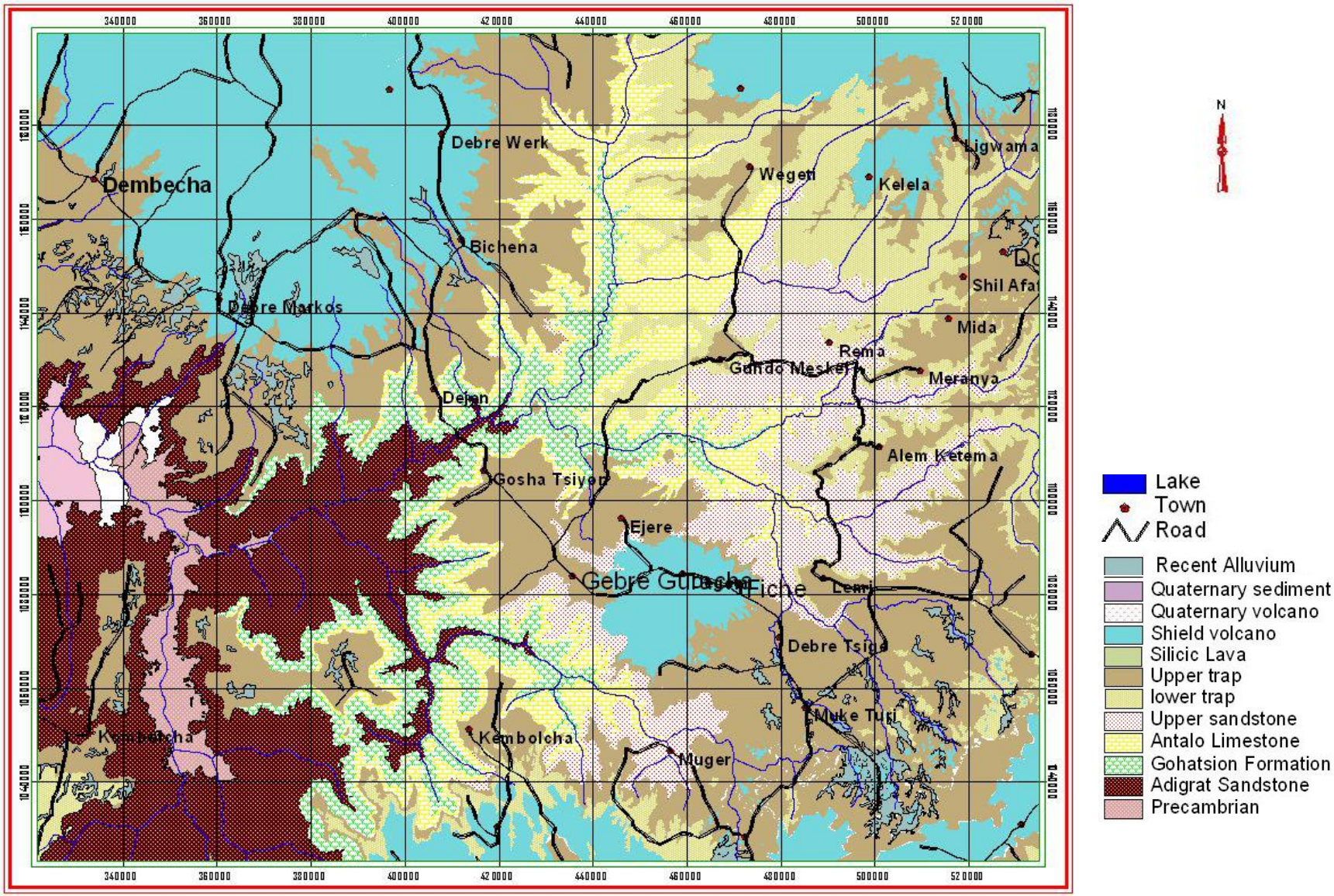

Fig.4.5. Lithological map of Dera Sub basin as interpreted from satellite imagery.

4.2. Field mapping and description

The satellite imagery interpretation was accompanied by field survey of selected parts mainly at the Were Ilu and Dera areas. Many traverses were carried out in as many sections as possible. Lithologic units were described in the field, stratigraphic sections were drawn and geological cross-sections are super imposed on a cross section drawn from a DEM image. The results of this work are presented in this section. The Mesozoic sedimentary units and the Tertiary volcanic cover are mainly represented in the areas surveyed.

4.2.1. Stratigraphic Sections

Seven major composite stratigraphic columns of the area are constructed during the field survey with the aid of systematically selected traverses. The first stratigraphic column has been constructed from field measurements taken along the Kabe-north of Were Ilu-Jara stream traverse (Fig. 4.6a). This stratigraphic section along the Jara stream valley compromises a fossiliferous, micritic, white to gray limestone, which is overlain by sandstone. The sandstone unit generally grades upwards from silty sandstone to coarse conglomeratic sandstone. It is cross-bedded, and unconformably overlain by highly brecciated basalts and agglomerates. The brecciated basalt is, in turn, overlain by thick flows of columnar basalts, which in some places consist of intercalations of welded tuff and minor rhyolites. This unit has open, widely spaced joints.

The second stratigraphic column (Fig. 4.6b) represents the area between Welleba stream and Alem Ketema. This section reveals at the bottom a fossiliferous limestone overlain by gray to pink, weakly cemented and cross-bedded sandstone. The sandstone unit is unconformably overlain by thick flows of columnar basalt.

A third section from Rema to Jara stream (Fig. 4.6c) has the basal part made up of fossiliferous limestone overlain by pebbly sandstone. The sandstone unit is reddish due to iron-oxide cementing and contains lenses of shales. It becomes gray to pink, weakly cemented and cross-bedded towards the top and is unconformably overlain by thick basalt flows.

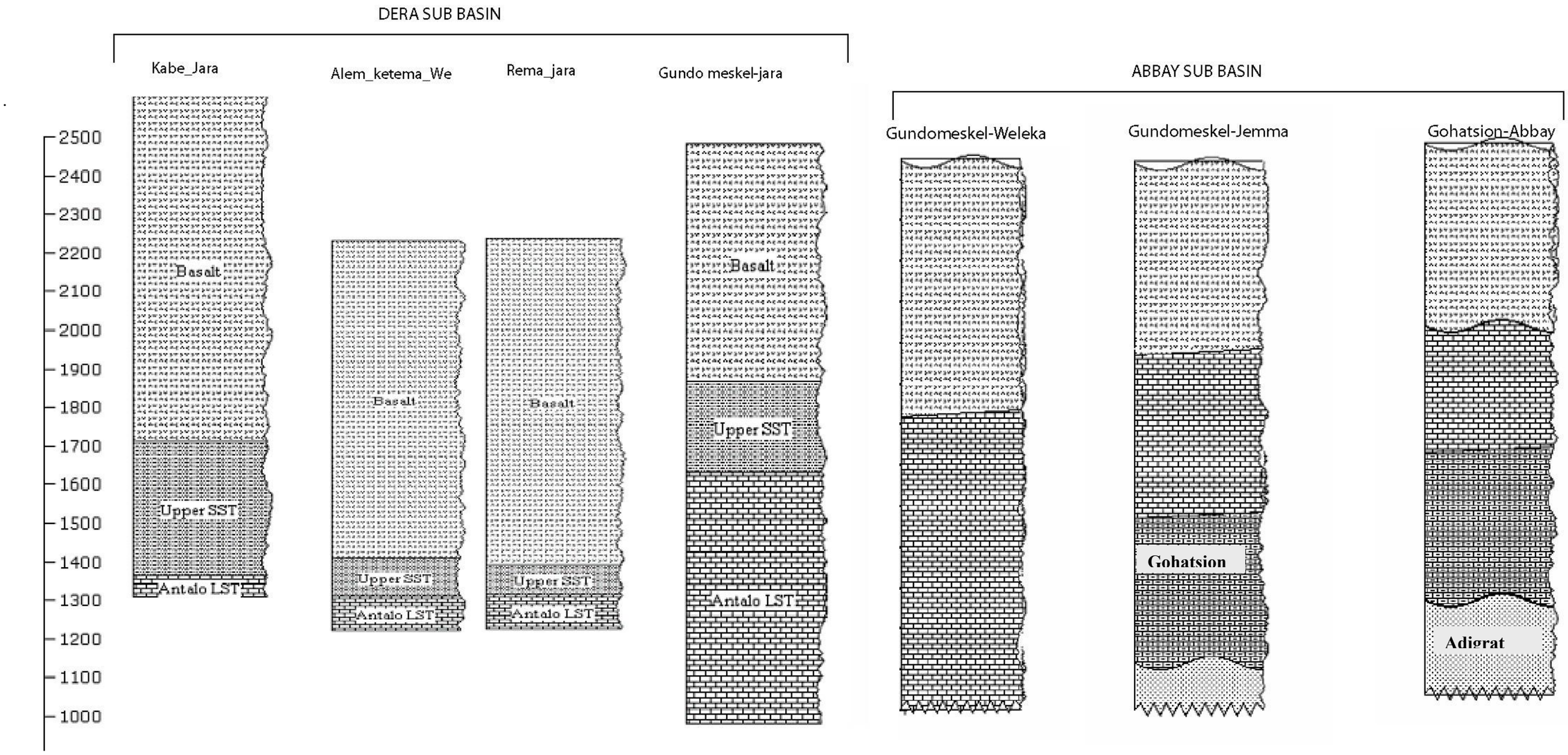

Fig. 4.6 Major composite Stratigraphic section of the area.

The fourth stratigraphic column represents the traverse from Gundo Meskel to Jara stream (Fig. 4.6d). This section represents Trap basalts on the elevated Gundo Meskel ridge unconformably overlying slightly tilted beds of Upper Sandstone. The sandstone beds are exposed along graben and half graben walls down to the flanks of the Jara stream where they overlie the Antalo limestone.

The fifth stratigraphic section is constructed from the traverse taken between the town of Gundo Meakel and Weleka River (Fig. 4.6e). This section, at the bottom consists of fossiliferous limestone. This limestone unit is very thick and forms three different multistory cliffs, and attains a thickness of about 728 m at the flank of Weleka stream even though its bottom part is not exposed. This unit is uncomformably overlain by thick flows of columnar basalt.

The sixth stratigraphic column represents exposures along the road cuts and river valleys between Gundo Meskel and Jemma river valley (Fig. 4.6f). The Adigrat sandstone generally fines upwards, especially along the Jemma river valley section. The Adigrat sandstone is uncomformably overlain by an intercalation of dolostone, shale, gypsum, limestone and siltstone. This member of rock units which belongs to the Gohatsion formation (Getaneh Assefa, 1981) is overlain by a thick fossiliferous limestone unit that attains a maximum thickness of 420m. The limestone is uncomformably overlain by thick flood basalts.

The seventh stratigraphic section represents the succession exposed along the road between Gohatsion to Abbay River (Fig. 5.6 g). The bottom unit lying on the bed of Abbay River is the Adigrat sandstone. This unit shows a general fining upward and forms cliffs uncomformably overlain by the Gohatsion formation. The latter is a hetrogeneous assemblage of mudstone, clay stone, limestone, dolostone, shale and gypsum. Unlike the underlying and overlying units, it forms gentle slopes and is uncomformably overlain by fossiliferous limestone unit, which has a thin intercalation of black shale in the upper part. The limestone unit is, in turn uncomfortably overlain by the trap basalts.

The entire sedimentary succession is almost horizontal, with the exception of low angle local tilts of a few degrees, which are related to minor faults and differential settlement**.** It should be noted

that the Upper sandstone shows up only in the first three sections. Another important finding is the thickening of the Antalo Limestone unit to about 728m at the Weleka river section, where it is exposed down to an elevation of 1154 m a.s.l. In general, it seems that depositional thickness of most facies decreases southwestward.

4.2.2. Lithologic Description

Adigrat sandstone: is exposed along the lower reaches of Abbay and Jemma river sections. Its vertical thickness, varying locally, attains a thickness of 250m to 350m and about 120m in the Abbay and Jemma river sections, respectively. The unit has a fining upward sequence character with reddish coarse sand at the base and siltstones at the top. The angular-sub angular, medium to coarse-grained sandstone beds show planar cross-bedding structures, in places. Sub-horizontal, single and multistory sandstone bodies characterize the unit. In some areas the horizontal beds vary in thickness from 1m, through 40cm-50cm down to 10 cm. Fresh cut sandstone has light yellow to light brownish–red color. Even though its lower contact is not exposed in the area surveyed, Wolela Ahmed (1997) reported that the Adigrat sandstone rests unconformably on the Precambrian basement or with slight disconformities on sedimentary rocks of the upper Paleozoic. The Adigrat sandstone shows alluvial fan, fluviatile facies tones (Bosellini, 1989; Russo et al., 1994; Wolela Ahmed 1997).

Gohatsion formation: in the area surveyed, the gypsum-containing formation overlies a transitional zone that in turn overlies the Adigrat sandstone. This unit attains measured thickness of 380m and 350m at the Jemma and Abbay river sections, respectively. It has a heterogeneous lithology containing an association of mudstone, claystone, limestones, dolostones, shale and gypsum. It forms relatively gentle slopes compared to the other sedimentary units. White to dark gray, soft, laminated gypsum is extensively exposed at the measured sections.

Based on field observations, satellite image and DEM interpretations, this formation can be divided into three sub units. The lower unit is composed mainly of terrigenous materials of fine-grained sandstone, siltstone and mudstone with an overall thickness of 30m in the Abbay canyon and 32m in the Jemma section. The middle unit is mainly dominated by white to gray, dark gray,

and pinkish massive gypsum, exhibiting gradational contact with the underlying lower unit but a clear sharp contract with the overlying unit. It is intercalated with dolomitized limestone and gray shale. At the bottom, the gypsum is characterized by nodular and chicken wire structures, whereas its middle and upper parts mainly depict tabular and layered structures. Between the layered and nodular gypsum lie yellow to gray clays. The hard dolomitized limestone attains a thickness varying from 2 to 20m. This unit forms steeper slope compared to the other two units. In the Abbay gorge, the gypsum has an overall thickness of 30m while the middle unit has an overall thickness of 135m. The upper unit is mainly composed of highly weathered and fractured light-yellow limestone, multicolored clayey rocks and white, weathered gypsum beds. Above the gypsum are multicolored, loose, calcite shale and siltstone with a total thickness of 3.5 meters.

Antalo limestone: this unit overlying the Gohatsion formation attains a maximum thickness of 728m at the measured Weleka river section where it directly underlies the Lower trap basalt; however, its lower contact is not exposed. Along the traverse from Gundo Meskel to Jemma River, the Antalo Limestone attains a maximum thickness of 380m and shows a clear contact with the underlying Gohatsion formation. Southeast of Gundo Meskel, the upper contact of the limestone unit is observed at an elevation of 1462m at Welleba stream (a tributary of Jemma River) with a maximum exposed thickness of 75m and at the Jara stream Fig 4.7 (a tributary of Wenchit river), at an elevation of 1428m with an exposed thickness of 35m. In this area, the upper sandstone unit overlies the limestone unit, while northwest and southwest of Gundo Meskel (in the Weleka and Abbay sections); the lower Trap basalt overlies the limestone unit.

Fig. 4.7 Photograph showing the fossiliferous Antalo Limestone bedding at the Jara stream.

The limestone unit is represented by three formations. The lower cliff-forming unit is composed of white, pale yellow limestone with shale intercalation and contains fossils of bivalves & brachiopods. The middle cliff forming limestone is intercalated with marl & mud rock. It forms gentle slopes and is the thickest part attaining up to 350m thickness in the Weleka section. The limestone is micritic, rich with fossils mainly of brachiopods and bivalves. It is characterized by horizontally bedded sedimentary structures. The upper cliff forming limestone unit has thin layers of marl and shale intercalations in the lower part but is pure limestone at the upper part. This limestone is more fossiliferous than the lower cliff forming limestone and is crystalline, medium to coarse-grained with interbeds of calcite nodules. In the Abbay and Jemma sections, black shale is observed as an intercalation in the upper limestone.

Upper sandstone: The Upper sandstone attains a variable thickness of 70m to 150m at the Welleba stream section and a maximum thickness of 320m along a section from Mida to Jara stream. In places this unit directly overlies the Antalo limestone unit while in others it is underlain by a transitional zone of alternating beds of red clay, calcareous sandstone and limestone. It is overlain by the lower Trap basalt or brecciated agglomerate beds (fig 4.8). This unit is predominantly composed of reddish brown to light gray sandstones and thin layer of conglomerate. It generally coarsens upward. At its bottom part, the sandstone is thinly bedded and silty in texture; in its middle part, it is ferruginous and cross-bedded and calcritic; and becomes gravely and massive at its top part. It should be noted that this unit is totally absent in the Abbay gorge, Jemma river valley (near Jemma River bridge along Gundo Meskel to Ejere) and at the Weleka river section. It is restricted to the area east of the Gundo Meskel ridge.

Tertiary and Quaternary Volcanic Cover: constitute the lower Trap, upper Trap, shield volcanoes and quaternary volcanics (Fig 4.8). Thick beds of massive to columnar-jointed flood basalts and associated tuff beds characterize the Trap sequences. These sequences in the study area attain maximum thickness of 550m and 350m for the lower and upper Traps, respectively. It should be noted, however, that along the Were Ilu – Jara stream traverse, a 415m thick sequence of agglomerate and brecciated basalt is exposed below the lower trap. The major shield volcanoes in the study area are restricted to north of Were Ilu in the Akesta area and west of the Abay canyon. Quaternary volcanics are exposed in the Tana rift.

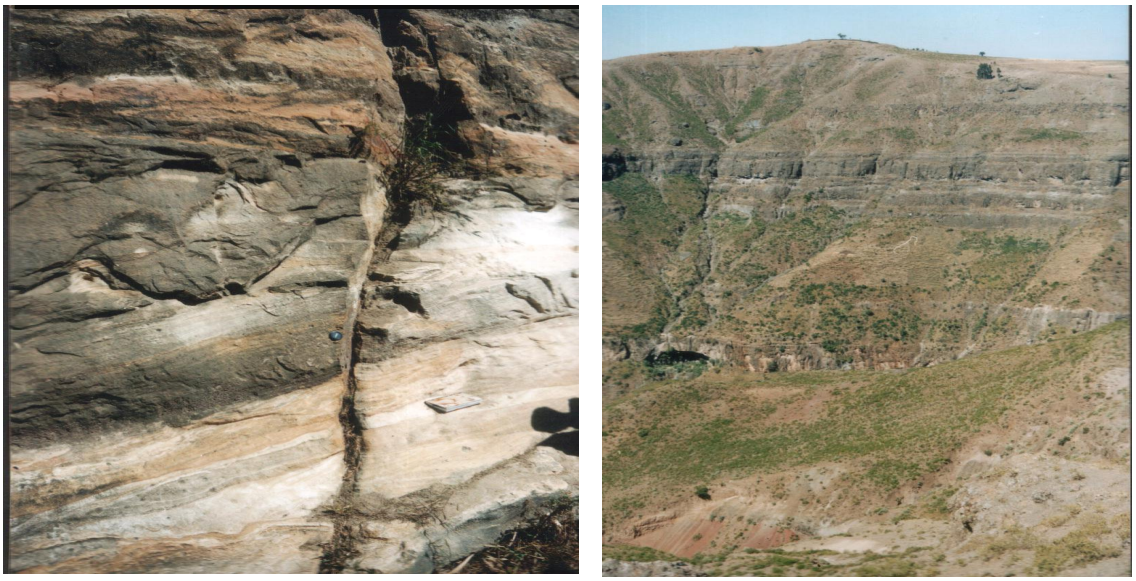

Fig. 4.8. The Left panel showing the coarsing upward upper sandstone around Wenchit stream and the right panel showing the upper and lower Traps at Were Ilu.

4.2.3. Cross sections

Four different topographic cross-sections constructed from digital elevation models provide clue on the basin's structural configuration and evolution (Fig4.9). The first topographic cross section made across the Abbay and Jemma rivers, from Dejen via Gohatsion to Weleka river trends SW-NE (Fig. 4.10a and b). This section reveals that the Antalo limestone thickens to the northeast, whereas the Gohatsion formation pinches out in the same direction. The former corresponds to the early flooding of the craton and the marine sediments occur only in depressions of aborted rift basins. In the Callovian- early Oxfordian time, a major transgression, probably related to the drifting phase and a major sea level high stand with the drowing of the craton caused the deposition of the Antalo limestone (Russo et al., 1994).

The second cross section is constructed along NW-SE direction from Weleka River via Gundo Meskel towards the Jara stream (Fig. 4.10c). NE–SW trending horsts, grabens and half grabens

restricted the deposition of the Upper sandstone to the southeast. This section reveals the presence of growth faults within the sedimentary sequence especially in the vicinity of Dera. Another cross section runs from Meragna to Jara stream along a generally NE-SW direction (Fig. 4.10d). This cross section shows several NE–SW striking faults which produce half graben structures on the Mesozoic sediments whereas the NW–SE structures cut the whole stratigraphic sequence of the area, especially at the vicinity of Were Ilu. The fourth cross section (Fig. 4.10e) crossing the Mechela River in SW-NE direction shows the presence of N-S to NNW-SSE oriented faults cutting through the trap basalts forming grabens oriented in the same direction. The seepage of Were Ilu is related to the fractures associated with this fault trend.

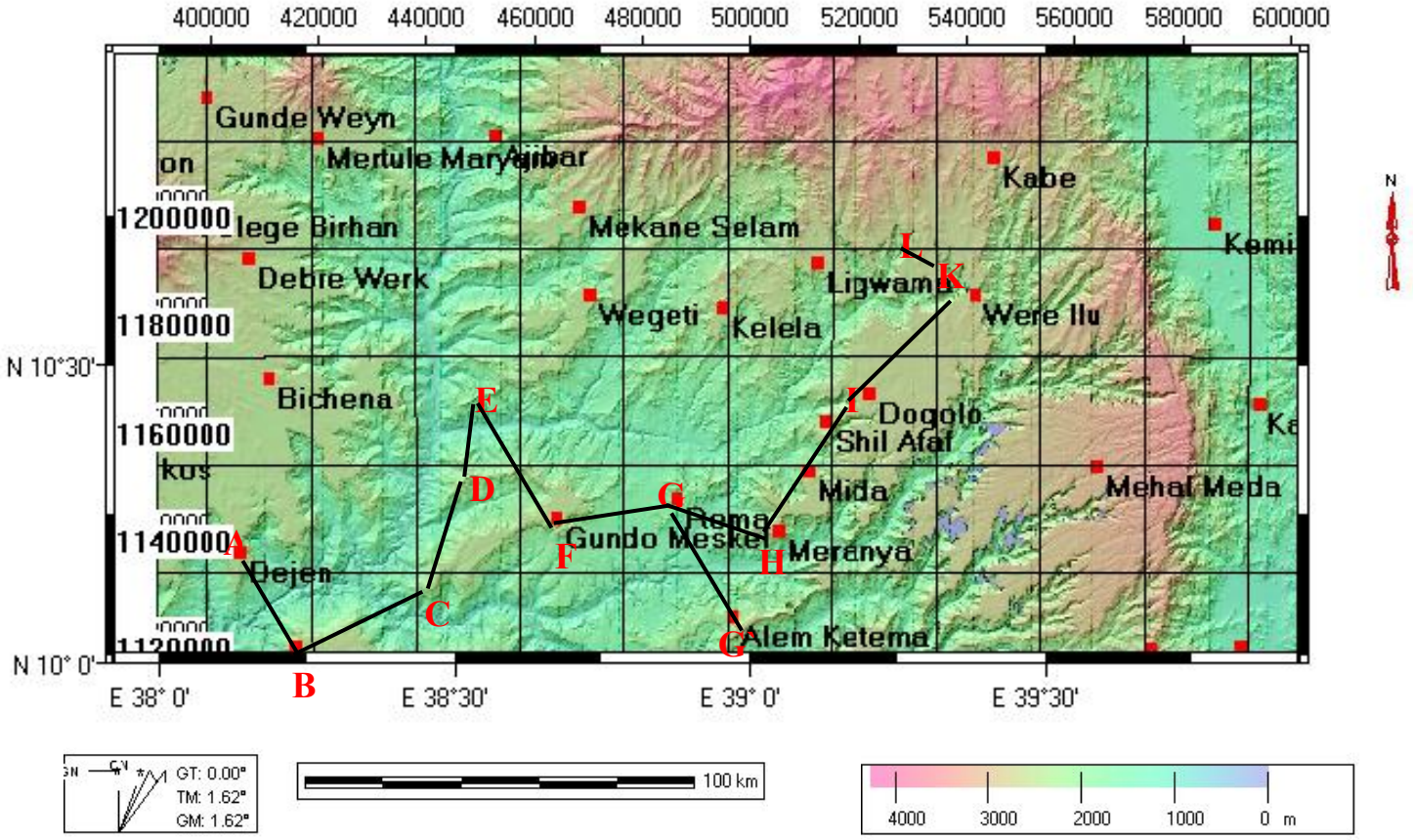

Fig. 4.9 DEM of the central and west part of the study area.

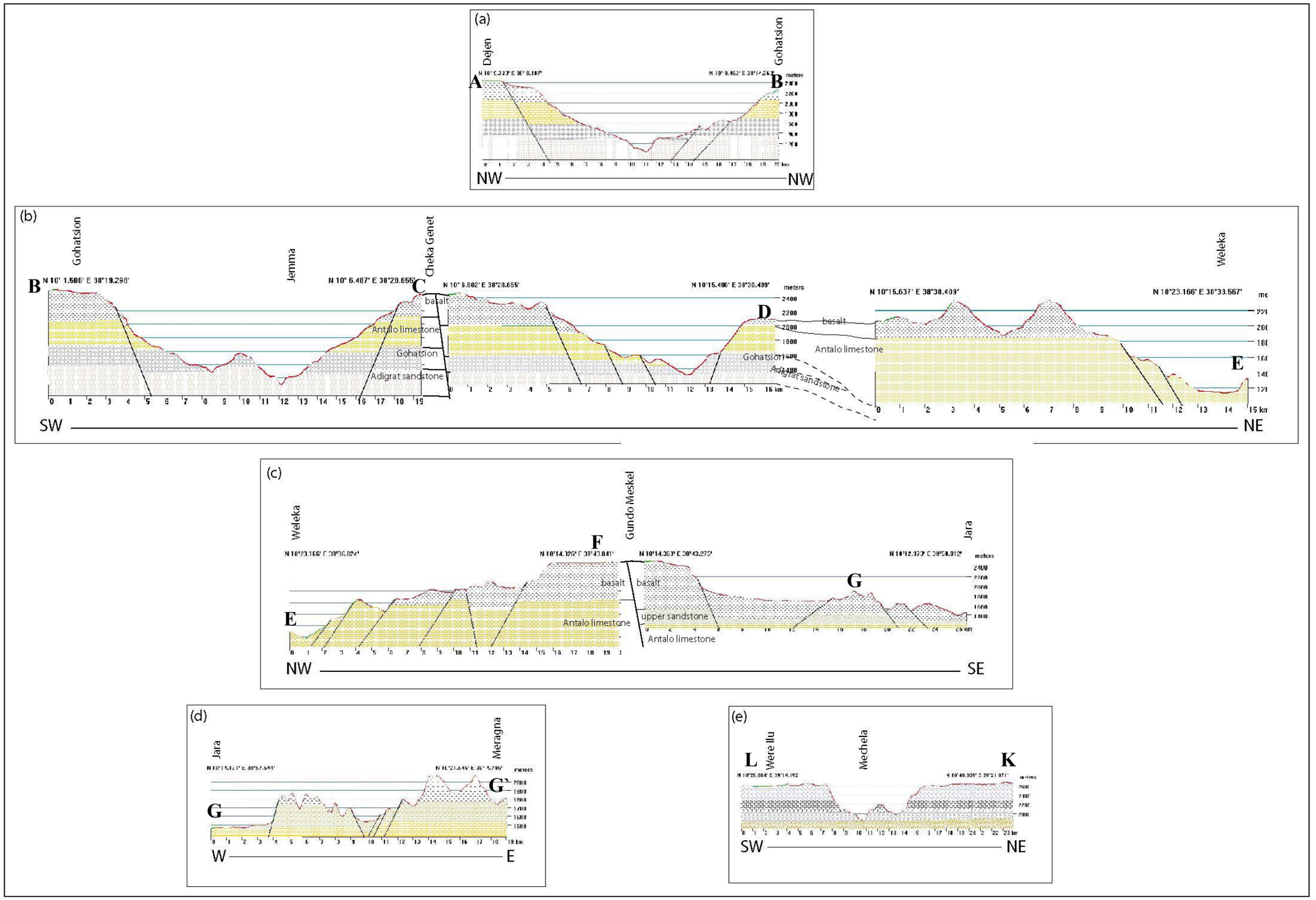

Fig 4.10 Profile section

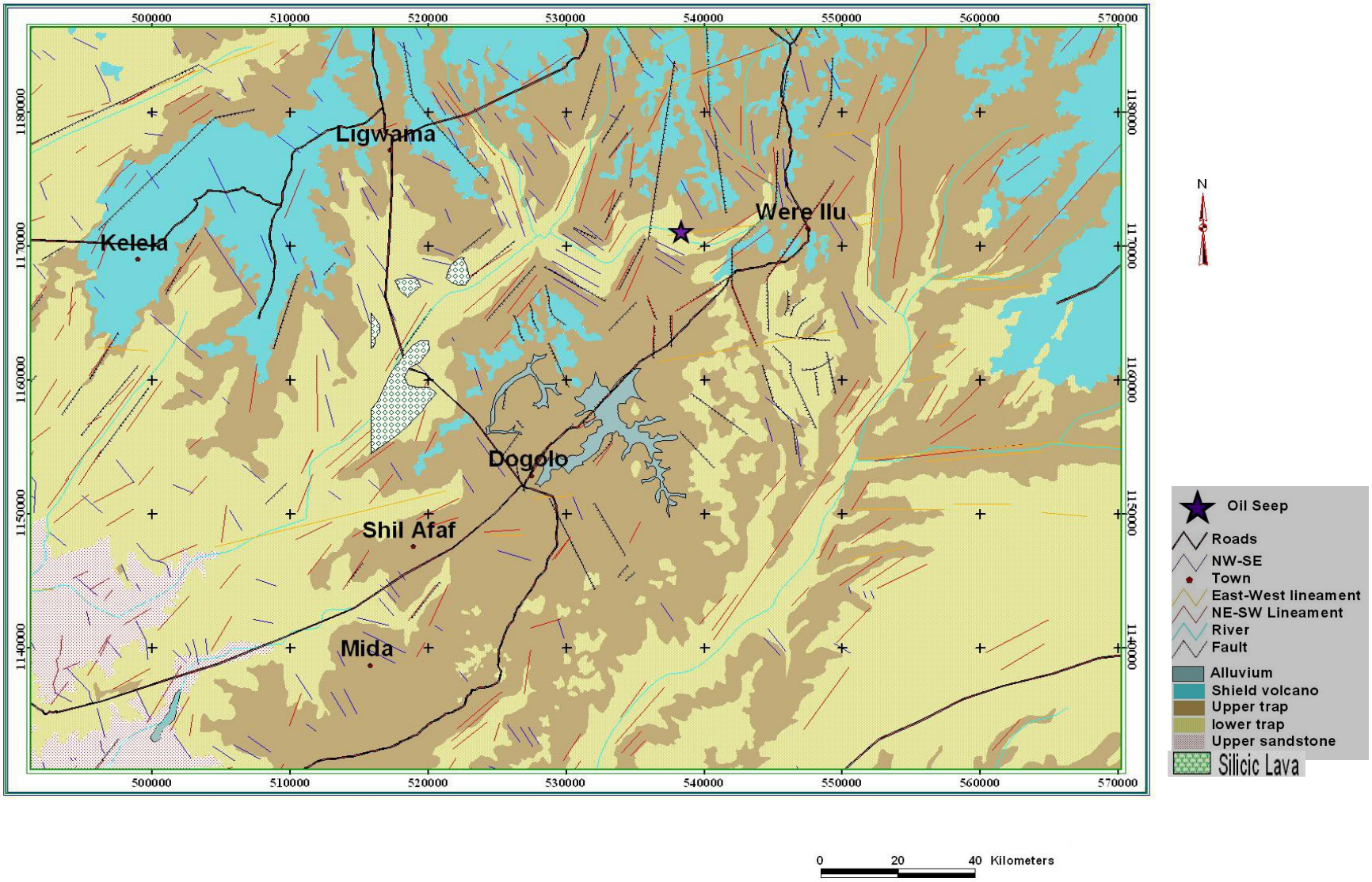

Fig. 4.11. Geological Map of Were Ilu

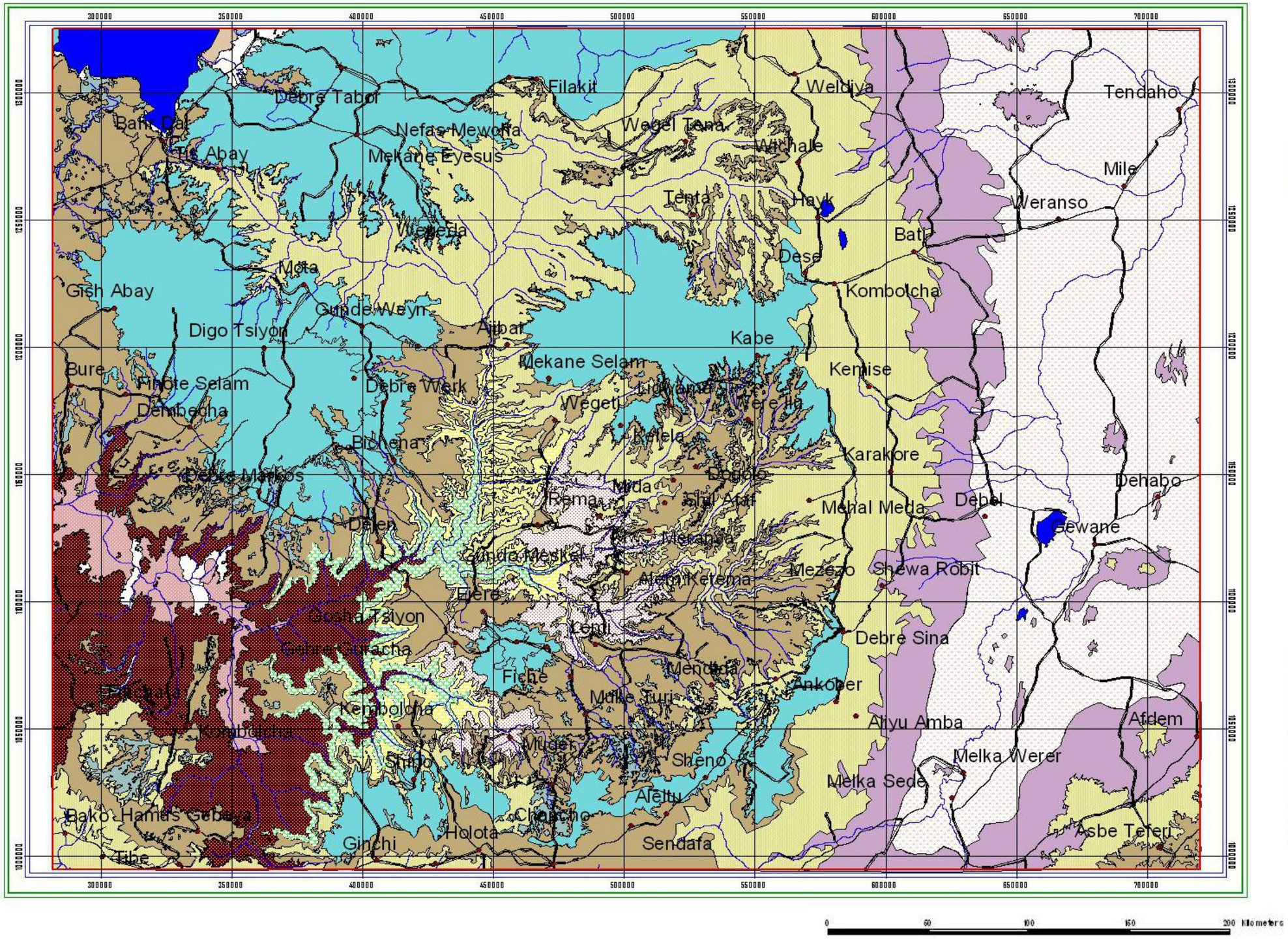

Fig. 4.12. Lithological Map of The study area.

CHAPTER 5

STRUCTURAL MAPPING AND ANALYSIS

5.1. Image Interpretation

The general study area covers parts of the Blue Nile basin in the central plateau, the western rift margin and rift floor. Elevation changes from about 1100m in the Abay valley west of Wereilu, to 3500m near Mehal Meda and falls to about 600m in the Afar floor. The central part of the Ethiopian plateau, covered by the land sat ETM^+ scene 169-53, shows numerous linear features which are not often strongly expressed on the raw satellite imagery due mainly to the lack of significant displacement across most of them. The area is characterized by widespread lineaments developed with three predominant trends: NNE-NE, NW-WNW and E-W.

The general structural pattern in the area shows three, tectonically distinct zones: the rift margin with the outer rift floor, the central area dissected by NE-SW and NW-SE structures and the westernmost part with NW-SE oriented structurally controlled river valleys. The eastern third of the area covers the northern MER margin, part of the western Afar margin and the adjacent rift floor. The boundary area is marked by dense faults cutting Oligo-Miocene flood basalts to produce marginal grabens and tilted blocks, which gradually lower the topography by nearly 3000m. South of 10°20’ N latitude, faults of the rift margin are generally oriented NNE-NE, assuming a NNW-SSE strike north of Kara Kore. The rift floor faults shows both NNE and NNW trends (Fig. 5.1).

5.1.1. NW-SE to WNW-ESE lineaments

Detailed image interpretation exhibits strong, NW-SE and WNW-ESE lineaments, especially in the western and north central parts of the area. Among these, the most prominent are segments of the Blue Nile, Muger and Jema rivers. The landsat ETM^+ imagery reveals the straight nature of some segments of these rivers indicating probable structural control by faults of the same trend. Emerging from Lake Tana, the Blue Nile course makes a big loop

around Mengistu and Choke volcanoes. North and south of these volcanic edifices, the course of the Blue Nile is nearly WNW-ESE.

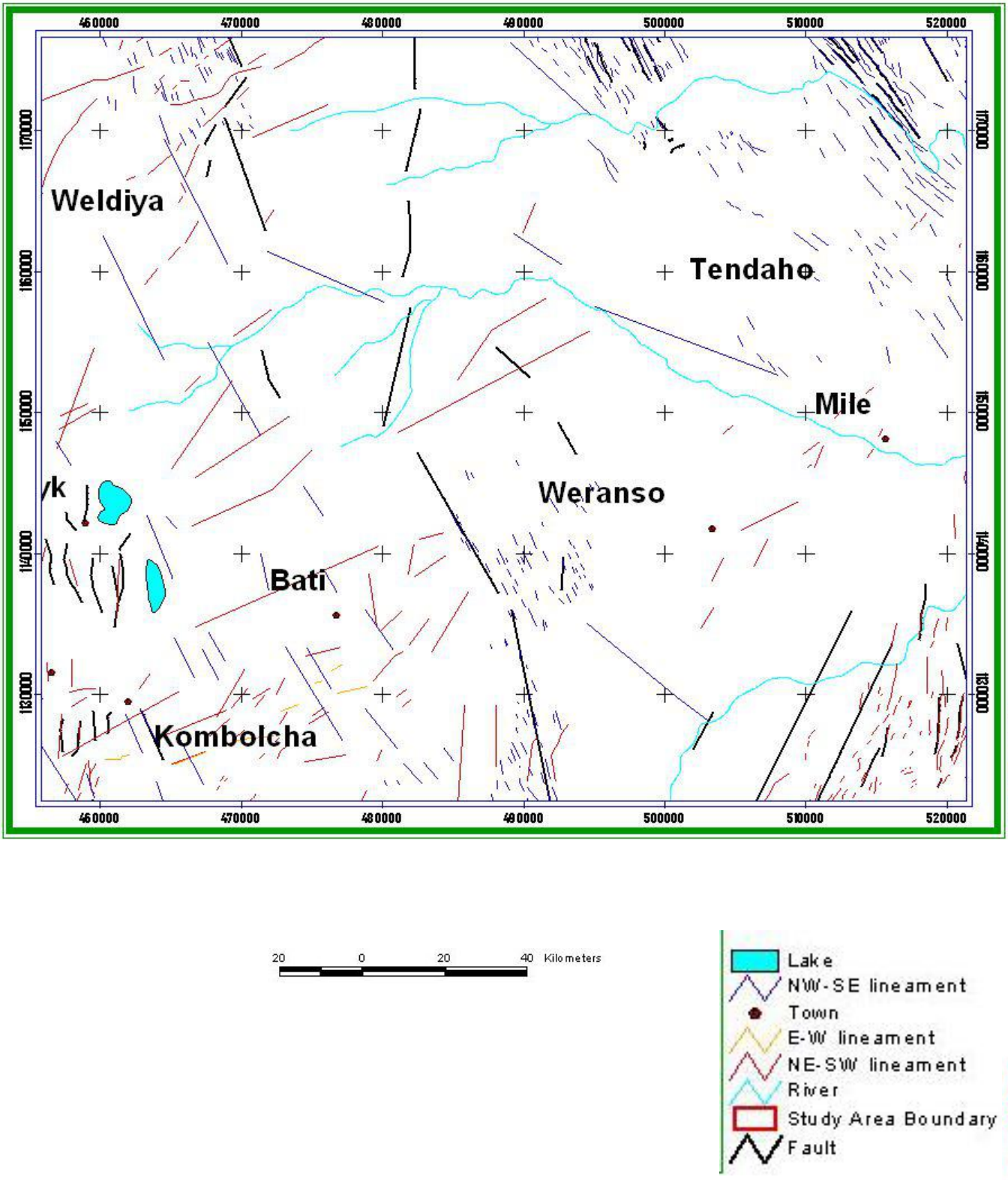

Fig. 5.1. Lineaments identified in the western escarpment of the MER and Afar.

The segments of Muger and Jema before joining the Blue Nile also represent major northwesterly lineaments. The NNW-NW trending fault system of the western Afar margin north of Kara Kore also belongs to this group of faults. North and northeast of Dejen and west of Wereilu, short, NW-SE trending lineaments show crosscutting relationships with the NE-SW faults. Automated strike & dip measurement computed on the digital imagery & DEM data depict these faults in general as striking on the average N40W & dipping to the SW and NE. Co-registered satellite imagery, DEM & lithological GIS ancillary data nearly indicate, these NW-SE trending fault system dissects the whole Stratigraphic sequence in Goha Tshion, Jema river valley, Debre Libanose, Goha Tshion - Dejen & Fincha areas (Fig. 5.2).

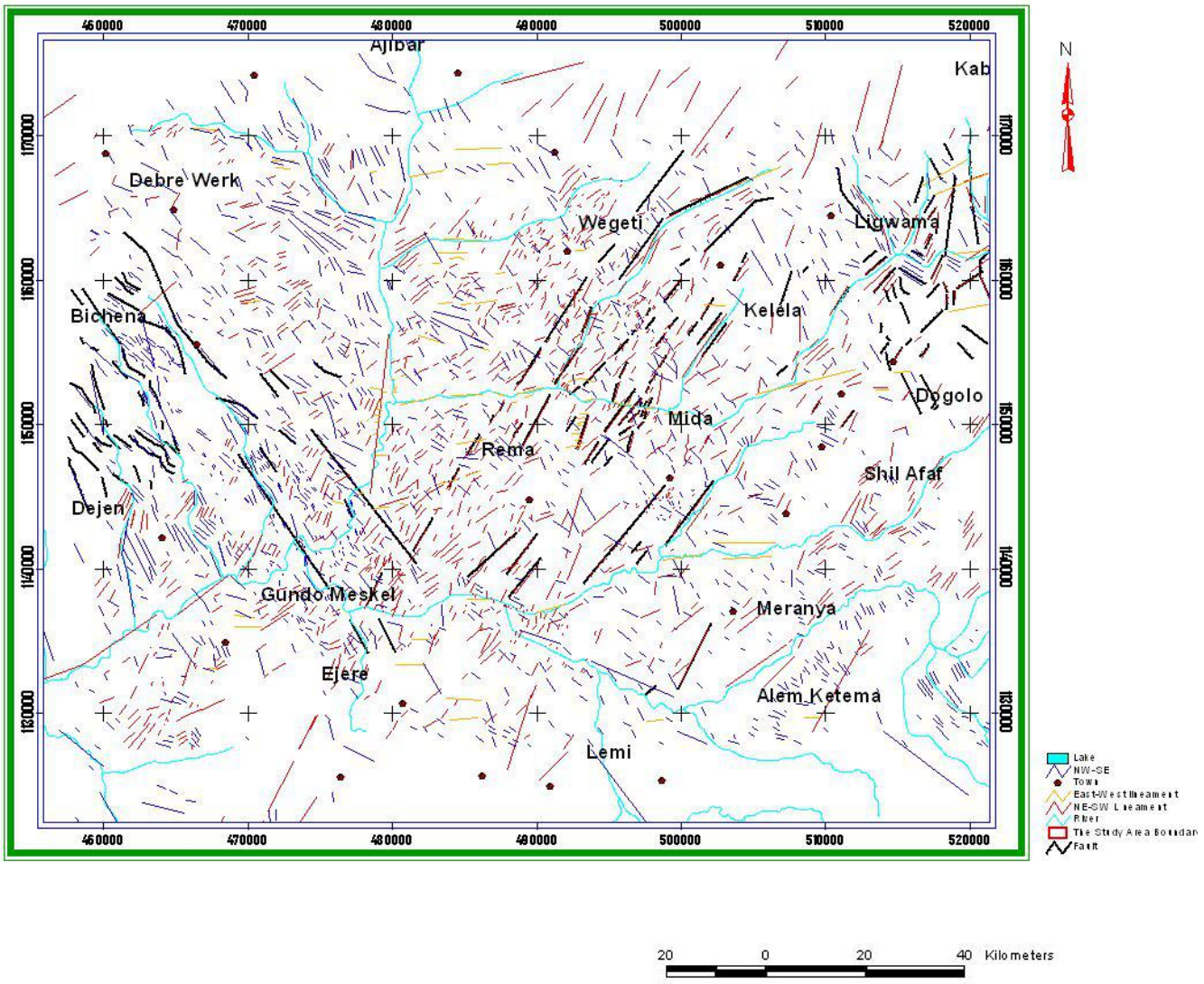

Fig. 5.2 NW-SE and NE-SW Lineament.

5.1.2. NE-SW lineaments

NE-SW lineaments occur in two distinct zones. The first is the transition area between the Main Ethiopian Rift and the southern Afar, whereas the second is restricted to the central part of the area that lies between Jema River and Wereilu (Fig.6.3). In both areas, these set of faults follow the general strike of the boundary fault segments. Automated attitude measurements from Drape landsat ETM^{+} on the SRTM (Shuttle Radar Terrain Model) DEM has demonstrated, that most of these NE-SW faults in the area have an average strike of N40°E and dip both to the SE and NW. Most of these NE-SW faults in the Mesozoic sedimentary rocks of the Abay basin are clearly detected on satellite imageries covered by the overlying Tertiary flood basalts suggesting that they predate the main phase of trap volcanism. In the particular area between Jema River and Wereilu town, NE faults form a 30 km wide zone of sparse faulting, here called the Rema fault zone which extends along strike for over 80 kilometers. Near Wereilu, the fault zone interacts with short NW-SE trending faults forming rhomboidal structures and half grabens.

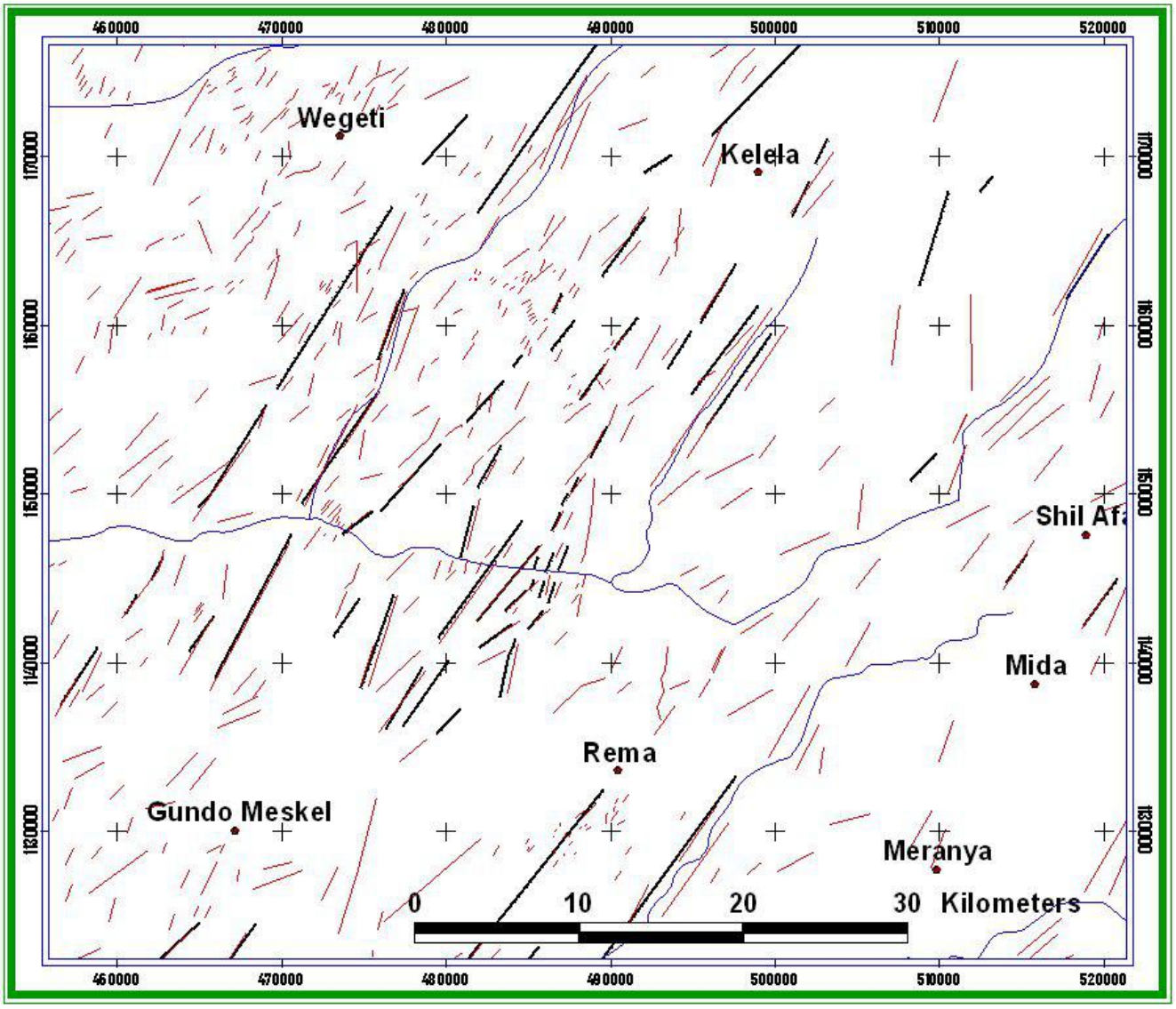

Fig 5.3. NE-SW lineaments.

5.1.3. E-W lineaments

Few, but persistent E-W lineaments are ubiquitous on the whole central Ethiopian plateau. The high pass and directional filters computed on the landsat ETM^{+} band 5 detect lineaments with this trend.

In the southernmost edge of the area, the Ambo lineament is a south downthrown major fault displacing Oligo-Miocene volcanic rocks of the trap series (Woldegebriel et al., 1990). The other prominent east-west line controls the course of the Weleka River (Fig. 5.4). This can be traced eastwards through discontinuous segments up to Mehal Meda. Farther north, in the central area, a more or less continuous east-west lineament cuts the Tertiary flood basalts north of Akesta. The fourth notable lineament passes near Debre Zebit town, east of Lake Tana.

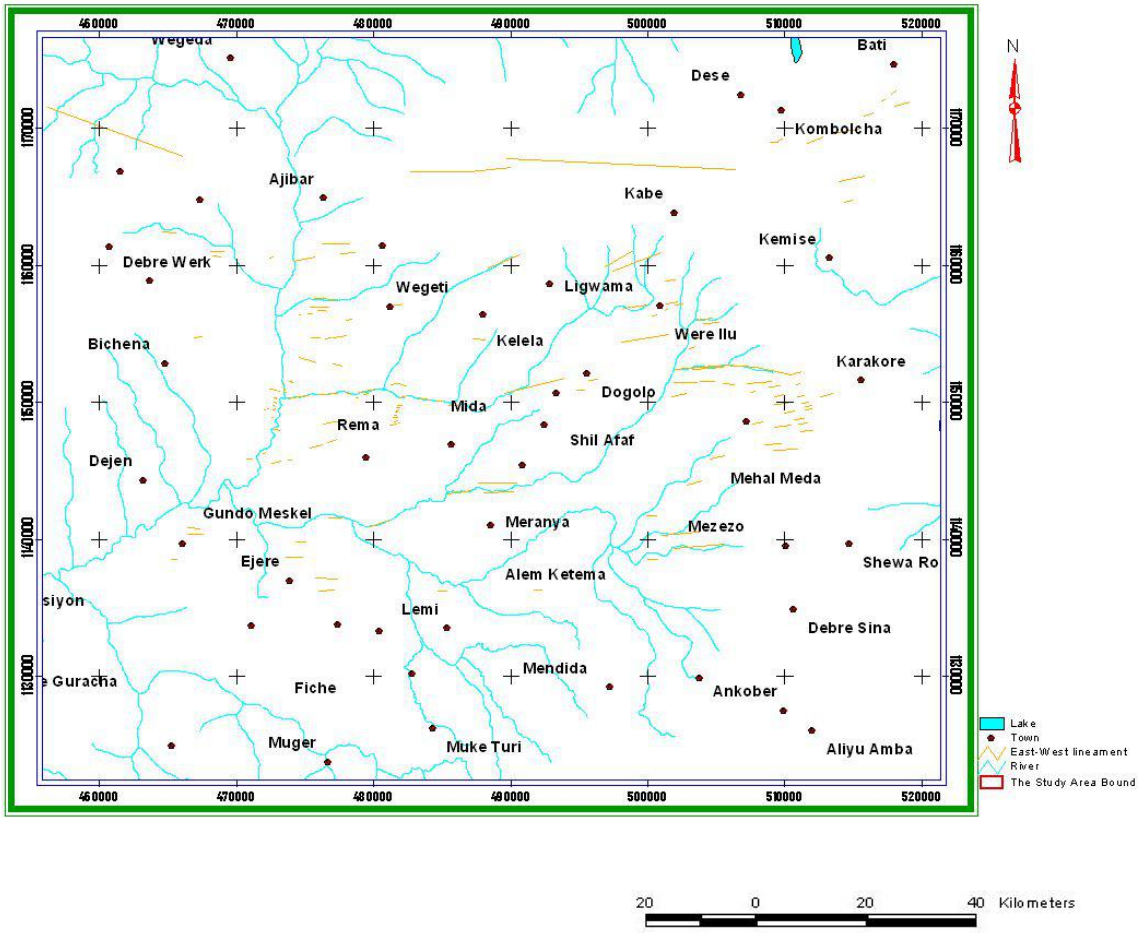

Fig. 5.4. E-W running lineament in the study area.

5. 2. Field Structural Mapping

In addition to structurally controlled lineaments and major faults identified from satellite imagery and Digital Elevation Model (DEM) interpretations, faults, systematic joints and dykes have been mapped during the field survey. The general description of the structures follows geographic criteria, starting from the eastern sector of the investigated area. A discussion on the structural relation between different faults will follow the descriptive sections.

The eastern side of the area is dominated by the tectonics in Afar and northern Main Ethiopian Rift (MER). The MER constitutes the northernmost part of the EARS, connecting the latter with the Afar triple junction where the Gulf of Aden and the Red Sea also meet. Extension in the Gulf of Aden and southern Red Sea commenced soon after flood basalts volcanism around 31 Ma whereas, the MER started to develop in the Mid-Miocene time at about 11-12 Ma (Davidson and Rex, 1980; Woldegebriel et al., 1990; Chernet et al., 1998, Wolfenden et al., 2004) following a broad doming centered on the present Afar depression (e.g. Ebinger et al., 1989). The generally NW, E-W and NE trends of the Red Sea, Gulf of Aden and East African Rifts control the rifting process in Afar, respectively.

In the central area between Dejen and Wereilu, numerous, small displacement faults have been mapped as a continuous zone of deformation (Figs. 6.3 and 6.4). Two orthogonal fault sets, namely the NE-SW set between Jema River and Wereilu and the NW-SE well developed on the edges of the previous fault zone, are the dominant structures affecting Mesozoic sediments and Cenozoic flood basalts.

The NE-SW fault zone is up to 30-40 km wide and 80 km long consisting of sparse, low displacement faults cutting across the Antalo limestone, the Upper sandstone and mildly the lower part of the trap basalts. Individual faults which are oriented N 35°-40°E, are often segmented and attain cumulative lengths which may exceed 50 km. They dip both to the NW and SE and show surprisingly small vertical displacements of only 5 to 10 m. Farther north in around Wereilu, this trend starts to loose its topographic expression and the entire fault zone dies south of the volcanic shields around Akesta and Guguftu. However, east of Wereilu, it continues northwards as linear river valleys in the upper course of the Jema valley. Interaction of small NS to NNE trending structures with NW-NNW structures west of

Wereilu town produced a graben with a strike varying between NNW and NNE. These structures are observed cutting the trap series.

The second major fault system, which is less developed than the NE-SW fault system comprises NW-SE trending faults east and north of Dejen and southwest of Were Ilu. They prevail around the town of Dejen west of the Jema-Blue Nile confluence. On the average, these faults strike N 320°E and they are west or east downthrown. This group of faults is relatively young compared to the NE-SW faults. They displace the entire volcanic succession whereas the NE-SW faults only slightly affect the basal part of the trap series. Another significant difference between the two fault sets is the fact that most NE-SW fault are long and with throws of a few meters to a few tens of meters, whereas the majority of the NW-SE faults are short and have large displacements. On a traverse taken across the Jema River, along the road between Gundo Meskel and Fiche, a small NW-SE graben shows a spectacular displacement of the Tertiary volcanics. These flood basalts, lying directly on the Antalo limestone are displaced by about 600m as seen on the southern side of the Jema valley. South and southeast of Mengistu volcano, this structural direction produced horsts, grabens and half grabens in the Tertiary volcanic succession.

Except the northwesterly faults around Dejen, the western part of the area is devoid of faults. The only significant lineaments are the northwesterly segments of Jema and Blue Nile. Outside the rift floor, Tertiary tectonic activity in the study area is limited to the Dejen and Rema fault zones.

East-west lineaments detected on satellite images do not exhibit clear topographic expressions in the field. The only sign of fault displacement is observed across the Weleka river valley where negligible displacements along a once, north-dipping fault occurred.

During the field survey, an E-W striking fault system that cut the lower trap unit and runs parallel to the basaltic dykes swarms North of Kabe town is observed. This fault system cuts the area at a regular interval and controls the local attitude of beds. About 10 Km south of Werilu a south dipping E-W fault caused a local tilt of strata by about 7^0 to the north.

Two sets of dyke orientations were measured in the study area. These are, on the average NNE (N 15-25^0) and ENE (N70-80^0). The ENE dykes observed near Kabe Village (Fig. 5.5)

ID	Easting	Northing	Strike	Dip	Altitude	Depth	Remark
1	561084	1214509	N 25 E	N85	3058	10	Weathered & Intermediate to felsic
2	561084	1211912	N 20 E	70	3195	3	Columnar, Horizontal joint basalt. Backing effect observed.
3	560009	1208688	N 15 E	75	3448	4	Several parallel dykes with regular spacing.
4	551283	1197414	N 80 E	N 35	2122	1	Basaltic (apharic) highly weathered.
5	551283	1197409	N 70 E	N 40	2122	1	Basalt
6	551283	1197402	N 75 E	N 49	2122	1	Multiple injection 80 cm + 20 cm
7	551283	1197399	N 102 E	N 75	2122	1	Multiple injection
8	551283	1197390	N 80 E	N 45	2122	1	

Table 5.1 Table presenting the measurement and characteristics of dyke swarm studied during the field survey.

form swarms of few centimeters to meters wide with spacing of the order of 3 meters. Around Akesta, another set of dykes trending ESE (110^0) was observed. Some of the dykes show multiple phases of injection and they are predominantly basaltic in composition. The similarity in attitudes of faults and the dykes is consistent with the same kinematic history.

Fig. 5.5. Dikes close to Kabe village.

Several joint sets developed in Antalo limestone and the upper sandstone whereas those affecting the flood basalts are not systematic. Variable joint orientations of $N20^0E$, $N60^0E$ and E-W were measured in the Abbay river valley on the limestone and they show variable dips of 80^0-85^0. Joints observed on the upper sandstone are sub-vertical (87^0-$90^{0)}$ with preferred orientations of $N70^0E$ and 140^0E. In the Mechela river where oil seepage is observed, two major set of joints were measured, the dominant and persistent trend being $N110$-125^0E.

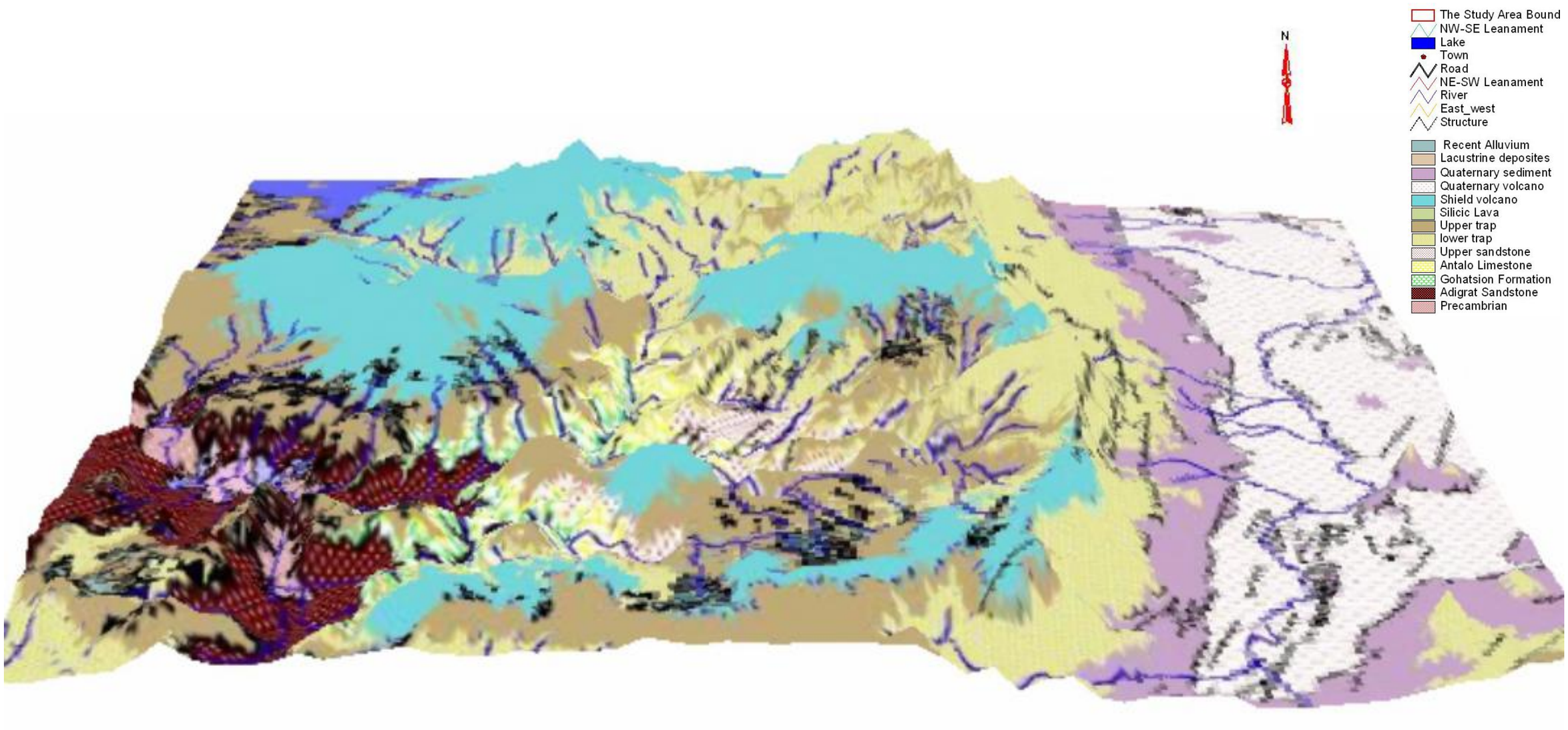

Fig. 5.6 Digital Terrain Model of the study area, presenting the general morphology, structure, lithology , and geology.

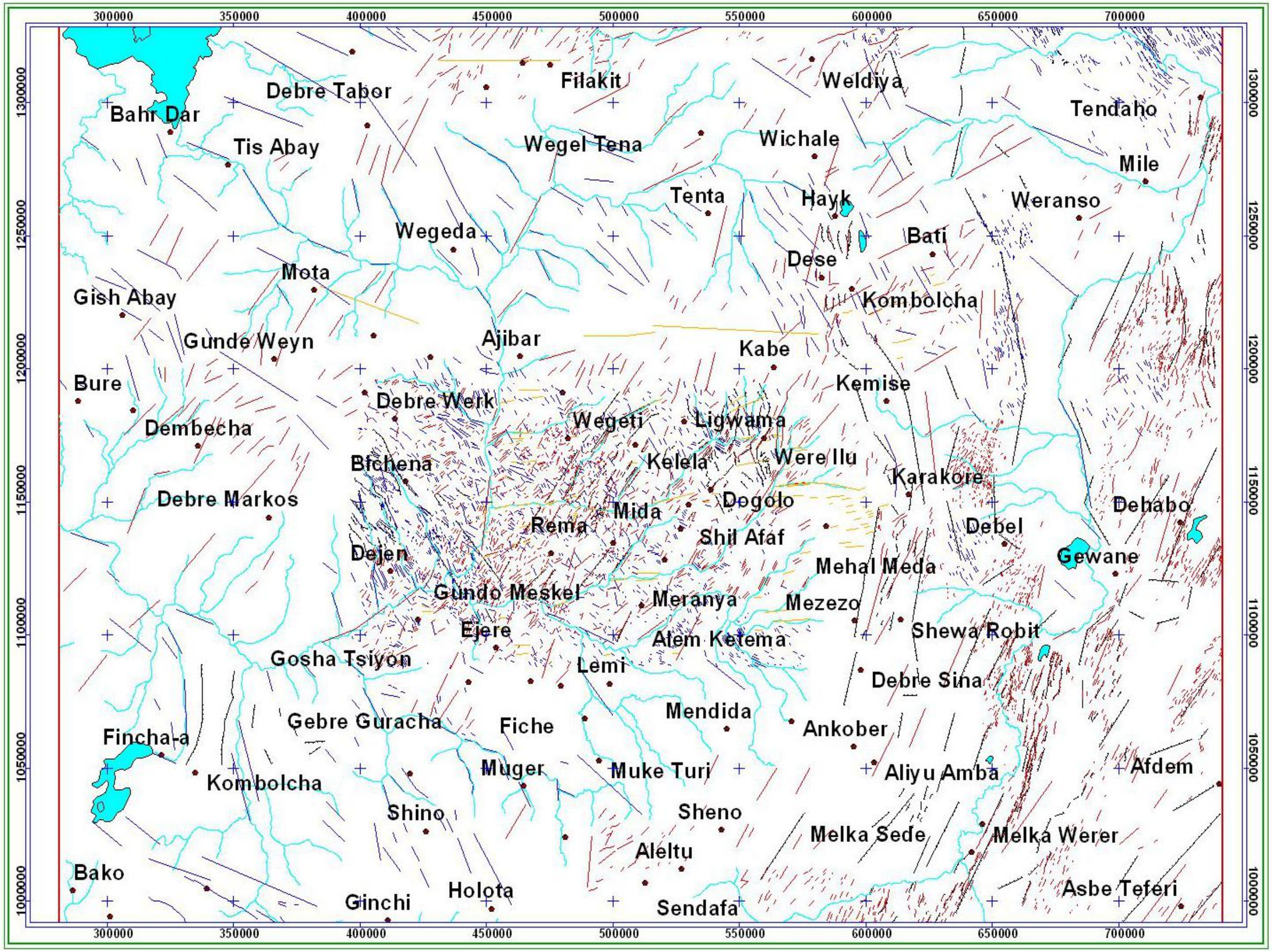

Fig. 5.7. Structural map of the study area.

CHAPTER 6

CONCEPTUAL MODEL AND DISCUSSION

6. 1. Structural and Stratigraphic Interpretations

The structural framework of a given sedimentary basin is related to and determined by the regional tectonic framework in which it develops. The discussion here focuses on the deformational and sedimentation history of the Blue Nile basin. The stratigraphic sequence to be reviewed is limited to the Triassic-Liasic Adigrat sandstone & younger rocks of the basin.

The following general interpretations have been drawn on the basis of standard remote sensing & GIS techniques, field observations, stratigraphic columns and geological cross sections.

The Precambrian basement anisotropy in Ethiopia is known to have strongly influenced later tectonic and sedimentation events (Bocalletti et al., 1998, Korme et al., 2004 and references therein). In Ethiopia, four major fault systems (N-S, E-W, NW and NE) inherited from the Precambrian (Pan African) structure are recognized (Korme et al., 2004 and references therein). The initiation of Cenozoic rifting in the Horn of Africa also seems to influence the youngest episodes of faulting outside the rift in the study area.

With the aim of understanding the petroleum potential of the area, emphasis for detailed field investigation has been given to the central part of the area which provides a unique sedimentary and tectonic setting marked by a distinct sub-basin and intermittent faulting.

Field relationships among the various trends and their effects on the Mesozoic and Cenzoic succession clearly suggest that the various trends experienced episodic reactivation. Supporting evidences for this come from the central part of the area between the Afar margin and Dejen which shows the youngest fault activity. Two orthogonal sets of faults of NE-SW and NW-SE orientations are evident from image interpretation and field survey. The NE-SW fault zone (here named the Dera fault zone), is predominant between Jema river and Wereilu and experienced intermittent reactivation. The absence of the Upper sandstone west of the

Dera fault zone demonstrates the existence of a high barrier (possibly grabens, half grabens and horst) separating this sub-basin from the western side prior to the deposition of the Upper sandstone and made the Blue Nile basin to deepen toward north east direction. Another episode of reactivation dissected the sandstone and the basal part of the Tertiary flood basalts.

In the vicinities of Dejen and the Blue Nile-Jema confluence, NW-SE faults persistently dissect and produce large displacements of up to 600m in the volcanic sequence. These faults trends have the same orientations with the fracture that are found at the Mechala river, which probably affect the reservoir rocks that accumulate the oil.

The NE-SW faults in the Jema-Wereilu area are parallel to the border faults in the transition between MER and Afar which suggests possible reactivation in time of rift initiation in early Miocene. The former is parallel to the transition zone between the MER and Afar. The NW-SE striking fault zone around Dejen and Wereilu imitate the NW-NNW strike of the western Afar border faults north of Kara Kore. The NE-SW faults are responsible for creating the Dera sub-basin which was already isolated from the Abbay sub basin during the deposition of the Cretaceous upper sandstone which misses from the succession west of the Dera fault zone.

The E-W lineaments controlling some of the major drainage lines (e.g. Weleka) show poor topographic expression. Taking only the latest structural events as seen from the current fault geometry and pattern which are evident in the Landsat imageries, these E-W lineaments are cut by NE-SW faults which, in turn are affected by the NW-SE faults.

The cross sections reveal the pinching out of the Gohatsion Formation from the SW to the NE direction in both the Abbay and Dera sub basins. In contrast the Antalo limestone becomes thicker towards NE achieving its maximum observed thickness of 728 m in the Weleka river section of the Abbay Sub basin. This implies that a thicker sequence of Antalo limestone may lie beneath the Trap basalts of Were Ilu where the seepage of petroleum is observed. It can also be concluded that the Blue Nile basin deepens towards the NE direction.

Generally it can be concluded that faults trending NE-SW, NW-SE and in some cases E-W, played a vital role in determining basin development by defining the basin and sub basin boundaries, forming structural depressions and highs (grabens, half grabens and horsts) which

in turn may have influenced the localization of sediment accumulations and subsequent erosional activities.

Based on the observation referred to above and with reference to the previous work, the structural configuration of the Blue Nile basin can be placed as follows:

1. The NW-SE extensional stress of Gondwanaland associated with extensive crustal break up initiated a number of rift zone in eastern Africa (Bosellini 1989, 1992). Some of them developed into oceans like the Indian ocean while few of them aborted and acts like as an aulacogen. The Blue Nile basin is one of such aulacogen.

2. The Blue Nile basin might have been the site of a hidden Paleozoic and Mesozoic rift system, which has been filled with great thickness of Karoo sediments (Bosellini, 1989, 1992 an Russo et al., 1994) active since the Carboniferous into the Middle Jurassic.

3. During Liassic to Triassic, Adigrat Sandstone Formation deposited in the Blue Nile basin. An early transgression during Liassic to late Bathonian would have deposited the Gohatsion Formation, followed by a major transgression during Callovian to early Oxfordian resulting in the Antalo Limestone sequence. The sea began to withdraw from the Horn of Africa from the late Jurassic to early Cretaceous resulted in the deposition of the Upper Sandstone (Russo et al., 1994).

4. The NE-SW trending rifts may have acted as planes of weakness in the Blue Nile basin and have been reactivated intermittently from Jurassic to Miocene. Movement along these major faults resulted in a complex structural history that led to the formation of several deep-fault bounded troughs. These fault systems play a vital role for the vertical movement of the Blue Nile basin and significant amount of sediment accumulation during various stages of basin development. The NE-SW faults are responsible for creating the Dera sub-basin which was already isolated from the Abbay sub basin during the deposition of the Cretaceous upper sandstone which misses from the succession west of the Dera fault zone.

5. The most recent rifting and opening phase started in the late Eocene and led the development of the Red Sea, Gulf of Aden and East Africa Rift system.

6.2. Conceptual model

Based on a synthesis of the possible effect of the faults, taking into account episodic reactivation characteristics of the major faults, the Geodynamic stages and events proposed to the Blue Nile basin by Russo et al.,(1994) and the stratigraphic and structural interpretations presented in chapter 5 and chapter 6, a conceptual model for the development of the Blue Nile basin is proposed below. This model indicates the Blue Nile basin has a general asymmetric geometry shape and as well as divided it in two sub basins. However, it should be noted that in the absence of adequate geophysical data, nonexistence of borehole data and inadequate surface and subsurface control, the model should be considered as a conceptual interpretation of the subsurface depending only on surface geological data. The stratigraphic and structural evolution of the Blue Nile basin occurred in the following stages (Fig. 6.1):

Stage 1: Peneplation and denudation of Basement rocks. Fractures were developed at the end of the period as a precursor for Karoo rifting.

Stage 2: "Karoo rifting" followed by the deposition of the Calub sandstone, Bokh Shale and Gumburo sandstone at early rifting stage. Adigrat sandstone was deposited at the syn-rifting stage.

Stage 3: Further subsidence resulting in early transgression event depositing the Gohatsion formation. From Callovian to Oxfordian a major transgression caused the deposition of Antalo limestone which was followed by regression sequences that deposited the Upper sandstone in the Blue Nile basin.

Stage 4: The NE-SW faults are responsible for creating the Dera sub-basin which was already isolated from the Abbay sub basin during the deposition of the Cretaceous upper sandstone which misses from the succession west of the Dera fault zone. Further subsidence and rifting followed by Basement uplifting with subsequent erosion that caused the removal of probably very thin sequence of Upper sandstone from the Abbay sub basin.

Stage 5: During Alpian to Apatian time, rejuvenation of older faults resulted in complex horst-graben structures which may later reactivated along the East African Rift system.

Stage 6: Volcanic activity outpoured the plateau basalts and shield volcanoes. Further subsidence, uplift, rifting and erosion has caused the present geomorphologic setting of the Blue Nile basin.

In conclusion, the structural and stratigraphic interpretations and the conceptual models show that there is a thickening of the Antalo Limestone sequence from southwest to Northeast implying a general basin deepening in the same direction. Moreover, the oil seepage at the Mechela river is associated with the NE-SW and NW-SE faults close to Were Ilu. Considering the sub-horizontal nature of the sedimentary strata and the thickness of the entire volcanic succession (ca. 800 m), the upper surface of the reservoir must be encountered at a shallow depth.

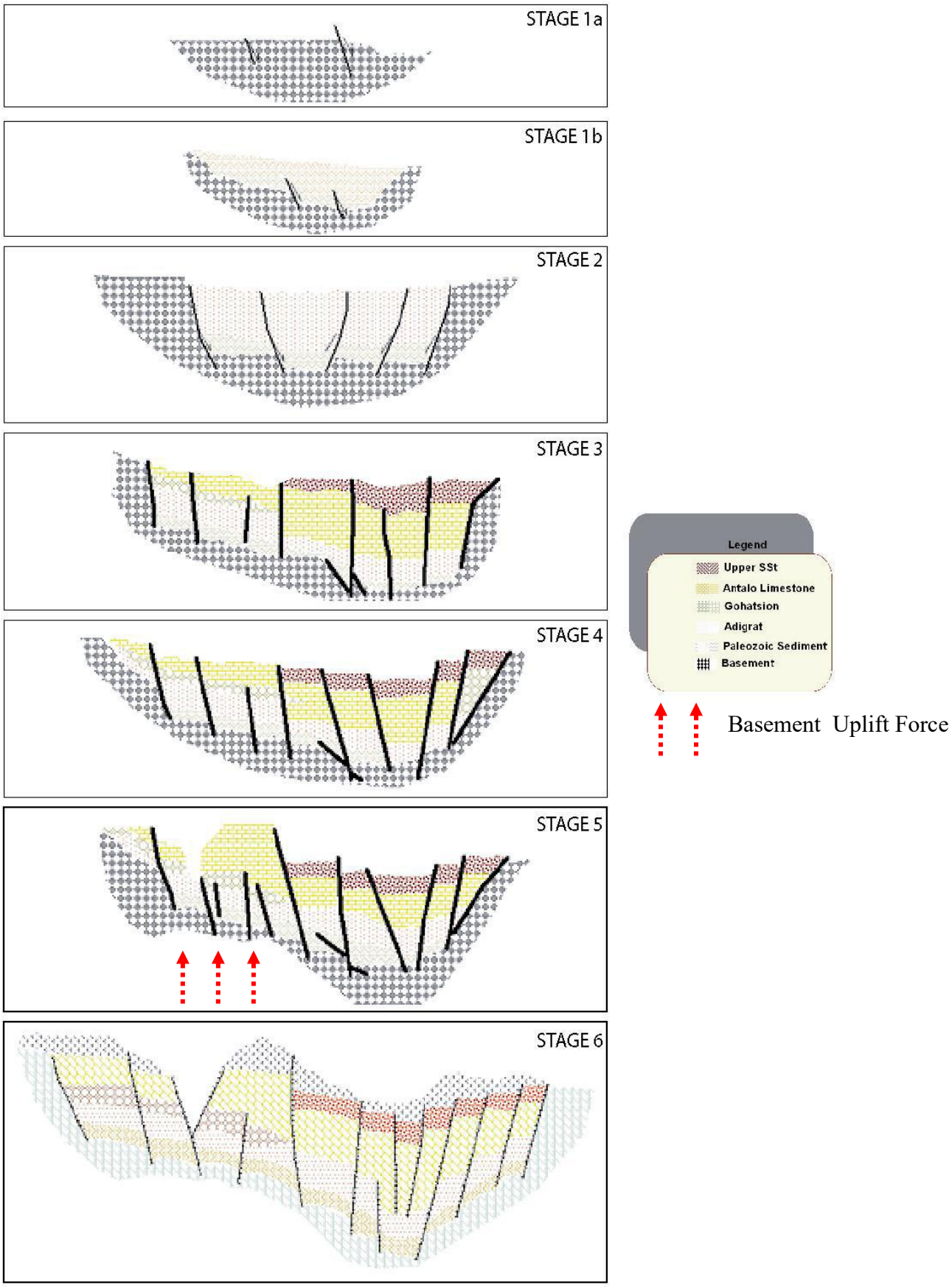

Fig. 6.1. Conceptual Model of the Blue Nile basin.

6.3 Implications to Petroleum Potential of the Blue Nile Basin

The assent of the oil seepage at the floor of the Mechela River is associated with dominantly NNW oriented fractures (Fig. 6.2). It has been reported earlier by Wolela Ahmed (2004) that in the Blue Nile basin there are four potential petroleum source rocks (the Antalo limestone, the Gohatsion formation, the dark to gray shale of the Karoo sediments and interbeds of carbonaceous material in the uppermost part of the Adigrat Sandstone formation).

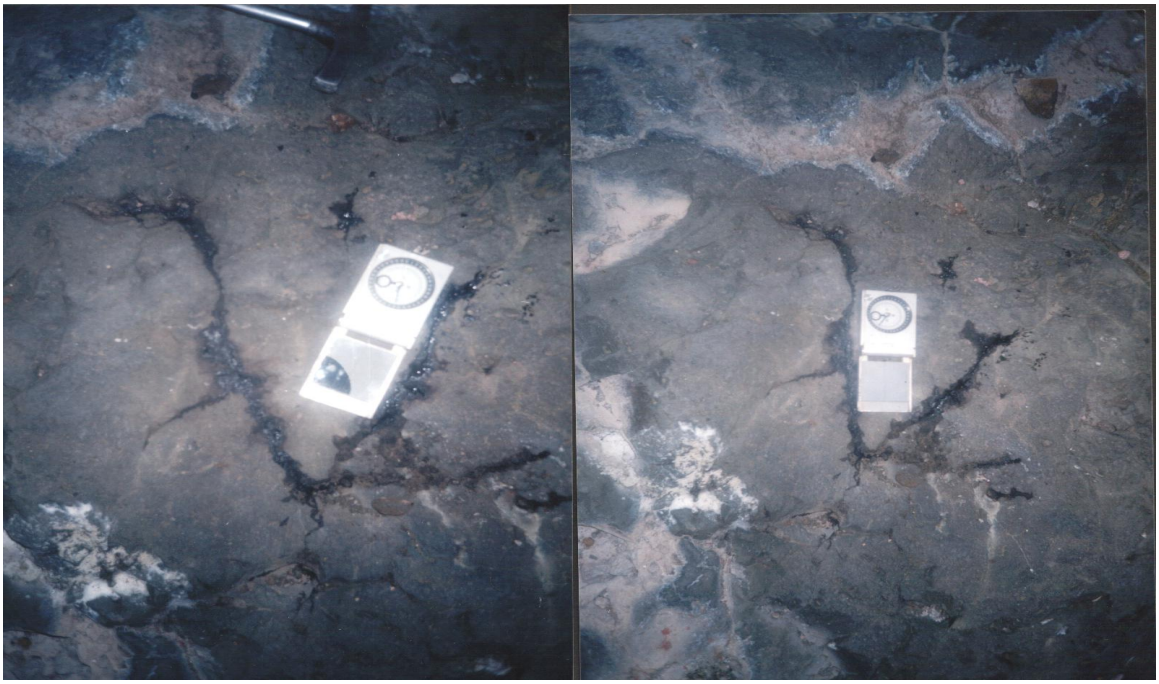

Fig. 6.2. Oil seepage along fractures at the Mechela river bed.

The structural and stratigraphic interpretations imply that the Antalo limestone should be given emphasis as potential source rock among the above indicated formations, for the oil seepage at the Mechela river.

Wolela Ahmed (2004) indicated that the black shales in the Antalo limestone are probably the sources of petroleum in the Blue Nile basin. However, the depth of occurrence of the black shale layers in the Dejen section is found out to be only 459m from the present day surface. This shallow burial depth makes the shale immature to generate oil as it is far below the optimum depth range for the formation of oil which is given at about 1.2 Km (Tissot, 1974).

However the structural interpretations and models suggest that the Antalo limestone sequence thickens towards the NE and may have been affected by both the NE-SW and NW-SE faults

resulting in a significant downward displacement which together imply an optimum depth of occurrence of the limestone (at least greater than 1.2 Km) for the generation of oil. This is corroborated by the stratigraphic columns of the area, which indicate that the Antalo limestone is found at the depth of 1800 meters beneath the Werilu oil seepage. In conclusion, the Antalo limestone unit could be the best source rock potential for oil generation in the area.

The upper sandstone, which gets coarser upwards and becomes conglomeratic, exhibits good reservoir quality at the top part (Wolela Ahmed, 2004). In addition to the Upper sandstone, the highly brecciated agglomeratic basalt that overlay the sandstone could as well be good reservoir. The highly fractured Trap basalt is associated with basic volcanic agglomerate associated with late Cretaceous conglomeratic sediments. The finding of economic oil accumulation from basic volcanic agglomerate associated with basaltic flows intercalated with late Cretaceous sediments in the interior coastal plain region of Texas (Conybeare, 1979) may be a good support for this conclusion.

Significant oil accumulation can be accumulated in oil traps. Structures could be major trapping mechanisms in the study area. The NW-SE faults, which may have created down warping structures, could be considered as effective oil traps. Moreover, the intersecting NE-SW and NW-SE faults in many localities in the study area may have resulted in a wide variety of structural traps such as step fault blocks, horsts, grabens and half grabens. These structural traps which may have been formed before or concurrent with oil migration period can be considered as suitable traps for significant oil accumulation in the Blue Nile basin.

However, it should be noted that the pinching out of some facies (mainly the Gohatsion formation) might have provided significant stratigraphic traps. The presence of shales and claystones which may act as sealing (cap) rocks should also be stressed in this connection. Lateral variation and inter-fingering of units are also observed as interesting factors contributing to the possible stratigraphic traps. Generally, combination of structural and stratigraphic traps is the possible oil trap in the Blue Nile basin.

CHAPTER 7

CONCLUSION AND RECOMMENDATION

7.1 Conclusion

This study was intended to improve the geological information available in the central and North western plateau of Ethiopia and the lithological and structural knowledge for further petroleum exploration in the Blue Nile basin. Using the satellite imagery in collaboration with remote sensing and GIS Data integration techniques; a number of geological features has been identified and separated into map products such as rock type, lineaments, faults, and others. In connection with these different maps have been generated; the lithological map, the structural map and the geological map. With reference to the result obtained from the structural interpretation and lithological description; various representative stratigraphic columns, profile sections, and finally conceptual model have been produced that indicates the blue Nile basin evolution.

By visually interpreted the enhanced image distinction has been made on the co-registered image data and DEM data among the basement complex, the Mesozoic sedimentary sequence and the tertiary volcanic cover. The upper trap, lower trap and the shield volcanoes have been identified by their distinct tonal variations, with subtle slope breaks on the cliff faces, texture and drainage pattern. In the Mesozoic sedimentary sequences of the study area, lithological boundaries are easily recognized yielding more information on the imagery, especially, in the Abbay canyon, Jemma and Mugher river valleys.

This work also addresses the spatial and temporal relationships between lineaments and faults identified in the study area as interpreted visually from the enhanced Landsat ETM+ and the DTM. The work identified, the central part of Ethiopia is characterized by wide spread lineaments developed with three predominant trends: NNE-NE, NW-WNW and E-W. The NW-SE trending faults crosscut some of the northeast faults and the entire trap series indicating their youthfulness. The NE-SW faults only slightly affects the basal parts of the trap series. Most of

the NE-SW faults are long and with throws of a few meters to a few tens of meters, where as the majority of the NW-SE faults are short and have large displacement. In addition, structurally controlled lineaments and major faults are identified from satellite imagery and DEM; faults, joint systems and dykes are described as was documented during the field survey.

The work put emphasize on the temporal relationships of structures acted as planes of weakness in the Blue Nile basin and have been reactivated intermittently from Jurassic to Miocene. These fault systems are parallel to the border faults and are responsible for creating the Dera sub-basin which was already isolated from the Abbay sub basin during the deposition of the Cretaceous upper sandstone which misses from the succession west of the Dera fault zone. The profile sections reveal the pinching out of the Gohatsion formation from the SW to NE directions both in Abbay and Dera Sub basins. In contrast the Antalo limestone becomes thicker towards NE achieving its maximum observed thickness of 728 m in the Weleka river section of the Abbay sub basin. This implies that thicker sequence of Antalo limestone may be beneath the trap basalts of Wereilu where the seepage of petroleum is observed. It can also be concluded the Blue Nile basin deepens towards the NE direction. Moreover, this analysis discus on faults trending NE-SW, NW-SE and in some cases E-W, played a vital role in determining basin development by defining the basin and sub basin boundaries, forming structural depressions and high (grabens, half grabens and horsts) which in turn may have influenced the localization of sediment accumulations and subsequent erosional activities.

In the final analysis, a schematic conceptual model is prepared based on the data integration approaches from previous works and the result obtained from structural and Stratigraphic interpretations. The Model shows evolution of the Blue Nile basin, the sedimentation process and the possible effect of the structures in basin evolution. It is constructed with six general schematics draw of the basin's configuration and tectono-stratigraphic evolution developmental stages.

The final analysis, in addition explains important implications to petroleum potential of the Blue Nile basin, besides the oil seepage at the floor of the Mechela river. Taking into consideration the structural and stratigraphic interpretations, this work gives emphasis to the Antalo limestone

which should be as potential source rock, for the oil seepage at the Mechela River floor. The upper sandstone, which gets coarser upwards and becomes conglomeratic, exhibits good reservoir quality at the top part. In addition to the upper sandstone, the highly brecciated agglomeratic basalts that overlay could as well be considered as good reservoir. The NW-SE faults which may have created down warping structures and the intersecting NE-SW faults and NW-SE faults could be the possible structural traps in the basin. Pinching out of some facies (mainly the Gohatsion formation) might have provided significant stratigraphic traps. The presence of shales and claystones which may act as sealing (cap) rocks should also be stressed in this connection. Lateral variation and inter-fingering of units are also observed as interesting factors contributing to the possible stratigraphic traps. Generally combination of the structural and stratigraphic traps could be possible oil traps in the Blue Nile basin.

7.2 Recommendation

Finally, the following recommendations are forwarded:

- Geophysical works including Seismic, gravity and magnetic together with GIS data integration techniques. Based on the data collected, to produce combined modeling of basement structures and topographic features in the Dera sub basin and particularly at Wereilu.

- The study area is characterized by rugged morphology, so that air borne geophysical surveys are recommended rather than ground geophysical survey.

- The geophysical work will be conducted both parallel and orthogonal to the basin elongation directions which will allow to construct different models to define the shape of the basin, to confirm the thickness of major rock units, and the possible effect of the deep seated structures.

List of Appendix Page

Appendix I.....83

Appendix II.....90

Appendix III.....93

Appendix IV.....94

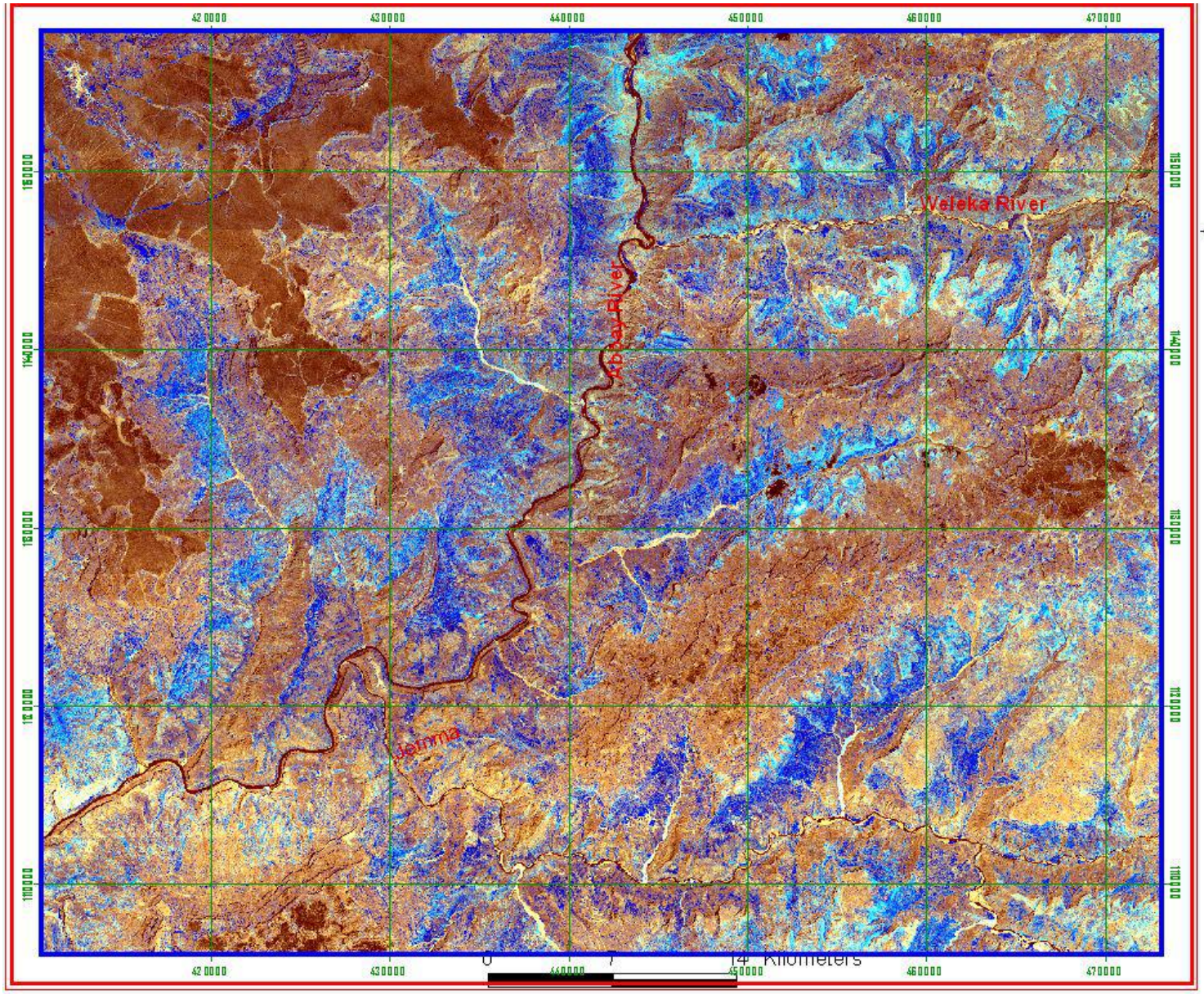

Band combination to enhance the visibility of the different soils resulting from alteration of the bed rock. The false color composite of the sum of ratio of band 4/5 + 7/4+ 3/7 as red, 5/4+7/4+3/7 as green and 4+7 as blue. This help tin mapping indirectly the rocks from which some of the soils are derived.

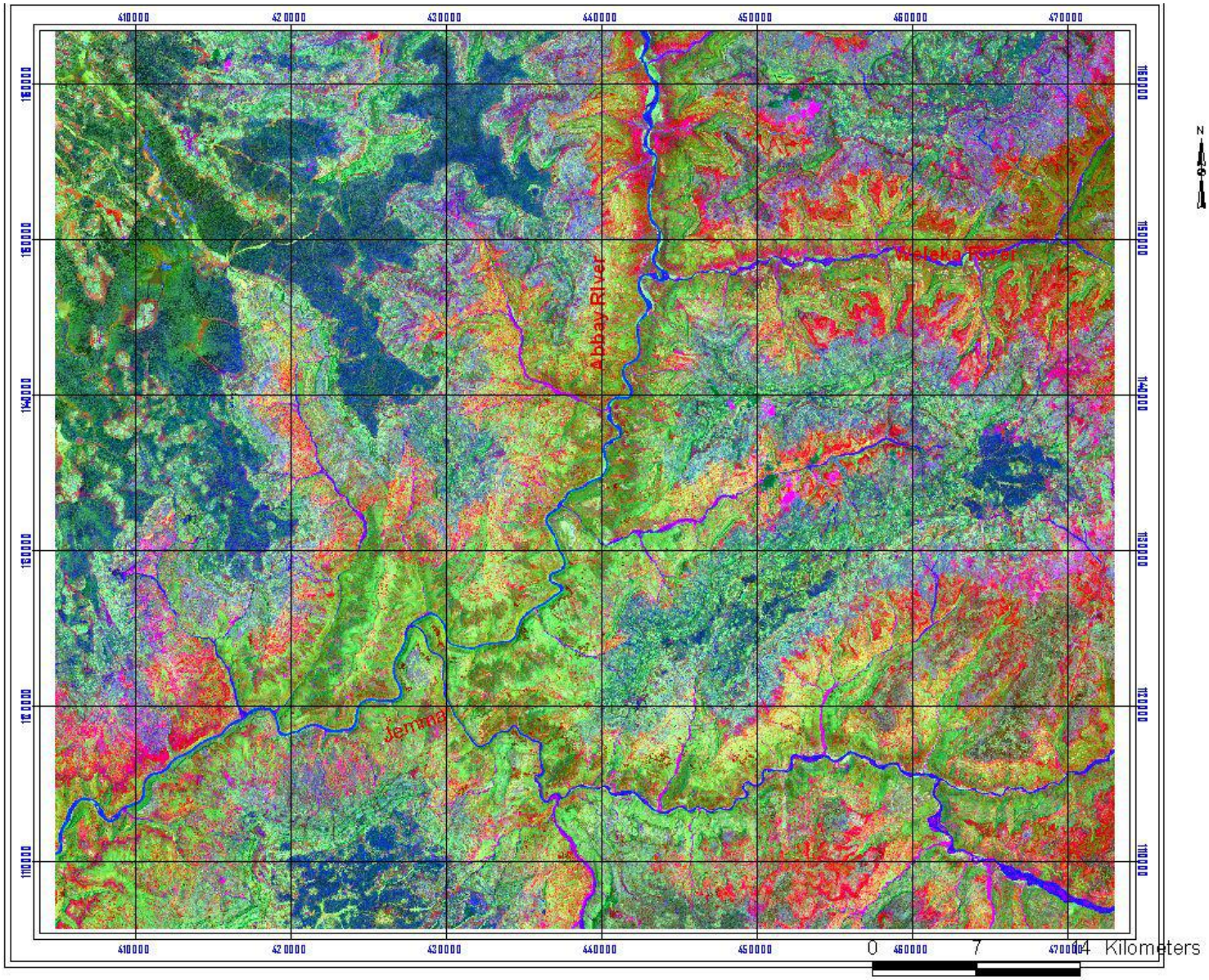

Principal Component Analysis (PCA) of Landsat ETM+ of band 7,5,4,3,2,1 of PC1, PC2 and PC3 in RGB order that help to identify the sandstone unit which appears red in color..

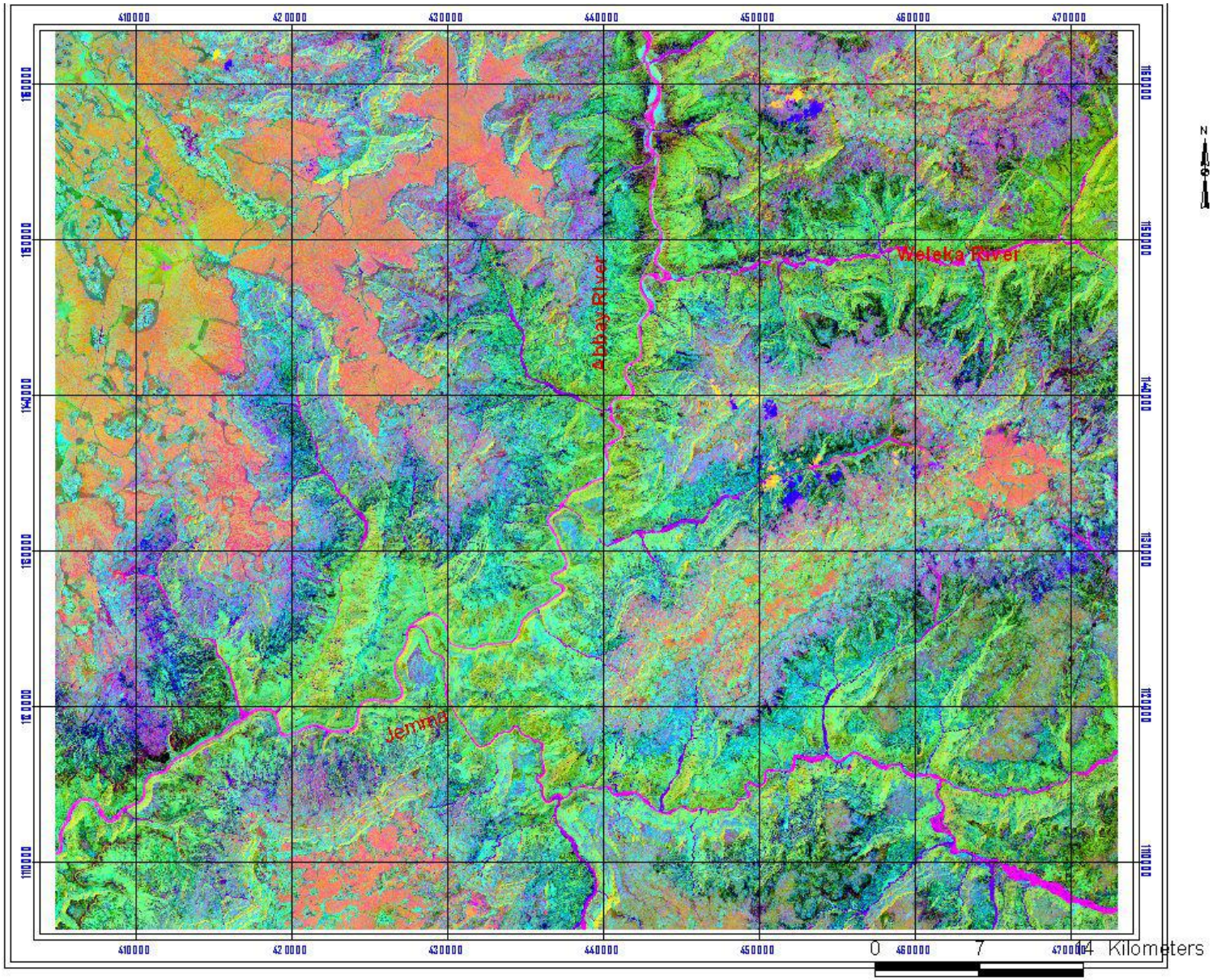

false color ratio image of the area using ETM+ 5/4 as red, 3/2 as green and 5/7 as blue. Though producing excellent discrimination of the rock type. In the principal components processing ; only PC1 (with 85% of egien value) gave the best result for general aspect of geology while PC2 and PC3 (with 15% of egien value) only can enhance some aspect of geology.

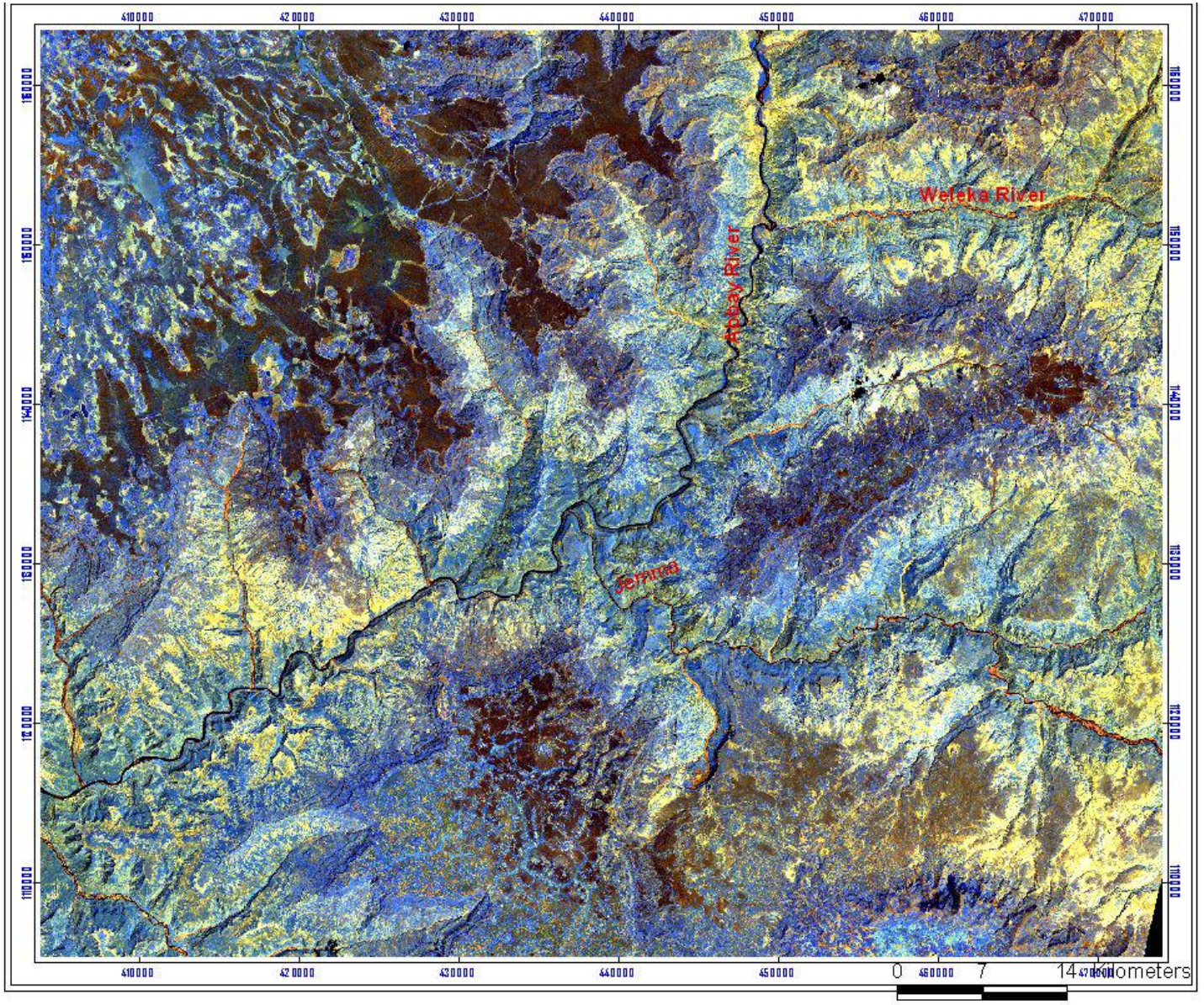

False Color Composite of Landsat ETM+ band 754 In RGB order relieving the sand stone unit in yellow, the Limestone unit in light blue, the upper trap in dark brown, and the lower trap in light brown.

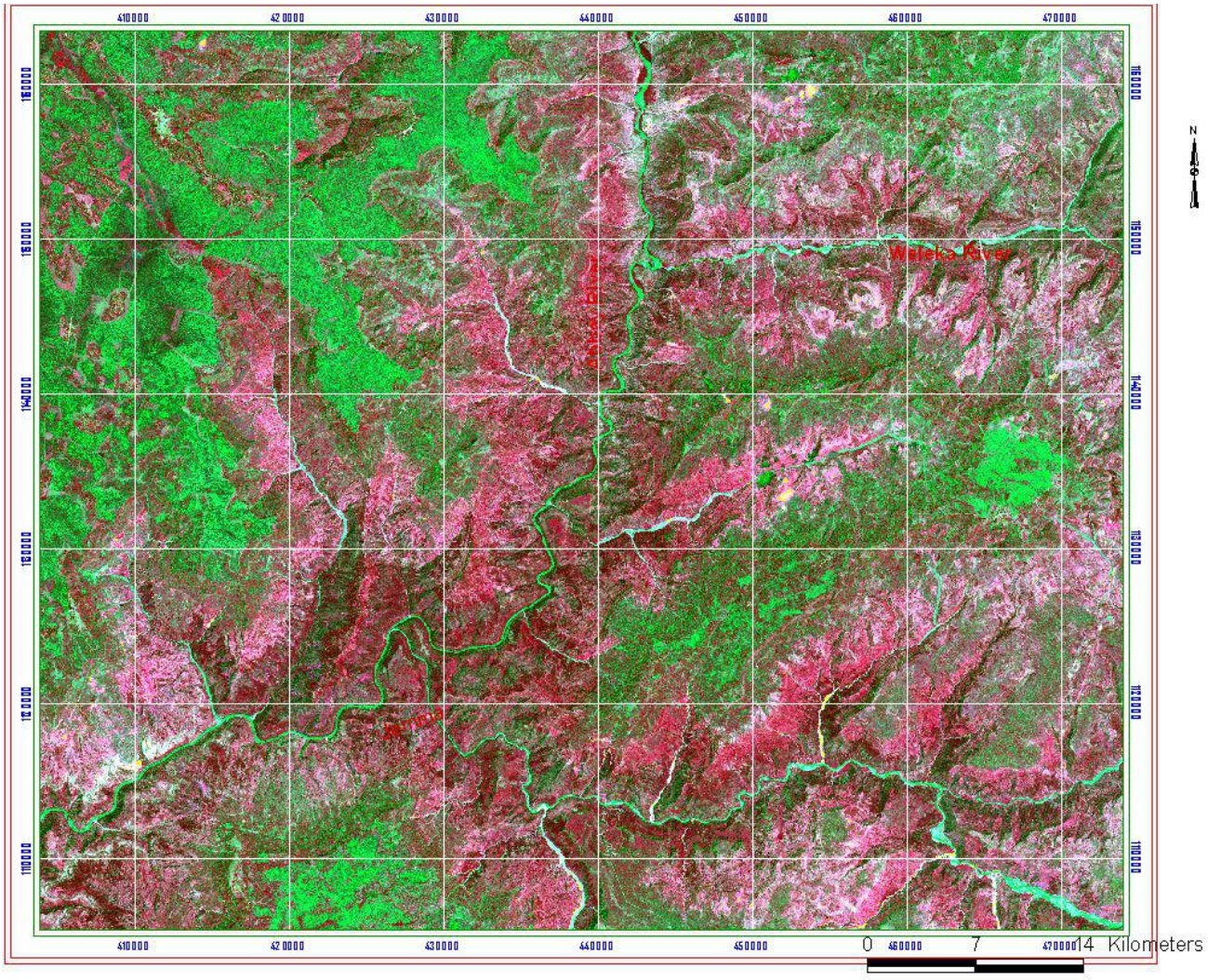

This image combines the first principal component of Bad 7,5,4,3,2 of landsat ETM+ as red, the sum of Band 7 and band 3 as green and the band 7/3 ratio as blue. The Mesozoic –cretaceous sediment sharply etched on the imagery as red color, where as the trap basalt distinguished as green colored seemed found associated with vegetation color.

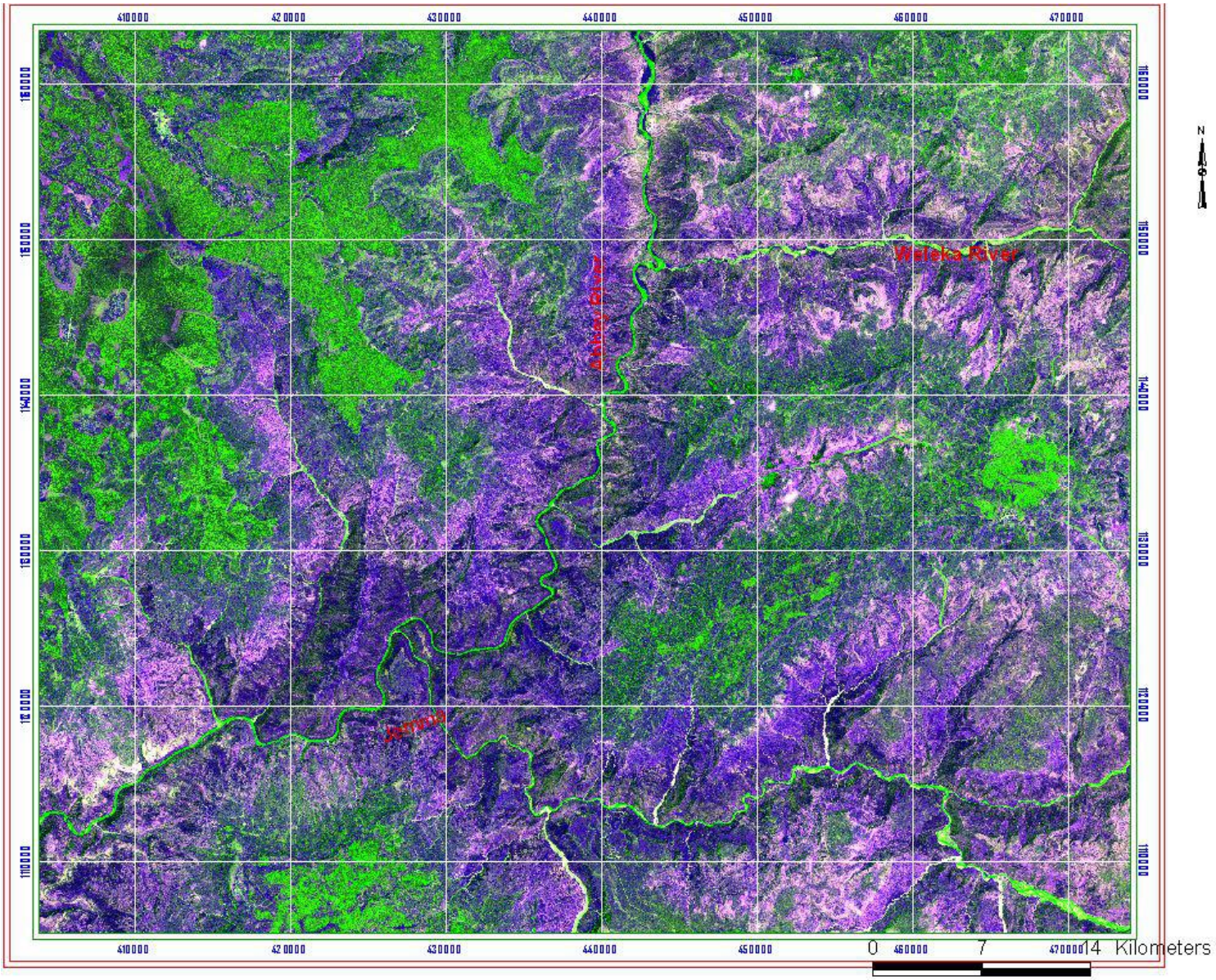

Filtering the IHS (Intensity, Hue and Saturation) color combination with edge enhancement so that it increase the visibility of contacts for interpretation.

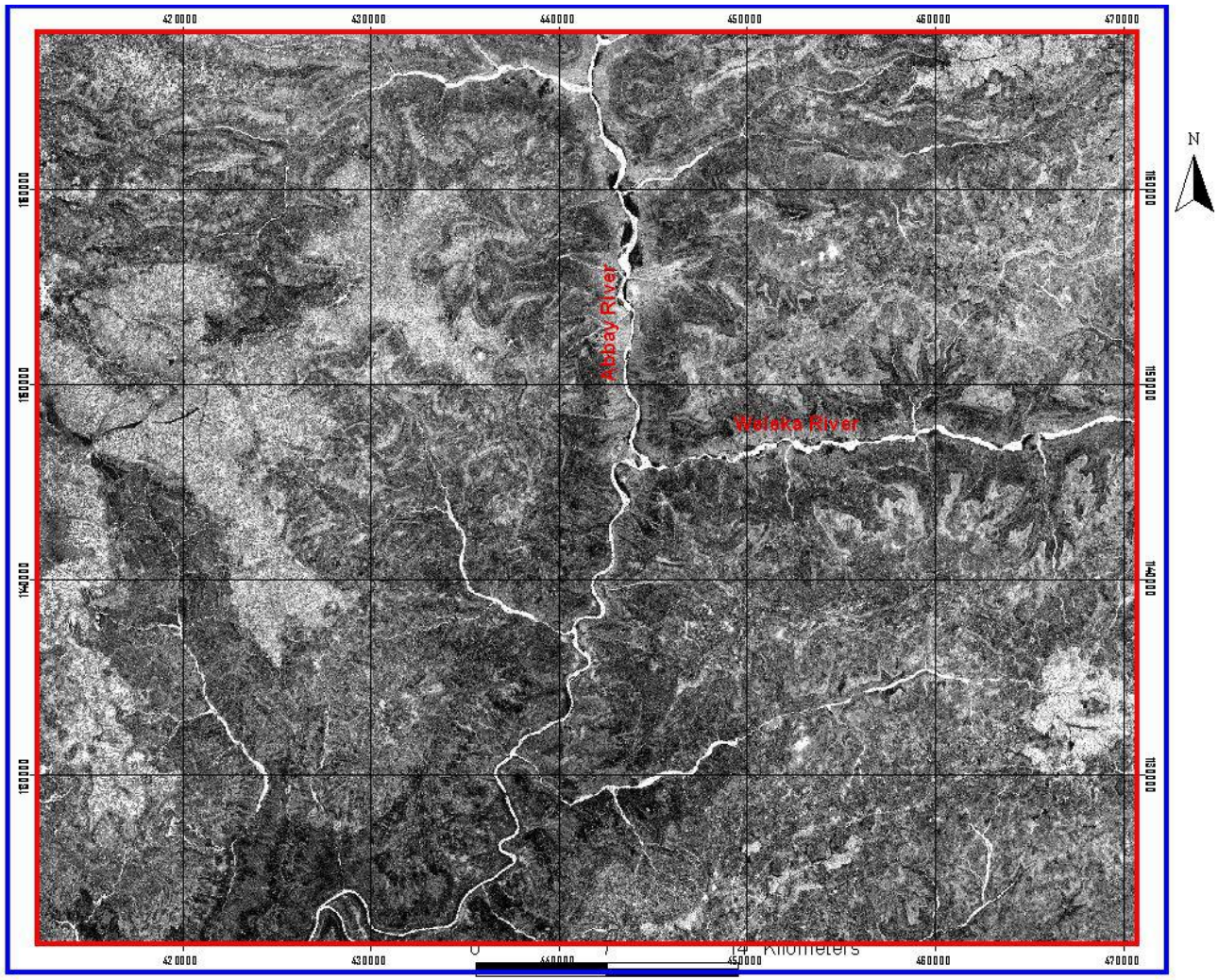

Band Ratio: ratio of LAndsat ETM+ band 7 over band 5. This techniques help to clearly identify linear features, and shows the basalt unit in light grey color while the sedimentary unit in black color.

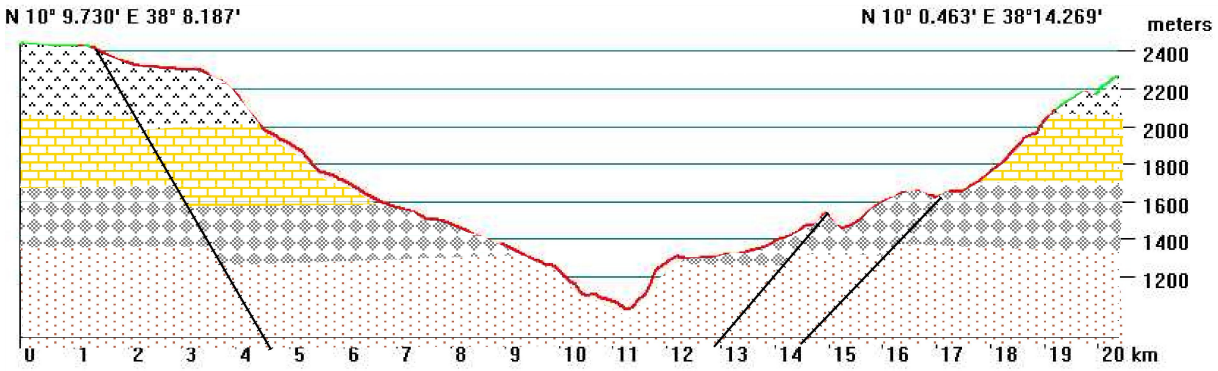

Dejen to Gohatsion

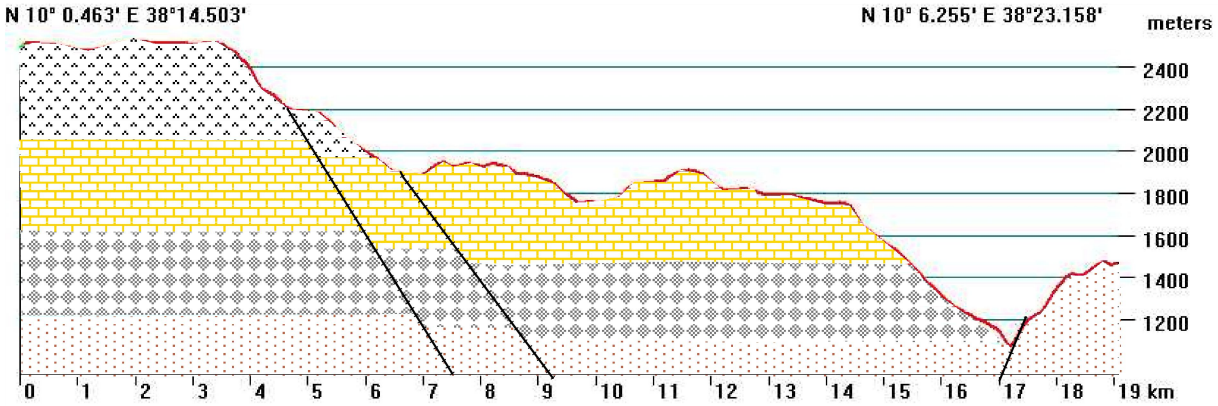

Gohatsion to Jema

Jema to Chekagenet

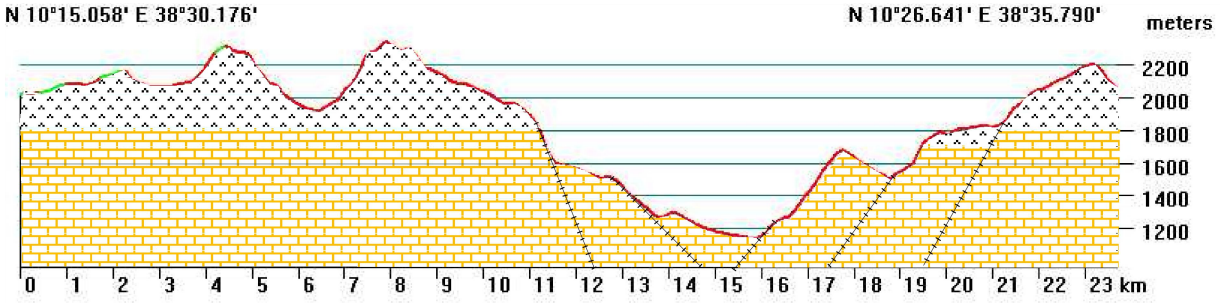

Profile Chekagenet to Weleka

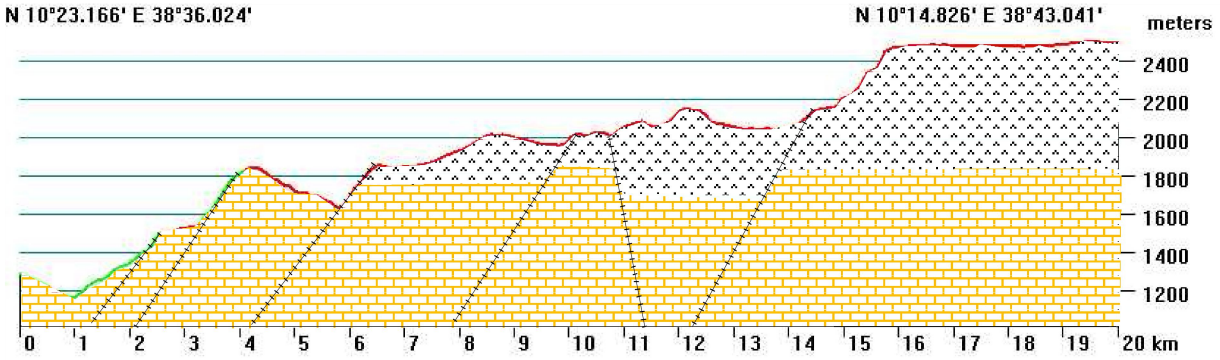

Weleka to Gundomeskel

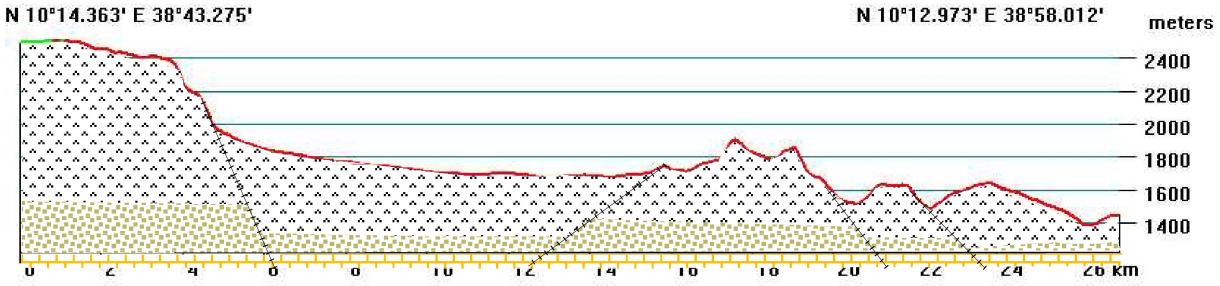

Gundomeskel to Jara

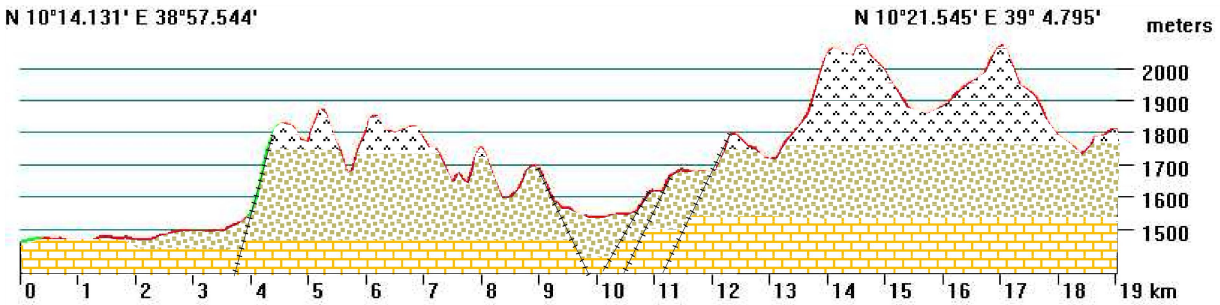

Jara to Meregna

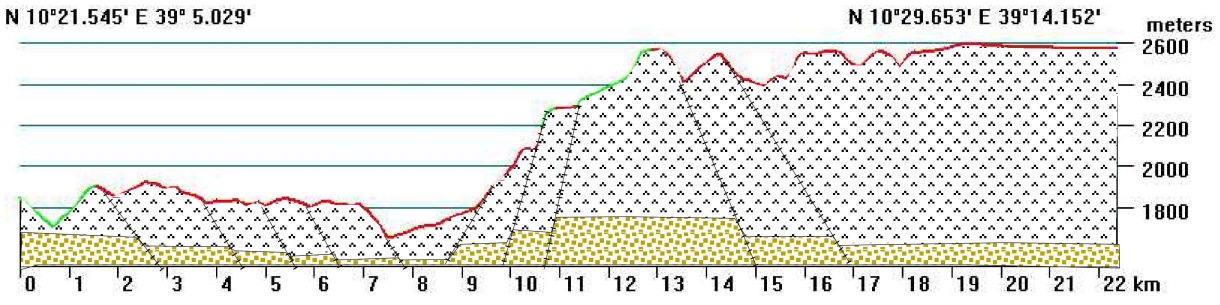

Meregna to Mida

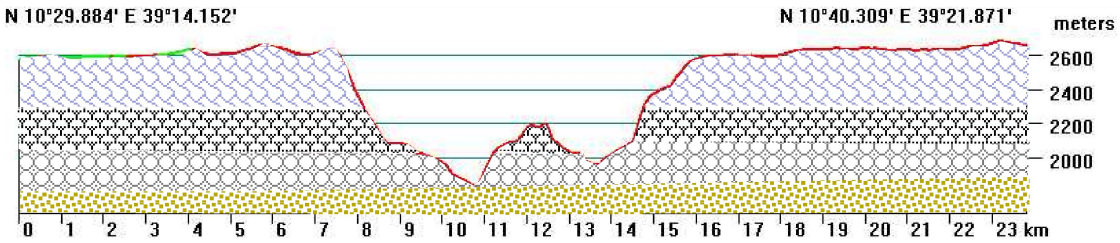

Mechela

```
GROUP = METADATA_FILE
PRODUCT_CREATION_TIME = 2004-02-12T17:29:50Z
PRODUCT_FILE_SIZE = 656.5
STATION_ID = "EDC"
GROUND_STATION = "EDC"
GROUP = ORTHO_PRODUCT_METADATA
SPACECRAFT_ID = "Landsat7"
SENSOR_ID = "ETM+"
ACQUISITION_DATE = 1999-10-23

WRS_PATH = 169
WRS_ROW = 053

SCENE_CENTER_LAT = +10.1307865
SCENE_CENTER_LON = +37.9942732
SCENE_UL_CORNER_LAT = +11.0627536
SCENE_UL_CORNER_LON = +37.3445896
SCENE_UR_CORNER_LAT = +10.8213895
SCENE_UR_CORNER_LON = +38.9971686
SCENE_LL_CORNER_LAT = +9.4373894
SCENE_LL_CORNER_LON = +36.9951753
SCENE_LR_CORNER_LAT = +9.1972592
SCENE_LR_CORNER_LON = +38.6407202

SCENE_UL_CORNER_MAPX = 319171.500
SCENE_UL_CORNER_MAPY = 1223419.500
SCENE_UR_CORNER_MAPX = 499690.500
SCENE_UR_CORNER_MAPY = 1196230.500
SCENE_LL_CORNER_MAPX = 279870.000
SCENE_LL_CORNER_MAPY = 1043841.000
SCENE_LR_CORNER_MAPX = 460531.500
SCENE_LR_CORNER_MAPY = 1016680.500

BAND1_FILE_NAME = "p169r053_7t19991023_z37_nn10.tif"
BAND2_FILE_NAME = "p169r053_7t19991023_z37_nn20.tif"
BAND3_FILE_NAME = "p169r053_7t19991023_z37_nn30.tif"
BAND4_FILE_NAME = "p169r053_7t19991023_z37_nn40.tif"
BAND5_FILE_NAME = "p169r053_7t19991023_z37_nn50.tif"
BAND61_FILE_NAME = "p169r053_7k19991023_z37_nn61.tif"
BAND62_FILE_NAME = "p169r053_7k19991023_z37_nn62.tif"
BAND7_FILE_NAME = "p169r053_7t19991023_z37_nn70.tif"
BAND8_FILE_NAME = "p169r053_7p19991023_z37_nn80.tif"

GROUP = PROJECTION_PARAMETERS

REFERENCE_DATUM = "WGS84"
REFERENCE_ELLIPSOID = "WGS84"
GRID_CELL_ORIGIN = "Center"
UL_GRID_LINE_NUMBER = 1
UL_GRID_SAMPLE_NUMBER = 1
GRID_INCREMENT_UNIT = "Meters"
GRID_CELL_SIZE_PAN = 14.250
GRID_CELL_SIZE_THM = 57.000
GRID_CELL_SIZE_REF = 28.500



FALSE_NORTHING = 0
ORIENTATION = "NUP"
RESAMPLING_OPTION = "NN"
MAP_PROJECTION = "UTM"
END_GROUP = PROJECTION_PARAMETERS
GROUP = UTM_PARAMETERS
ZONE_NUMBER = +37
END_GROUP = UTM_PARAMETERS
SUN_AZIMUTH = 132.0508651
SUN_ELEVATION = 58.4136104
QA_PERCENT_MISSING_DATA = 0
CLOUD_COVER = 0

PRODUCT_SAMPLES_PAN = 17120
PRODUCT_LINES_PAN = 15306
PRODUCT_SAMPLES_REF = 8560
PRODUCT_LINES_REF = 7653
PRODUCT_SAMPLES_THM = 4280
PRODUCT_LINES_THM = 3827
OUTPUT_FORMAT = "GEOTIFF"

END_GROUP = ORTHO_PRODUCT_METADATA
GROUP = L1G_PRODUCT_METADATA
BAND_COMBINATION = "123456678"
CPF_FILE_NAME = "L7CPF19991001_19991123_11"
GROUP = MIN_MAX_RADIANCE
LMAX_BAND1 = 191.600
LMIN_BAND1 = -6.200
LMAX_BAND2 = 196.500
LMIN_BAND2 = -6.400
LMAX_BAND3 = 152.900
LMIN_BAND3 = -5.000
LMAX_BAND4 = 157.400
LMIN_BAND4 = -5.100
LMAX_BAND5 = 31.060
LMIN_BAND5 = -1.000
LMAX_BAND61 = 17.040
LMIN_BAND61 = 0.000
LMAX_BAND62 = 12.650
LMIN_BAND62 = 3.200
LMAX_BAND7 = 10.800
LMIN_BAND7 = -0.350
LMAX_BAND8 = 243.100
LMIN_BAND8 = -4.700
END_GROUP = MIN_MAX_RADIANCE
GROUP = MIN_MAX_PIXEL_VALUE
QCALMAX_BAND1 = 255.0
QCALMIN_BAND1 = 1.0
QCALMAX_BAND2 = 255.0
QCALMIN_BAND2 = 1.0
QCALMAX_BAND3 = 255.0
QCALMIN_BAND3 = 1.0
QCALMAX_BAND4 = 255.0
QCALMIN_BAND4 = 1.0
QCALMAX_BAND5 = 255.0
QCALMIN_BAND5 = 1.0
QCALMAX_BAND61 = 255.0
QCALMIN_BAND61 = 1.0
QCALMAX_BAND62 = 255.0
QCALMIN_BAND62 = 1.0
QCALMAX_BAND7 = 255.0
QCALMIN_BAND7 = 1.0
QCALMAX_BAND8 = 255.0
QCALMIN_BAND8 = 1.0
END_GROUP = MIN_MAX_PIXEL_VALUE
GROUP = PRODUCT_PARAMETERS

CORRECTION_METHOD_GAIN_BAND1 = "CPF"
CORRECTION_METHOD_GAIN_BAND2 = "CPF"
CORRECTION_METHOD_GAIN_BAND3 = "CPF"
CORRECTION_METHOD_GAIN_BAND4 = "CPF"
CORRECTION_METHOD_GAIN_BAND5 = "CPF"
CORRECTION_METHOD_GAIN_BAND61 = "CPF"
CORRECTION_METHOD_GAIN_BAND62 = "CPF"
CORRECTION_METHOD_GAIN_BAND7 = "CPF"
CORRECTION_METHOD_GAIN_BAND8 = "CPF"
CORRECTION_METHOD_BIAS = "IC"

END_GROUP = PRODUCT_PARAMETERS
GROUP = CORRECTIONS_APPLIED
STRIPING_BAND1 = "NONE"
STRIPING_BAND2 = "NONE"
STRIPING_BAND3 = "NONE"
STRIPING_BAND4 = "NONE"
STRIPING_BAND5 = "NONE"
STRIPING_BAND61 = "NONE"
STRIPING_BAND62 = "NONE"
STRIPING_BAND7 = "NONE"
STRIPING_BAND8 = "NONE"
BANDING = "N"
COHERENT_NOISE = "N"
MEMORY_EFFECT = "N"
SCAN_CORRELATED_SHIFT = "N"
INOPERABLE_DETECTORS = "N"
DROPPED_LINES = N
END_GROUP = CORRECTIONS_APPLIED
END_GROUP = L1G_PRODUCT_METADATA
END_GROUP = METADATA_FILE
END
```

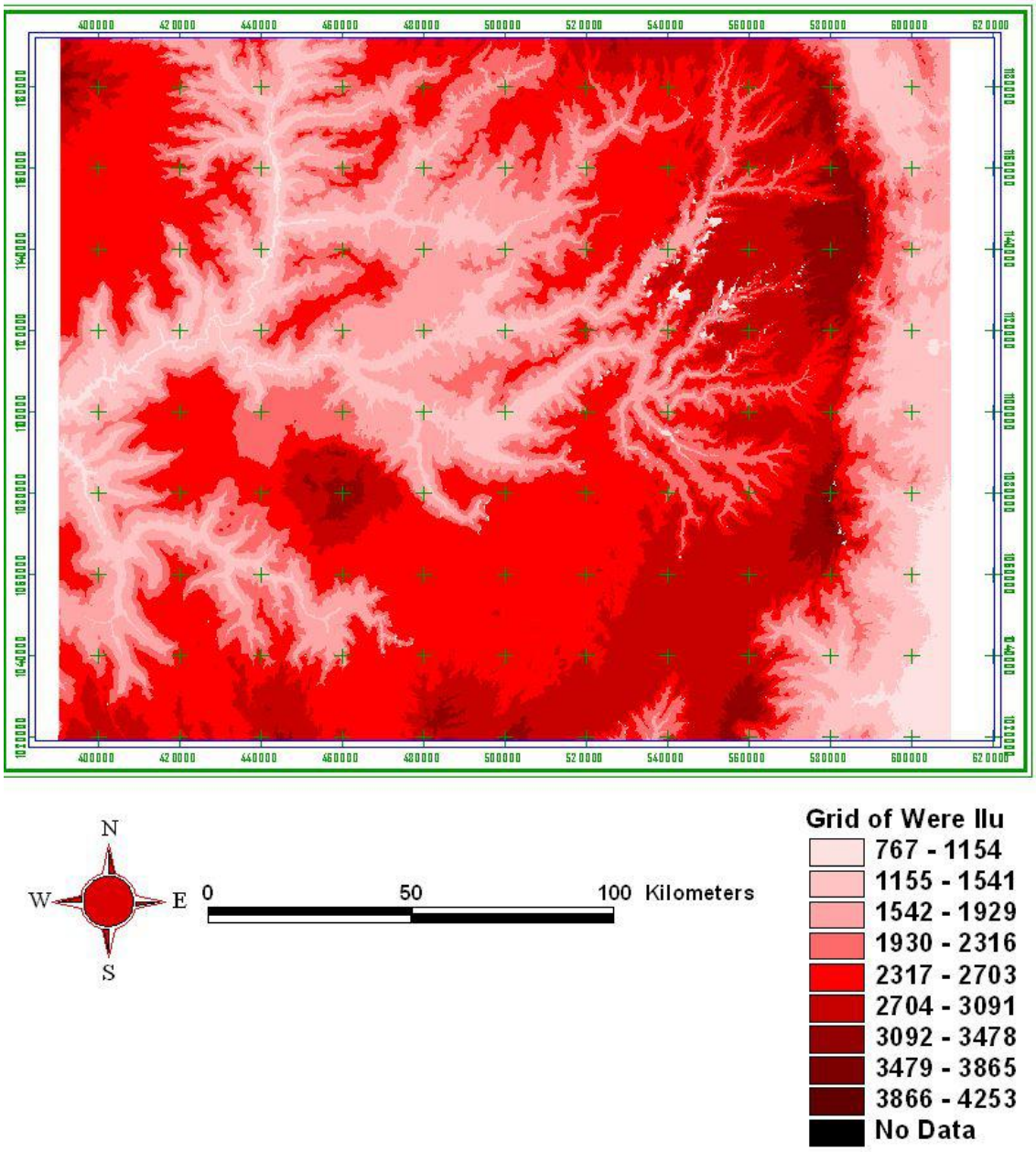

DEM of the Dera and Were Ilu.

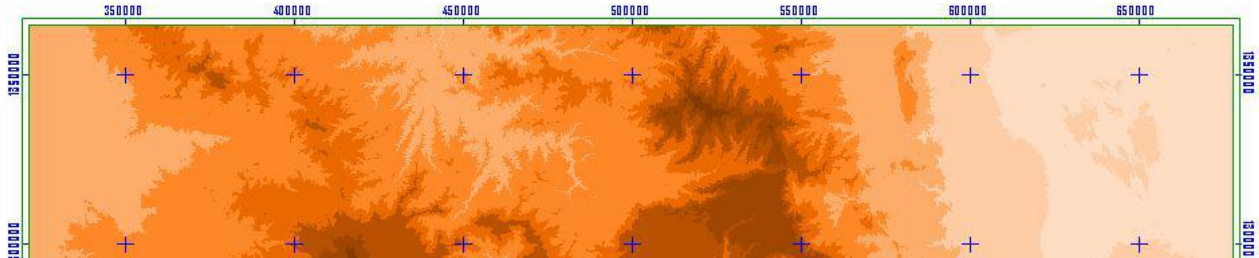

-116 - 370
371 - 856
857 - 1342
1343 - 1828
1829 - 2315
2316 - 2801
2802 - 3287
3288 - 3773
3774 - 4260
No Data

Dem of the Study area.

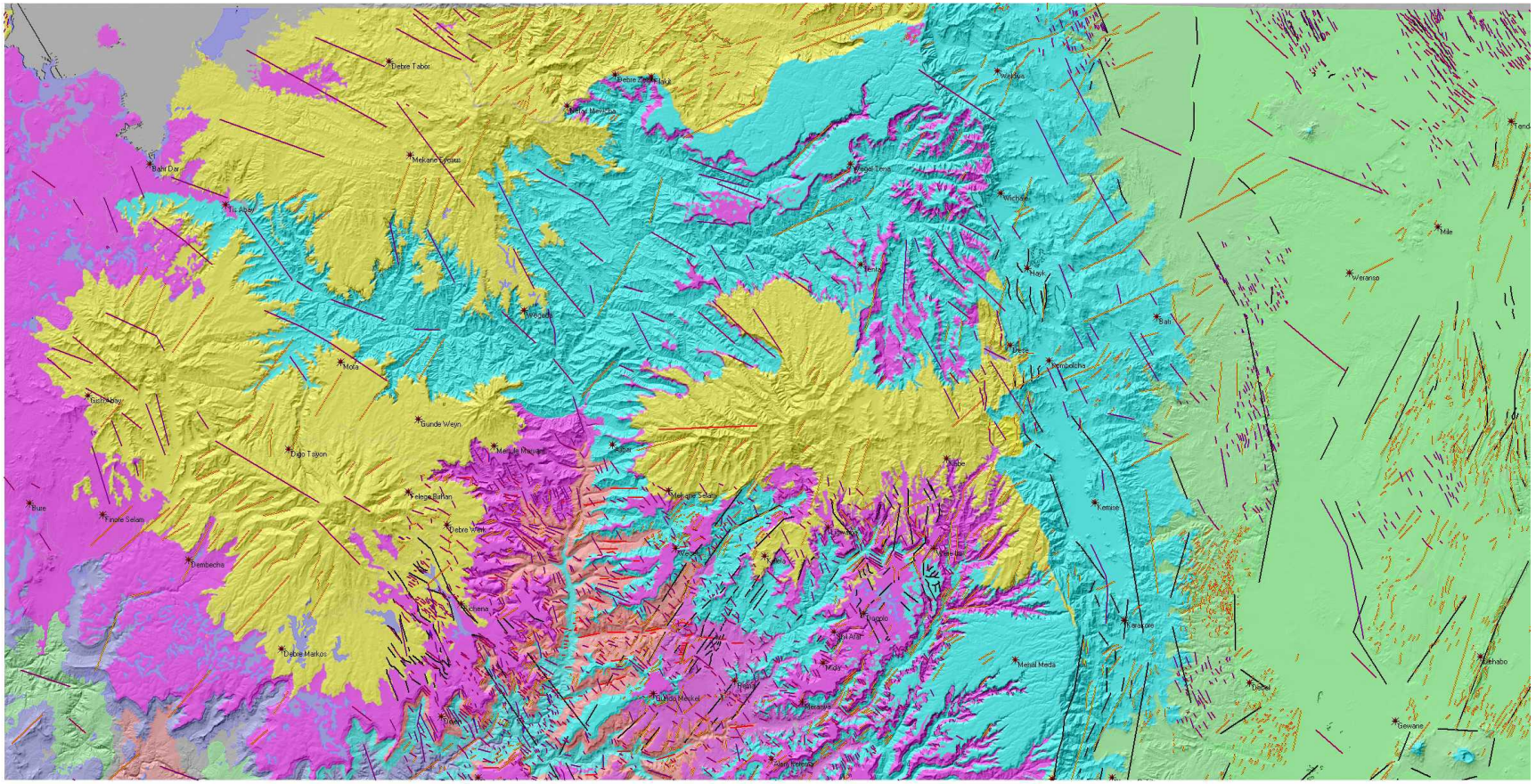

DTM of the study area.

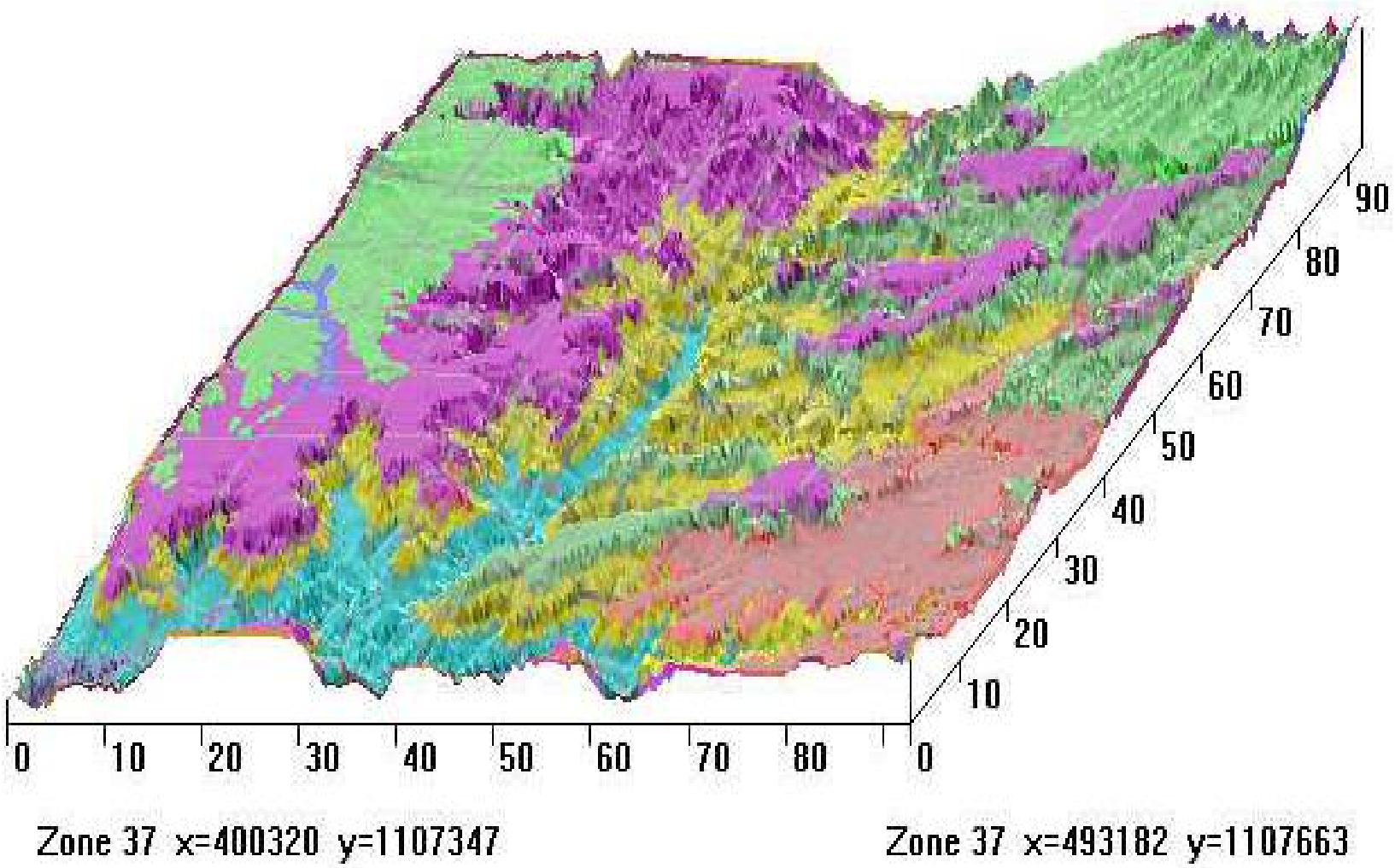
0
10
20
30
40
50
60
70
80
0
10
20
30
40
50
60
70
80
90
Zone 37 x=400320 y=1107347
Zone 37 x=493182 y=1107663

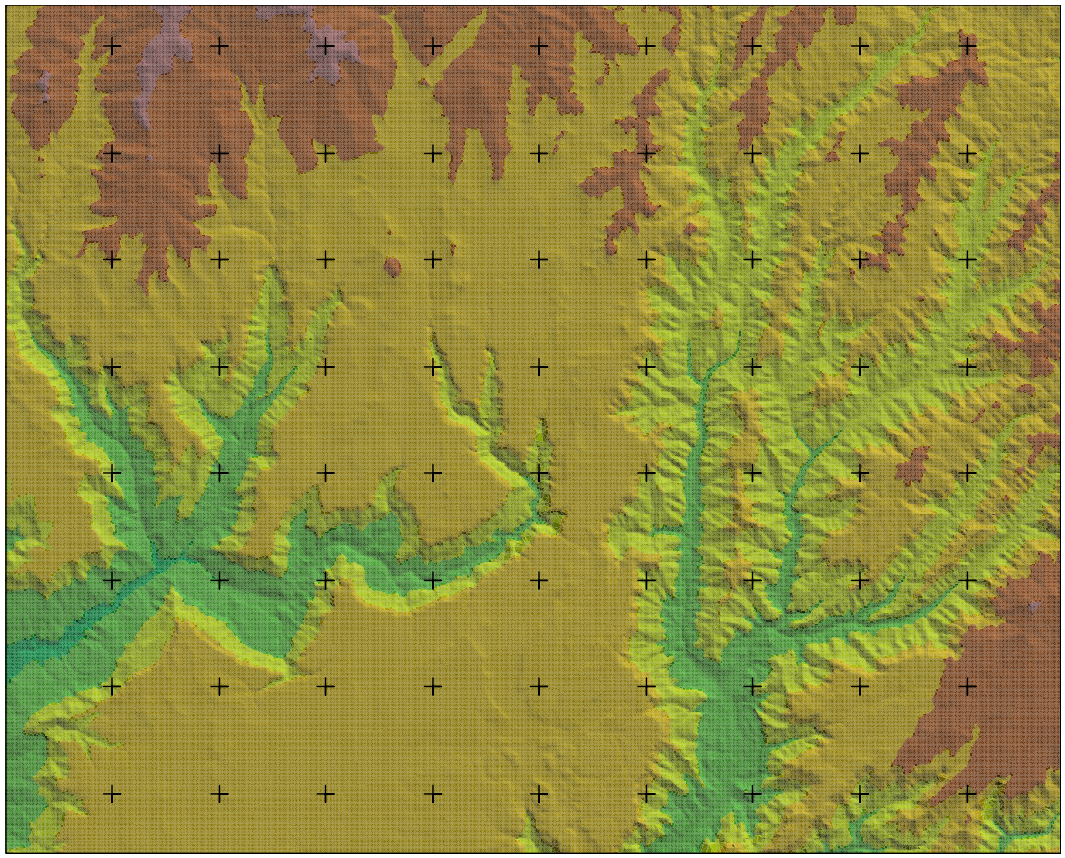

REFERENCES:

Arkell, W.J. (1956) Jurassic Geology of the World. Oliver and Boyd (eds). *Edinburgh, P. 297-332.*

Beicip (1985) Geological report of the Ogaden Malmasion, 1:1000000 scale. *Paris, France.*

Blanford, W.T. (1869) On the Geology of a portion of Abyssinia. Quart. *Journa. Geol. Soc. London, Vol. 25, pp. 491-406.*

Bocaleti, M., Bonini, M. Mazzuoli, R., Abebe, B., Piccardi, L., Tortrici, L. (1998). Quaternary Oblique extensional tectonics in the Ethiopia Rift (Horn of Africa). *Tectonophysics 287: 97-116.*

Bosellini, A. (1989) The East African Continental Margins. *Geology, 14: 76-78.*

Bosworth, W. (1992) Mesozoic and early Tertiary rift tectonics in East Africa, *Tectonophysics, 20, 115-137.*

Conybeare, B. (1979) Lithostrtigraphic Analysis of Sedimentary Basins. *Vol I, Academic Press (eds), New York, PP. 438-494.*

Dainelli, G. (1943) Geologia dell' Africa Orientale: *4 vols., Academia d' Italia, centro studi A.O.I., Roma.*

Davidson, A. and Rex, D.C. (1981) Age of volcanism and rifting in southwestern Ethiopia. *Nature, 283: 371-373.*

Drury, S.A. (1993) Image Processing in Geology. 2nd edn, Allen and Unwin (eds.), Digital image processing in the visible and Near-Infrared, *Cambrige, Uk. PP. 124-149.*

Ebinger, C.J., Yemane, T., Gidey Woldegebriel, Arson, J.L. and Walter, R.C.(1989) Tectonic development of the Western Branch of East African Rift System. *Geological society of America Bulletin 101: 885-903.*

Ethiopia Hunt Oil Company (1992) Geneale River Area, Ogaden basin, unpuplished report. *Addis Ababa, Ethiopia.*

Ethiopia Mapping Agency (1988) National Atlas of Ethiopia, Addis Ababa, Ethiopia.

Ethio Geo-Technical Services (2000) Report on Hydrogeological and Geophysical investigation to identify potential ground water field and test/productive well drilling

in Ajibar and surrounding areas, Amhara National regional State, Water Mines and energy Resource Development Bureau.

Getaneh Assefa (1991) Lithostratigraphic and enviroment of deposition of late Jurassic–Early cretaceous sequence of the central part of Northwestern Plateau, Ethiopia. N. Jb. Geol. Palaont. *Abb. 182(3): 255-284, Stutgart.*

Getaneh Assefa (1987) Gohatsion Formation: A new Lias- Malm Lihostratigraphic Unit from the Abay River basin, Ethiopia. *Geoscience Journal Vol. II no. 1, PP. 63-88.*

Giday Weldegabriel, Jaes, L., Aronson and Robert C. Walter, (1990) Geology, Geochronology, and rift basin development in the central sector of the Main Ethiopian Rift. Geol. Soc. Of America *Bull., Vol. 102, pp. 439-458.*

Gregnanin, A. (1969) Magmatismo precoce Ethiopico. La Serie in Frarenacea.Mem-mus Tridentino *Sci. Nat., Vol. 18, pp. 137-172.*

Guiraaud and Maurin(1992) Early Creataceous rifts of western and Central Africa: an overview, *Tectonophysics, 213: 153-168.*

Jansen, M.E. Torne, M., Cloetingh, S. and Banda E. (1995) Temporal and Spatial correlations between changes in plate motions and the evolution of rifted basins in Africa, *Geol. Soc. Am. Bull., 107: 1317-1332.*

Jepsen, D.H. and Athearn, M.J. (1961) Geological plan and section of the left bank of Blue Nile Canayon near crossin of Addis Ababa- Debre Markos Road. U.S. department of interuior, Ethiopia's Resources Department, Addis Ababa, Ethiopia.

Jepsen, D.H. and Athearm, M.J., (1964) Land and water Resources of the Blue Nile Basin. Apendx II, 221 P. Geology, U.S. Dept. Interior. Addis Ababa. Ethiopia.

Kazmin, V. (1972a) The Geology of Ethiopia, Geological Survey of Ethiopia, Addis Ababa. Ethiopia.

Kazmin, V. (1972b) The Geology of Ethiopia, Geological Survey of Ethiopia, 1:2000000 scale. Printed by Hunting surveys Ltd. London, E.I.G.S., Addis Ababa, Ethiopia.

Kazmin, V., (1975) Explanation of the geological map of Ethiopia, Ethiopian Geological survey. *Bull., 1:1-15.*

Kent, P.E., (1974) Continental Margin at East Africa: A rgion of Vertical movement. In: Bark, A. and Drake, C.l. (eds). The Geology of Continental Margins. *Sprinnger-Verlag, New York, P. 313-320.*

Kernel, E. (1926) Abessomalein (Abessinien und Somalien) in Handbuch, Regionalische *Geologie, vol. 7, Heidelberg.*

Kovacik, J. (1975) Report on oil seepage occurrence south of Dessie in the Province of Wollo. Unpub. Report, MME, Addis Ababa, Ethiopia.

Le Bas, M.J., and Mohr, P.A. (1970) Tholeiite from the Simien alkali basalt center, Ethiopia. *Geol. Mag., Vol. 107, PP. 523-529.*

Lillesand, T.M and Kifer, R.W. (2000) Remote Sensing And Image Interpretaion, 2nd ed, *Jhon Willey (eds.) PP: 513-518.*

Merla, G., and Minucci, E. (1938) Missione geologica nel Tigrai, Reale Accad. Ital., Roma, Vol. 1, 363 PP.

Merla, G., Abbate, E., Canuti, P., Sagri, M. and Tacconi, P., (1973) Geological map of Ethiopia and Somalia. Consigilo Nazionale delle Ricerche, Firenze.

Merla, G., Abbate, E., Sagri, M. Azzuroli, A., Bruni, P., Canuti, P., Fazzuoli, A., Bruni, P., and Tacconi, P., (1979) Explanation of the Geological Map of Ethiopia and Somalia with the majo land forms. Consigilo Nazionale delle Ricerche, Firenze.

Ministry of Mines and Energy (1993) Petroleum potential of Ethiopia unpub. Report, Addis Ababa, Ethiopia.

Minstry of Water Resource (1999) Integrated Master Plan Of The Abay Basin. Addis Ababa, Ethiopia.

Mohr, P.A, (1962) The geology of Ethiopia. Univ. Coll. Addis Ababa press, 268 PP.

Mohr, P.A. (1963) Occurrence of the Karroo System Sediments in Ethiopia. *In Garland, C.R., 1972-1975.*

Mohr, P.A. (1967b) Major volcano-tectonic lineament in the Ethiopian Rift System, *Nature, 213, 664-665.*

Mohr, P.A. (1971a) Ethiopia Tertiary dike Swarms. Simithsonian Astophysics. *Obs. Spec. Rep. No. 339. 53 pp.*

Mohr, P.A., and Rogers, A.S. (1966) Gravity traverses in Ethiopia (second interim report). Bull. Geophys. Obs. Addis Ababa, Vol. 9, PP 7-58.

Mohr, P.A. (1974) Mapping pf the major structures of the African rift system. Smithsonian Astrophysical Observatory, Special Report 361.

Peccerillo a. and Bekele Megersa (1992) Petrological and geochemical variations associated with the transition from plateau basalt to central volcanos along the Mugher-

Tarmaber transect. Programs and abstracts of the second Ethiopian Geoscience and Mineral Engineering congress. P 10-13.

Raaben, V.P., Komenyev, S.p, Lissin,V.N. and Kitachew W.T. (1979) Preliminary report on the evaluation of petroleum prospects of the Ogaden Basin, Ethiopia. Ethiopian institute of Geological Survey, Note, 112.

Russo, A., Getaneh assefa, and Balemual Atnafu (1994) Sedimentary Evolution of the Blue Nile Basin. N.Jb. *Geol. Palaont., Abh., 182: 255-284.*

Serawit, A. and Tamrat, M. (1996) The Geology of Gundo Meskel and Ejere area, North Shoa, Abbay Basin. Ministry of mines and Control, Petroluem operations Department, Addis Ababa. Ethiopia.

Serawit, A. and Tamrat, M. (1995) The Geology of Jema River valley, North Shoa, Abbay Basin. Ministry of mines and Control, Petroluem operations Department, Addis Ababa. Ethiopia.

Serawit, A. and Tamrat, M. (1999) The Geology of Mugher Cement Factory, North Shoa, Abbay Basin. Ministry of mines and Control, Petroluem operations Department, Addis Ababa. Ethiopia.

Shackelton, R.M., (1978) Structural development of the east African Rift system. In: Bishop, W.W. (ed). Geological Background to Fossil Man: Recent research in the geology rift, East Africa. *Scottish Academic press. 55P.*

Stefanini, G. (1933) Saggio di una carta geologica dell'Eritrea, della Somalia e dell'Ethiopia, 1:2000000. *Note instrative.-195 PP.;Firenze (I.G.M.).*

Tadiows Chernet, Hart, W., Aronson, J.L., Walter, R.C. (1998) New age constraints on the timing of volcanism and tectonism in the northern Main Ethiopian Rift-Southern Afar transition Zone (Ethiopia). *Journal of volcanology and geothermal Research 80: 885-903.*

Tamrat, M.and Tibebe, G.S. (1997) The Geology of Ginde Mendbert- Jeldu and Amuru_jarti areas (East Wellega and Western Shoa), Abbay Basin. Ministry of mines and Control, Petroluem operations Department, Addis Ababa. Ethiopia.

Tesfaye Korme, Acocella and Bekele Abebe (2004) The role of pre-existing structures in orgin, propagation and architecture of faults in the Main Ethiopian Rift. *Gondwana Resurch, 7. 467-479.*

Tissot, B., Durand, B., Espitalie, J. and Combaz, A. (1974) Influence of nature and Diagenesis of organic matter in formation of petroleum. *American Association. Petroleum Geologists Bull., 58: 499-506.*

Ukistins A. I., Renne R.P., Wolfenden E., Barker J., Dereje Ayalew, Menzies M., (2002) Matching Conjugate volcanic rifted Margins :^{40} Ar/ ^{39}Ar Chrono-stratigraphy of pre- and syn-rift bimodal flood volcanism in Ethiopia and Yemen. Jour. *Earth and planetary science letter. 198: 289-306.*

UNFAO (1984) Agro-climatological data for Africa: Food and Agricultural Organization of the United nations, Rome Ialy.

Wolfenden E., Ebinger C., Gezahegn Yirgu, Deino A., Dereje Ayalew (2004) Evolution of the northern Main Ethiopia rift : Birth of triple Junction. Jour. *Earth and planetary science letter. 224: 213-228.*

Wolela Ahmed (2004) A review of the Hydrocarbon potential of the Blue Nile basin, Central Ethiopia. ministry of Mines, Petroluem operation Department, Addis Ababa.

Wolela Ahmed (1997) Sedimentology, diagenesis and hydrocarbon potential sandstones in hydrocarbon prospective Mesozoic rift basins (Ethiopia, UK, USA). Phd thesis, The Queen's University of Belfast, UK.

Wycisk, P., Klitzsch, C. Jas, and Reynolds, O. (1990) Intracratonal sequence development and structural control of phanerozoic strata in Sudan, Berlinear Geowiss, Abh., (A), 120.1, 45-86.

Zanettin, B. and Justin-Visentin, E., (1973) The Volcanic Succesion in the central Ethiopia: The Volcanics of Western Afar and Ethiopian Rift Margins. Mem. Ist. *Geol. Miner. University. Padova, V.31, P.1-19.*

Zanettin, B., Gregnanin, A., Justin-Visentin, E., Mezzacasa, G. and Piccirillo, E.M., (1974) Petrochemistry of the volvcanic series of the central Eastern Ethiopian Plateau and relationships between Tectonics and Magmatology. Mem. Ist. *Geol. Miner. University. Padova, 31. P 1-34.*

Zanettin, B., Gregnanin, A., Justin-Visentin, E., Mezzacasa, G. and Piccirillo, E.M., (1976) New Chemical Analysis of Tertiary volcanics from the central Eastern Plateau CNR. *Padova, P.1-43.*

Zanettin, B., Justin-Visentin, and Piccirillo, E.M., (1976) Volcanic Succession, Tectonics and Magmatology in central Ethiopa. In ARTI V (ed) Atti Mem. *Accad. Sci. Lett. Art. 11, p. 1-19.*

Zanettin, B., Justin-Visentin, and Piccirillo, E.M., (1980) Correlation among Ethiopian Volcanic Formation with special reference to the chronological and stratigraphic problems of the Trap series, *Academia Nazionale Dei Lincei, 47, 231-252.*